Multi-Rate Coding Schemes for Gaussian Multiple Access Channel

Meilin HE

Kyoto, Japan

November, 2017

Abstract

In multi-rate communication systems, multiple users attempt to communicate simultaneously, at various transmission rates, with a common receiver through the multiple access channel (MAC), even in the presence of Gaussian noise. A central problem in multi-rate coding for the multiple access communication system is to assign K constituent code to K transmitters so that they can communicate simultaneously, at various transmission rates, with a common receiver through the Gaussian MAC. However, it is impractical for users to employ different encoders.

In this dissertation, we propose multi-rate coding schemes for Gaussian MAC. In our schemes, each user employs a same structure of encoder serially concatenated with a spreader and a user-specific interleaver. Here, the different interleavers are used for user separation, and the spreader is employed to lower the transmission rate and thus to combat the multi-user interference. The different rate transmission is realized by adjusting the parameter of the encoder and the length of spreading. We analyze the decoding performances of our coding schemes, and obtain the optimal coding parameters and spreading lengths, which gives the maximum sum rates and approach the theoretical limits of the channel. The proposed coding schemes support multimedia services, and avoid employing multiple channel encoders to implement the multi-rate transmission.

Our three multi-rate coding schemes, roughly speaking, have almost the same structure with the same encoder, spreader, and interleaver. We discuss the optimization of the multi-rate coding based on three decoding algorithms employed in the multiple access communication systems. The three decoding algorithms are the belief propagation (BP) with the maximum a priori (MAP) detection, elementary signal estimation (ESE), and successive interference cancellation (SIC).

First, we introduce a multi-rate transmission in two-user multiple access communication sys-

tems with the MAP detection. Each user employs the same repeat accumulate (RA) encoder but with different parameters, i.e., the repeat numbers, in the encoder. Here, we perform the coding-only (without spreading) scheme, since multi-user interference is small for two users. At the receiver, we perform the BP decoding on a single factor graph, where at sum (two-user superimposed signals) node, the MAP detection is carried out. We develop a univariate fixed point analysis to obtain a system equation array of parameters of RA codes. This makes it possible to represent the parameters of RA codes explicitly as functions of the fixed point. We find the optimal parameters of RA codes that give the maximum sum rate. Numerical results show that our optimized two-user multi-rate RA code is superior to the conventional equal rate code in maximum sum rate, and approach the Shannon limit.

Second, we introduce a multi-rate transmission in multi-user multiple access communication systems with the ESE detection. We equally divide K users into multiple groups, and users in identical group has a same transmission rate. For each user, we employ a RA code serially concatenated with a spreading sequence and a user-specific interleaver pattern to implement various rates by adjusting both repeat number in RA encoder and length of spreading in spreader. Here, the interleaver patterns are different for user separation, and the spreading sequence is to lower the rate and thus to combat the user interference, since an increase in the number of users results in very serious multi-user interference. At the receiver, we perform a joint iterative BP decoding (Iterative Joint Decoding, IJD) on a single factor graph, where at sum (multi-user superimposed signals) node, the ESE detection is carried out. We develop a bivariate fixed point analysis to obtain the optimal parameters (repeat numbers) of RA code and spreading lengths, which give the maximum sum rate. With the increment of groups, the maximum sum rates of our optimized multi-rate code increase, and approach the Shannon limit, and exceeds those of conventional equal-rate transmission.

Instead of global IJD above, in the receiver we perform hybrid interference cancellation (HIC) decoding, where SIC is employed between the groups, and IJD is employed within the group. The HIC scheme provides much lower decoding complexity than the global IJD scheme with little degradation in the maximum sum rate, and outperforms the pure SIC scheme.

Finally, we also consider the multi-rate transmission in the multi-user systems but with the SIC decoding. The SIC decoding has lower decoding complexity, compared with IJD and HIC schemes. We give the optimal rate and power profile and provide the sum rate which also approach the Shannon limits.

Contents

List of Figures

List of Tables

Chapter 1

Introduction

This chapter introduces the fundament of channel coding and decoding for Gaussian multiple access channel (MAC). In multiple access communication systems, from practical consideration, it is required for users to employ the same encoder for supporting multi-rate transmission. We briefly introduce our basic idea for the multi-rate transmission, and give our contributions.

1.1 Gaussian Multiple Access Channel

There are numerous examples of multiple access communication, such as a set of mobile telephones communicating with a base station and many ground stations transmitting to a satellite. In this multiple access communication systems, multiple transmitters sends information to a single receiver simultaneously over a common communication channel. The receiver receives a superimposed signal of all the transmitters. This is often modeled as a multi-input single-output channel, referred to as a multiple access channel (MAC).

A K-user MAC model is depicted in Fig. 1.1. Let $X^{(k)} \in \{+1, -1\}$ denote the transmitted symbol of user k. Received symbol Y is a superposition of $X^{(k)}, k = 1, ..., K$, and noise Z. When Z is a Gaussian variable, with mean zero and variance σ^2, i.e., $Z \sim \mathcal{N}(0, \sigma^2)$, this channel is referred to as a Gaussian MAC.

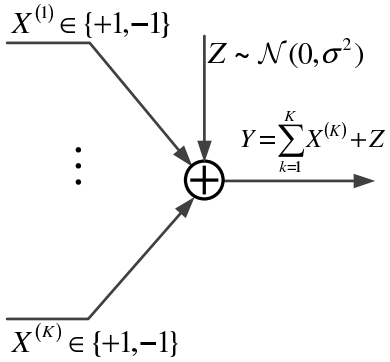

Figure 1.1: K-user Gaussian MAC.

1.2 Multi-Rate Coding Scheme

In multiple access communication systems, it is required to support multi-rate transmission to meet the requirements for various multimedia services such as voice, data, and video. For example, data message is transmitted at lower rates, and video message is transmitted at higher rates.

Multi-user information theory tells us that multi-rate transmission can provide the sum rate to approach the capacity of K-user Gaussian MAC [1, 2]. Unfortunately, a practical multi-rate coding scheme is not provided by the multi-user information theory. This leads communication researchers to design a practical multi-rate coding scheme for the Gaussian MAC, and optimize it to approach the Shannon limit.

A central problem in multi-rate coding scheme for the multiple access communication system is to assign a K-user multi-rate code so that they can communicate simultaneously, at various transmission rates, with a common receiver through the MAC, even in the presence of Gaussian noise.

We consider a multi-user multi-rate coding scheme, where the kth user employs a channel code C_k serially concatenated with a spreading sequence $\mathcal{S}_k$ and an interleaver pattern $\pi^{(k)},\ k = 1, \cdots, K$. Denote by $\{(C_1, \mathcal{S}_1, \pi^{(1)}), (C_2, \mathcal{S}_2, \pi^{(2)}), \cdots, (C_K, \mathcal{S}_K, \pi^{(K)})\}$ a K-user multi-rate code. The block diagram of K-user multi-rate coding scheme is depicted in Fig. 1.2. In this system, K independent users are attempting to transmit information to a single receiver. For the kth user, a length-B_k information bit vector of $\boldsymbol{u}^{(k)}$, is encoded by a rate-r_k channel encoder k into a length-B_k/r_k coded

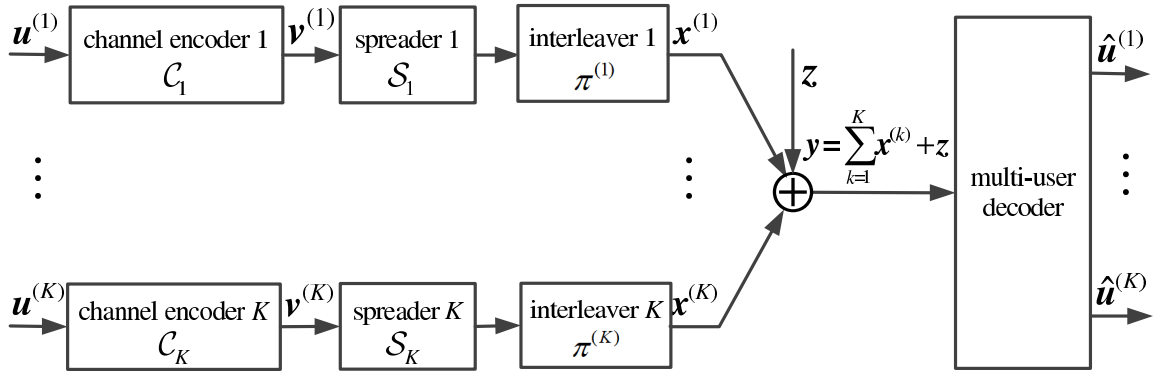

Figure 1.2: K-user multi-rate coding scheme.

vector $\boldsymbol{v}^{(k)}$. The employed channel code is an error correction code, such as a repeat accumulate (RA) code, a convolutional code, a low-density parity-check (LDPC) code, and so on. After that, a length-L_k spreading sequence $\mathcal{S}_k$ and a user-specific chip-level interleaver pattern $\pi^{(k)}$ are employed to produce a length-B_kL_k/r_k vector $\boldsymbol{x}^{(k)}$, which is transmitted to the Gaussian MAC. Here, the spreader is employed to lower the transmission rate and thus to combat the multi-user interference, and the different interleaver patterns are used for user separation. For transmission, we will favor $x_j^{(k)} \in \{+1, -1\}$ over $x_j^{(k)} \in \{0, 1\}$ under the mapping $\{0 \leftrightarrow +1, 1 \leftrightarrow -1\}$. The transmission rate of the kth user is $R_k = r_k/L_k$. And the different rate transmission is realized by adjusting the parameter r_k of the encoder and the length L_k of spreading sequence. Note that although the transmission rates of different users vary, it is not difficult to have identical signal length N by an adjustment of information bit lengths B_k, i.e., $B_kL_k/r_k \triangleq N$, to realize multi-rate transmission with rate profile $(R_1, \cdots, R_K)$. The overall transmission rate, i.e., the sum rate, is

$$R_{sum} = \sum_{k=1}^{K} R_k. \tag{1.1}$$

The symbol synchronization is assumed. The receiver gets a superimposed signal vector $\boldsymbol{y} = (y_1, \cdots, y_N)$ with

$$y_j = \sum_{k=1}^{K} x_j^{(k)} + z_j, \quad j = 1, \cdots, N, \tag{1.2}$$

where z_j is a zero-mean Gaussian variable with a variance of σ^2. Based on this received signal

vector, a multi-user decoding is performed to recover the transmitted information bit vectors and output estimations of $\hat{\boldsymbol{u}}^{(k)}, k = 1, ..., K$.

In Fig. 1.2, a channel code C_k, a spreading sequence $\mathcal{S}_k$, and an interleaver pattern $\pi^{(k)}$ are employed by the kth user. The problem of multi-rate coding becomes design of the K-user multi-rate code $\{(C_1, \mathcal{S}_1, \pi^{(1)}), (C_2, \mathcal{S}_2, \pi^{(2)}), \cdots, (C_K, \mathcal{S}_K, \pi^{(K)})\}$ to approach the Shannon limit. When each user employs a random interleaver, the problem becomes to design $\{(C_1, \mathcal{S}_1), (C_2, \mathcal{S}_2), \cdots, (C_K, \mathcal{S}_K)\}$ to achieve the maximum sum rate, and to approaches the Shannon limit. For convenience, we abbreviate K-user multi-rate code as $\{(C_1, \mathcal{S}_1), (C_2, \mathcal{S}_2), \cdots, (C_K, \mathcal{S}_K)\}$.

1.3 Previous Works

In the section, we review the previous related work on multi-user coding for MAC.

When each user transmit at an equal rate, the optimization of coding for MAC is reduced to optimize jointly the channel code C and spreading sequence $\mathcal{S}$, where $C_1 = \cdots = C_K \triangleq C$ and $\mathcal{S}_1 = \cdots = \mathcal{S}_K \triangleq \mathcal{S}$. Given C, the length of spreading sequence $\mathcal{S}$ is optimized by observing the extrinsic information transfer (EXIT) chart in [3–5]. However, this EXIT analysis is difficult to be extended to joint design of identical C and $\mathcal{S}$, since it is required to do a tremendous amount of observation on the EXIT charts for all various parameters of C and $\mathcal{S}$. Instead of EXIT analysis, the bivariate point analysis provides a good tool to jointly design C and $\mathcal{S}$, which approaches the Shannon limits in the equal rate of each user [6–8].

The first attempt to give a multi-rate coding schemes can be found in [9], where the multiple lengths of spreading sequence, i.e., $\mathcal{S}_1, \cdots, \mathcal{S}_K$, are optimized by a linear programming in an uncoded scenario. Since this work is restricted to no channel code and the all-ones spreading sequence, it decoding performance is about 5 dB away from the Shannon limit. The development of a multi-rate code $\{(C_1, \mathcal{S}_1), (C_2, \mathcal{S}_2), \cdots, (C_K, \mathcal{S}_K)\}$ is still a challenge work.

1.4 Our Contributions

We now briefly introduce our K-user multi-rate code $\{(C_1, \mathcal{S}_1), (C_2, \mathcal{S}_2), \cdots, (C_K, \mathcal{S}_K)\}$ for the Gaussian MAC.

In our multi-rate coding schemes (Fig. 1.2), the kth user employs a channel code C_k serially concatenated with a spreading sequence $\mathcal{S}_k$ and a user-specific interleave pattern $\pi^{(k)}$. Here, the same structure of encoder is employed for each user to implement various channel codes $C_k,\ k = 1, \cdots, K$. The spreading sequence $\mathcal{S}_k$ is employed to lower the transmission rate and thus to combat the multi-user interference. The different interleaver patterns are used for user separation. The different rate transmissions is realized by adjusting the parameter of the code C_k and the length of spreading sequence $\mathcal{S}_k,\ k = 1, \cdots, K$. We analyze the decoding performances of our coding schemes, and obtain the optimal coding parameters and spreading length, which gives the maximum sum rates and approach the theoretical limits of the channel. The proposed coding schemes support multimedia services, and avoid employing multiple channel encoders to implement the multi-rate transmission.

Our contributions in Chapters 3, 4, and 5 are illustrated as follows:

In Chapter 3, we introduce a multi-rate transmission in two-user multiple access communication systems with the MAP detection. Each user employs the same RA encoder but with different parameters, i.e., the repeat numbers, in the encoder. Here, we perform the coding-only (without spreading) scheme, since multi-user interference is small for two users. At the receiver, we perform a BP decoding on a single factor graph, where at sum (two-user superimposed signals) node, the MAP detection is carried out.

We develop a univariate fixed point analysis to obtain a system equation array of parameters of RA codes. This makes it possible to represent the parameters of RA codes explicitly as functions of the fixed point. We obtain a reliable region about repeat numbers of RA codes over which the decoding error rate is less than a given arbitrary small value. Then in the reliable region, we find the optimal parameters of RA codes that give the maximum sum rate. Numerical results show that our optimized two-user multi-rate RA code is superior to the conventional equal rate code in maximum sum rate, and approach the Shannon limit.

In Chapter 4, we introduce a multi-rate transmission in multi-user multiple access communication systems with the ESE detection. We equally divide K users into multiple groups, and users in identical group has a same transmission rate. For each user, we employ a RA code serially concatenated with a spreading sequence to implement various rates by adjusting both repeat number in RA encoder and length of spreading in spreader. Here, the interleaver patterns are different for user separation, and the spreading sequence is to lower the rate and thus to combat the user interference, since an increase in the number of users results in very serious multi-user interference. At the receiver, we perform a joint iterative BP decoding (Iterative Joint Decoding, IJD) on a single factor graph, where at sum (multi-user superimposed signals) node, the ESE is carried out.

We develop a bivariate fixed point analysis to explicitly represent repeat numbers q_m of RA code and spreading lengths L_m as a function of mutual information outputs, $m = 1, \cdots, M$. Based on these basic explicit representations, a united unreliable region is given, where users in at least one group are undecodable. The complementary set of the united unreliable region gives the optimal parameters (repeat numbers) of RA code and spreading lengths, corresponding to the optimal rate profile, that achieves the maximum sum rate. With the increment of groups, the maximum sum rates of our optimized multi-rate code increase, and approach the Shannon limit, and exceeds those of conventional equal-rate transmission.

Instead of global IJD above, in the receiver we perform hybrid interference cancellation (HIC) decoding, where SIC is employed between the groups, and IJD is employed within the group. The HIC scheme provides much lower decoding complexity than the global IJD scheme with little degradation in the maximum sum rate, and outperforms the pure SIC scheme.

In Chapter 5, we also consider the multi-rate transmission in the multi-user systems but with the SIC decoding. The SIC decoding has lower decoding complexity, compared with IJD and HIC schemes.

We propose a joint rate and power optimization (RPO) to obtain the optimal rate and power profile, that achieves the optimal sum rate by the assumption of equal-ratio power allocation. Our RPO employs multiple equal-ratio power, and choose the optimal ratio, which gives the power profile well matched with the rate profile. It shows that our optimized multi-rate code with joint

RPO, supporting the multi-rate transmission with the same structure of encoder, approaches the Shannon limit, and outperforms conventional rate-only optimization and power-only optimization.

Finally, conclusion of the dissertation is given in Chapter 6. We propose the multi-rate coding schemes for the Gaussian MAC, and analytically give the maximum sum rate which approach the theoretical limit of the channel. The proposed multi-rate coding schemes support multimedia services in practical communication systems.

Chapter 2

Preliminary: Repeat Accumulate (RA) Codes

In this chapter, we introduce coding and decoding of the repeat accumulate (RA) codes. RA codes are a class of the simplest forms of low density parity check (LDPC) codes that provide capacity-approaching performance over point-to-point Gaussian channel. Moreover, RA encoder can provide various rates by varying its coding parameter, i.e., the repeat number, and thus plays an important role in our multi-rate transmission.

2.1 Introduction

Repeat accumulate (RA) codes are a specific class of serially concatenated codes in which the outer code is a rate-$1/q$ repetition code and the inner code is a convolutional code with generator $1/(1+D)$. A $1/(1+D)$ convolutional code simply outputs the modulo-2 sum of the current input bit and the previous output bit, i.e. it provides a running sum of all past inputs and so is often called an accumulator. These two component codes give RA codes their name. Despite their simple structure, they were shown to provide good performance and, more importantly, they paved a path toward the design of efficiently encodable LDPC codes.

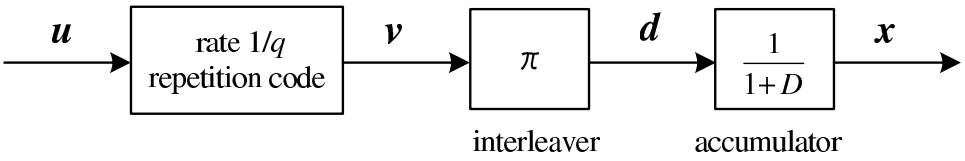

Figure 2.1: A repeat accumulate code.

2.2 Encoding and Decoding of RA Code

2.2.1 Encoding of RA Code

In the chapter, we introduce the encoding of RA code, as shown in Fig. 2.1.

The simple component codes of RA codes lead to a particularly straightforward encoding process. The message bits are copied q times, interleaved, then passed through a memory-1 convolutional encoder.

More precisely, the encoding process is as follows. The input is the K message bits $\boldsymbol{u} = (u_1, \cdots, u_K)$. The qK bits at the output of the repetition code are q copies of $\boldsymbol{u}$, in the form

$$\boldsymbol{v} = (v_1, v_2, \cdots, v_{qK}). \tag{2.1}$$

Here, $v_i = u_{f(i)}$, $f(i) = \lceil i/q \rceil$, where $\lceil x \rceil$ denotes the smallest integer greater than or equal to x.

The interleaver pattern $\pi = (\pi_1, \pi_2, \cdots, \pi_{qK})$ defines a permutation of the bits in $\boldsymbol{v}$ to

$$\boldsymbol{d} = (d_1, d_2, \cdots, d_{qK}) = (v_{\pi_1}, v_{\pi_2}, \cdots, v_{\pi_{qK}}). \tag{2.2}$$

Finally, the qK bits $\boldsymbol{x} = (x_1, x_2, \cdots, x_{qK})$ at the output of the accumulator are defined by

$$x_i = x_{i-1} \oplus d_i, \quad i = 1, 2, \cdots, qK. \tag{2.3}$$

The encoder for an accumulator can also be called a differential encoder.

Example 2.1 The message

$$\boldsymbol{u} = (1, 0, 0, 1) \tag{2.4}$$

is to be encoded using a length-10 RA code consisting of a $q = 3$ repetition code, and the interleaver $\pi = (1, 7, 4, 10, 2, 5, 8, 11, 3, 9, 6, 12)$.

Firstly, the message bits are each repeated three times to give

$$\boldsymbol{v} = (1, 1, 1, 0, 0, 0, 0, 0, 0, 1, 1, 1). \tag{2.5}$$

Secondly, $\boldsymbol{v}$ is interleaved to give

$$\boldsymbol{d} = (1, 0, 0, 1, 1, 0, 0, 1, 1, 0, 0, 1). \tag{2.6}$$

Lastly, the accumulator produces the running sum of $\boldsymbol{d}$ (from left to right),

$$\boldsymbol{x} = (1, 1, 1, 0, 1, 1, 1, 0, 1, 1, 1, 0). \tag{2.7}$$

2.2.2 Decoding of RA Code

In this chapter, we represent the RA code by a factor graph and introduce the BP decoding [10–13] of RA code on the factor graph.

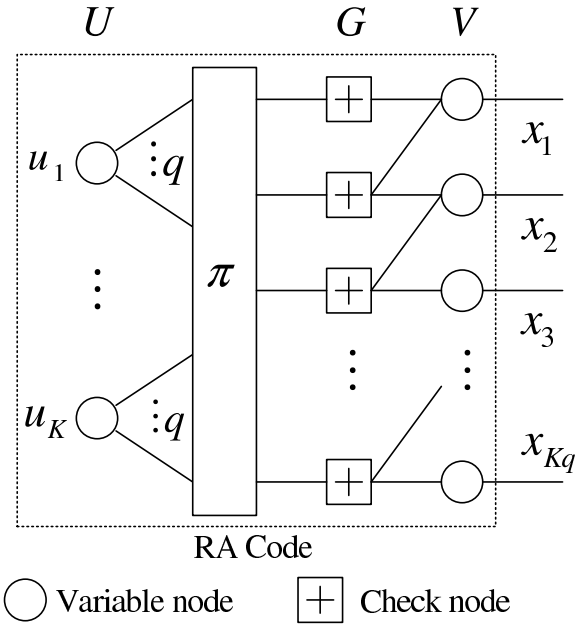

Figure 2.2: Factor graph representation of a repeat accumulate code.

Fig. 2.2 illustrates a factor graph of RA code. There are two kinds of nodes in the graph: variable and check nodes. Let U, G and V be three node sets that include the nodes below the

letters "U", "G" and "V" in Fig. 2.2, respectively. The variable node in U corresponds to an information bit. The check node in G denotes a constraint between the variable nodes connected to it, i.e., the mod-2 addition of the variable nodes connected to the same check node is 0. The variable node in V corresponds to an RA coded bit.

In BP decoding process, the decoder processes each variable node and each check node with a posteriori probability (APP) decoding. The iterative information exchange occurs between all of variable nodes and all of check nodes that are two types of component decoders. In precisely, the output extrinsic information of all variable (or check) nodes are input into their connected check (or variable) nodes as a priori information.

Now that we have asserted that, in the limit of infinite block length, factor graph of RA code is cycle-free, we can proceed with stating the message update rules for BP decoding. Before iterative update, we initialize each message passing from variable node j to check node i with $L_{ji}^{(0)} = L_j$. Here,

$$L_j = \log \frac{p(y_j|x_j = +1)}{p(y_j|x_j = -1)} \tag{2.8}$$

is the belief message of channel value at the variable node j, where x_j and y_j are transmitted bit and received value at the variable node j.

Consider the lth round iteration, $l = 1, 2, 3, ..., l_{\max}$, where $l_{\max}$ is the maximum iterative round. The local decoding at a variable node with g (Fig. 2.2, $g = q$ in U or $g = 3$ in V) connected edges is same as the decoding for a $[g, 1, g]$ repetition code [6,10,12,14–17] with code length g, information length 1, and minimum distance g. According to standard BP rules [11–13], the message passing from the variable node j to check node i in $V \to G$ is given by [18]

$$L_{ji}^{(l)} = L_j + \sum_{i'=1, i' \neq i}^{g-2} L_{i'j}^{(l)}, \tag{2.9}$$

where $L_{i'j}$ is the a priori information from check node i' to variable node j. The local decoding at the check node in G with g (Fig. 2.2, $g = 3$) connected edges is the same as the decoding for a $[g, g-1, 2]$ single-parity-check code [6, 10, 12, 14–17]. According to standard BP rules [11–13],

the message passing from check node i to variable node j in $G \to U$ is given by [18]

$$L_{ij}^{(l)} = 2\tanh^{-1}\left(\prod_{j'=1,j'\neq j}^{g}\tanh\left(\frac{L_{j'i}^{(l-1)}}{2}\right)\right), \tag{2.10}$$

where $L_{j'i}$ is the a priori information from variable node j' to check node i. Similarly, the message passing from the variable node j to check node i in $U \to G$ is given by [18]

$$L_{ji}^{(l)} = \sum_{i'=1,i'\neq i}^{g} L_{i'j}^{(l)}. \tag{2.11}$$

From check node i to variable node j in $G \to V$, the message passing is the same with Eq. (2.10).

When $l = l_{\max}$, the total belief message at each variable node in U is calculated by [18]

$$L_j^{\text{total}} = \sum_{i=1}^{g} L_{ij}^{(l_{\max})}. \tag{2.12}$$

From each L_j^{total}, $j = 0, 1, 2, ..., K-1$, the decision of each transmitted bit is obtained by

$$\hat{x}_j = \begin{cases} 0, & L_j^{\text{total}} > 0, \\ 1, & \text{else.} \end{cases}$$

2.3 Extrinsic Information Transfer (EXIT) Functions

The extrinsic information transfer (EXIT) chart technique is a graphical tool for estimating the decoding thresholds of RA codes via tracking the mutual information (MI) between transmitted random variable X and passed message L at each iteration. We suppose an infinite code length and an infinite number of decoding iterations. Moreover, assume that the a priori and the extrinsic passed messages are Gaussian variables (variance of each variable is twice of its mean).

2.3.1 Mutual Information (MI)

Recall that the mutual information,

$$I(X;Y) = H(X) - H(X \mid Y), \tag{2.13}$$

between two random variables X and Y gives the amount of uncertainty in X that is removed by knowing Y. In our case, $X \in +1, -1$ is a discrete-valued transmitted random variable and Y is a continuous received random variable, so the more successful the decoder the more uncertainty is removed by knowing Y.

The mutual information can be calculated as

$$I(X;Y) = \sum_{x\in\pm 1} \int p(x,y) \log_2 \frac{p(x,y)}{p(x)p(y)} \mathrm{d}y, \tag{2.14}$$

where $p(x,y)$ is the joint probability distribution of X and Y and $p(x)$ and $p(y)$ are the marginal probability distributions of X and Y, respectively. Using Bayes' rule,

$$I(X;Y) = \sum_{x\in\pm 1} \int p(y \mid x)p(x) \log_2 \frac{p(y \mid x)p(x)}{p(x) \sum_{x'\in\pm 1} p(y \mid x')p(x')} \mathrm{d}y, \tag{2.15}$$

and thus

$$I(X;Y) = \sum_{x\in\pm 1} \int p(y \mid x)p(x) \log_2 \frac{p(y \mid x)}{p(y \mid x=+1)p(x=+1) + p(y \mid x=-1)p(x=-1)} \mathrm{d}y, \tag{2.16}$$

In particular, for

$$y_i = \mu x_i + z_i \tag{2.17}$$

where z_i is Gaussian with mean zero and variance $\sigma^2 = 2\mu$, the conditional probability density function of $\boldsymbol{y}$ is

$$p(y_i \mid x_i = +1) = \frac{1}{\sqrt{2\pi\sigma^2}} \exp\left(-\frac{(y_i-\mu)^2}{2\sigma^2}\right), \tag{2.18}$$

$$p(y_i \mid x_i = -1) = \frac{1}{\sqrt{2\pi\sigma^2}} \exp\left(-\frac{(y_i+\mu)^2}{2\sigma^2}\right). \tag{2.19}$$

Substituting into (2.16), we obtain

$$I(X;Y) = \mathrm{J}(\sigma) \tag{2.20}$$

$$= 1 - \int \frac{1}{\sqrt{2\pi}\sigma} \exp\left(-\frac{(y-\sigma^2/2x)^2}{2\sigma^2}\right) \log_2(1+e^{-y}) \mathrm{d}y \tag{2.21}$$

The expression in (2.21) can be solved by integrating numerically, or it can be approximated. Here, we use the approximation from [19]:

$$\mathrm{J}(\sigma) \approx \begin{cases} a_{\mathrm{J},1}\sigma^3 + b_{\mathrm{J},1}\sigma^2 + c_{\mathrm{J},1}\sigma, & 0 \le \sigma \le 1.6363, \quad (2.22a) \\ 1 - \exp\left(a_{\mathrm{J},2}\sigma^3 + b_{\mathrm{J},2}\sigma^2 + c_{\mathrm{J},2}\sigma + d_{\mathrm{J},2}\right), & 1.6363 < \sigma < 10, \quad (2.22b) \\ 1, & \sigma \ge 10, \quad (2.22c) \end{cases}$$

where

$$a_{\mathrm{J},1} = -0.0421061,\ b_{\mathrm{J},1} = 0.2092520,\ c_{\mathrm{J},1} = -0.00640081,$$
$$a_{\mathrm{J},2} = 0.00181491,\ b_{\mathrm{J},2} = -0.142675,\ c_{\mathrm{J},2} = -0.08220540,$$
$$d_{\mathrm{J},2} = 0.05496080.$$

Here, $I(X;Y) = \mathrm{J}(\sigma)$, when $y_i = \mu x_i + z_i$ and z_i is sampled from a Gaussian random variable with mean zero and variance $\sigma^2 = 2\mu$. The inverse function

$$\sigma = \mathrm{J}^{-1}(I) \quad (2.23)$$

can be approximated by the function [19]:

$$\sigma = \mathrm{J}^{-1}(I) \approx \begin{cases} a_{\sigma,1}I^2 + b_{\sigma,1}I + c_{\sigma,1}\sqrt{I}, & 0 \le I \le 0.3646, \quad (2.24a) \\ -a_{\sigma,2}\log\left(b_{\sigma,2}(1-I)\right) - c_{\sigma,2}I, & 0.3646 < I < 1, \quad (2.24b) \end{cases}$$

where

$$a_{\sigma,1} = 1.095420,\ b_{\sigma,1} = 0.214217,\ c_{\sigma,1} = 2.33727,$$
$$a_{\sigma,2} = 0.706692,\ b_{\sigma,2} = 0.386013,\ c_{\sigma,2} = -1.75017.$$

2.3.2 MI Evolution for RA Codes

Now, substituting the conditional probability density function $p(y_j \mid x_j)$ into (2.8), we rewrite

$$L_j = \frac{2}{\sigma^2}(x_j + z_j) \quad (2.25)$$

with mean $\mu_L = 2/\sigma^2$ and variance $\sigma_L^2 = 4/\sigma^2$, when conditioned on $x_j = +1$. Thus, mean and variance of L are connected by

$$\sigma_L^2 = 2\mu_L. \quad (2.26)$$

Consider the lth round iteration, for a variable node with degree $g = 3$ in V of Fig. 2.2. Under the Gaussian Approximation, all messages passing from variable node to check node in $V \rightarrow G$, denoted $L_{v,g}$, follow a Gaussian distribution with mean $\mu_{v,g} = \mu_L + (g-2)\mu_{g,v}$ and variance $\sigma^2_{v,g} = 2\mu_{v,g} = \sigma^2_L + (g-2)\sigma^2_{g,v}$. The extrinsic MI $I^{(l)}_{v,g}$ of the variable node from V to G becomes at the lth iteration [12, 14, 17]

$$I^{(l)}_{v,g}\left(I^{(l-1)}_{g,v}, \sigma\right) = \mathrm{J}\left(\sqrt{\sigma^2_L + (g-2)\sigma^2_{g,v}}\right), \tag{2.27}$$

$$= \mathrm{J}\left(\sqrt{\frac{4}{\sigma^2} + \left(\mathrm{J}^{-1}\left(I^{(l-1)}_{g,v}\right)\right)^2}\right) \tag{2.28}$$

where $I^{(l-1)}_{g,v}$ is the a priori MI from check node to variable node in $G \rightarrow V$ at the $l-1$th iteration. Here, we initialize $I^{(0)}_{g,v} = 0$.

Subsequently, consider a check node with degree $g = 3$ in G of Fig. 2.2. Based on the duality relationship, which has been proven to be accurate for the binary-input AWGN channel [20, 21], the extrinsic MI for a degree-g check node (i.e., rate-$(g-1)/g$ single parity check (SPC) code) and that of a degree-g variable node (i.e., rate-$1/g$ repetition (REP) code) are related as

$$I_{\mathrm{E,SPC}}(g, I_{\mathrm{A,SPC}}) = 1 - I_{\mathrm{E,REP}}(g, 1 - I_{\mathrm{A,SPC}}). \tag{2.29}$$

We have the extrinsic MI $I^{(l)}_{g,u}$ of the check node from G to U at the lth iteration

$$I^{(l)}_{g,u}\left(I^{(l)}_{v,g} \times (g-1)\right) = 1 - \mathrm{J}\left(\sqrt{(g-1)\left(\mathrm{J}^{-1}\left(1 - I^{(l)}_{v,g}\right)\right)^2}\right) \tag{2.30}$$

$$= 1 - \mathrm{J}\left(\sqrt{2\left(\mathrm{J}^{-1}\left(1 - I^{(l)}_{v,g}\right)\right)^2}\right) \tag{2.31}$$

where $I^{(l)}_{v,g}$ is the a priori MI from variable node to check node in $V \rightarrow G$ at the lth iteration.

Similarly, for a variable node with degree $g = q$ in U, we get the extrinsic MI $I^{(l)}_{u,g}$ from U to G at the lth iteration

$$I^{(l)}_{u,g}\left(I^{(l)}_{g,u} \times (g-1)\right) = \mathrm{J}\left(\sqrt{(q-1)\left(\mathrm{J}^{-1}\left(I^{(l)}_{g,u}\right)\right)^2}\right). \tag{2.32}$$

For a check node with degree $g = 3$ in G, the extrinsic MI $I^{(l)}_{g,v}$ from G to V at the lth iteration is

$$I^{(l)}_{g,v}\left(I^{(l)}_{u,g}, I^{(l)}_{v,g}\right) = 1 - \mathrm{J}\left(\left(\mathrm{J}^{-1}\left(1 - I^{(l)}_{u,g}\right)\right)^2 + \left(\mathrm{J}^{-1}\left(1 - I^{(l)}_{v,g}\right)\right)^2\right). \tag{2.33}$$

When $l = l_{max}$, the final extrinsic MI $I_u^{(l_{max})}$ of variable node in U is

$$I_u^{(l_{max})}\left(I_{g,u}^{(l_{max})} \times g\right) = \mathrm{J}\left(\sqrt{q\left(\mathrm{J}^{-1}\left(I_{g,u}^{(l_{max})}\right)\right)^2}\right). \tag{2.34}$$

By updating (2.27)-(2.33), we can determine RA code emsembles' BP threshold

$$\sigma^{\mathrm{BP}} \triangleq \sup\{\sigma \in (0, +\infty) : I_u^{(I_{max})} \xrightarrow{I_{max}\to\infty} 1\}. \tag{2.35}$$

Chapter 3

Rate Optimization in Two-User Communications

In this chapter, we introduce a multi-rate transmission in two-user multiple access communication systems. Each user employs the same RA encoder but with different parameters, i.e., the repeat numbers, in the encoder. At the receiver, we perform a belief propagation (BP) decoding on a single factor graph, where at sum (two-user superimposed signals) node, the maximum a priori (MAP) detection is carried out. We develop a univariate fixed point analysis to obtain a system equation array of parameters of RA codes. This makes it possible to represent the parameters of RA codes explicitly as functions of the fixed point. We find the optimal parameters of RA codes, corresponding to the optimal pair-of-rates, that give the maximum sum rate. Numerical results show that our optimized two-user multi-rate RA code is superior to the conventional equal rate code in maximum sum rate, and approach the Shannon limit.

3.1 Introduction

In recent years, there are numerous examples of multiple-access communication, where each transmitter sends information to a single receiver simultaneously over a common communication channel. The receiver receive a superposed signal of all the transmitters. This is often called a

multiple access channel (MAC). An important model in the MAC is a Gaussian multiple access channel (GMAC), where the receiver receives a Gaussian noisy version of the superposition.

A number of works that focus on maximizing the sum rate of the GMAC were studied. Rimoldi *et al*. considered the rate splitting [22], relying on "single-user coding" and "successive cancellation". Ahlswede *et al*. studied the random coding and optimal joint decoding [23, 24]. Unfortunately, these theoretical results don't directly translate to practical systems maximizing the sum rate. This leads communication researchers to design practical multi-user code for the Gaussian MAC.

Declercq *et al*. considered a suboptimal but practical approach [25, 26]. Linear programming is used to optimize a two-user low density parity check (LDPC) code by maximizing the sum rate with iterative decoding. However, each LDPC code was restricted to have the same distribution of degree. That is, the code rate of each user was allocated to be equal. It is known that in some practical communication systems, different code rate is required by different user.

Yang *et al*. developed an unequal rate coding scheme employing iterative decoding [9], where a modified linear programming method is used to optimize the rate of code for each user. It is shown that with different rate for each user, the convergence of iterative decoding is facilitated since low rate user converge earlier than high rate user. However, due to the simple repetition code employed by each user, the performance is about 5 dB away from the Shannon limit. It is desirable to optimize the rate of code by employing a more sophisticated code for each user.

In this chapter, we consider a two-user unequal rate repeat accumulate (RA) code for a G-MAC with binary inputs, equal-power and symbol synchronization. In this system, we employ a rate-$1/q_k$ regular RA code for user k ($k = 1, 2$) with the sum rate of $1/q_1 + 1/q_2$. For two independent information bit sequences with different lengths, the corresponding adjustable repeat numbers q_k ($k = 1, 2$) of RA codes guarantee the same code length and thus realize unequal rate allocation. At the receiver, two-user message-passing decoding is performed on a single factor graph. To jointly design the two-user unequal rate RA code for the GMAC, we develop a fixed point analysis based on message-passing decoding. Thus, we obtain a system equation array of q_1 and q_2. This permits us to represent q_1 and q_2 explicitly as functions of the fixed point, respectively.

For a given channel noise level with unitary-power signal transmission, we obtain a reliable region of (q_1, q_2) over which the decoding error rate is less than a given arbitrary small value ϵ. Then in the reliable region, we find the optimal repeat numbers q_1^* and q_2^* that give the maximum sum rate of $1/q_1^* + 1/q_2^*$.

3.2 System Model

In this chapter, we describe the system model with a two-user unequal rate RA code for a MAC. The block diagram of the system is depicted in Fig. 3.1.

3.2.1 Coding Scheme

In this two-user Gaussian MAC, we consider pair $(1/q_1, 1/q_2)$ of unequal rates, where q_1 and q_2 are positive integers. Two independent information bit vectors $\boldsymbol{u}^{(1)}$ and $\boldsymbol{u}^{(2)}$, being sent to a single receiver. The length-K_k information bit sequence $\boldsymbol{u}^{(k)} = (u_1^{(k)}, u_2^{(k)}, \ldots, u_{K_k}^{(k)})$, $u_i^{(k)} \in \{0, 1\}$, $1 \le i \le K_k$, $k = 1, 2$, of user k enters a regular RA encoder, which is a serial concatenation of a rate-$1/q_k$ repeater with a $1/(1+D)$ accumulator linked by the different interleaver π_k [27]. The sum rate is $R_{sum} = 1/q_1 + 1/q_2$. Note that although the rates of the RA codes for different users are not the same, it is not difficult to have the same code length N via a adjustment of information bit lengths K_1 and K_2, i.e., $K_1 q_1 = K_2 q_2 \triangleq N$. The output coded vector is denoted as $\boldsymbol{x}^{(k)} = (x_1^{(k)}, x_2^{(k)}, \ldots, x_N^{(k)})$, $x_t^{(k)} \in \{0, 1\}$, $1 \le t \le N$. For transmission, we will favor $x_t^{(k)} \in \{+1, -1\}$ over $x_t^{(k)} \in \{0, 1\}$ under the mapping $\{0 \leftrightarrow +1, 1 \leftrightarrow -1\}$.

After that, $\boldsymbol{x}^{(1)}$ and $\boldsymbol{x}^{(2)}$ are transmitted to the Gaussian MAC. We assume that the average power of transmitted symbols is unitary, and the codewords and transmitted symbols for each user are synchronized.

The receiver receives a superimposed signal sequence $\boldsymbol{y} = (y_1, y_2, \ldots, y_N)$ with

$$y_t = x_t^{(1)} + x_t^{(2)} + z_t, \ t = 1, 2, \ldots, N \tag{3.1}$$

where z_t is a zero mean AWGN with variance σ^2. Two-user decoding is performed to recover

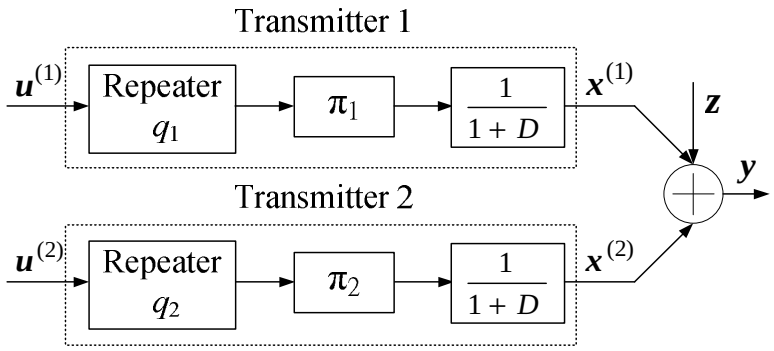

Figure 3.1: System model

information bit vectors $\boldsymbol{u}^{(k)}$, $k = 1, 2$.

3.2.2 Maximum A Posteriori Decoding

In order to jointly decode information bit vectors of the two users, we consider a factor graph representation [11] for regular RA codes and superposition of the MAC. Figure 3.2 illustrates the factor graph of two-user regular RA code and superposition of the MAC. The dotted box parts are the factor graph of the rate-$1/q_1$ and rate-$1/q_2$ regular RA codes [17], respectively. And the remaining part corresponds to the superposition of the Gaussian MAC. There are three kinds of nodes in the graph: variable, check, and sum nodes. Let U, G, V, and Y be four node sets that include the nodes below letters "U", "G", "V" and "Y" in Fig. 3.2, respectively. The variable node in U corresponds to an information bit. The check node in G denotes a constraint between the variable nodes connected to it, i.e., the mod-2 addition of the variable nodes connected to the same check node is 0. The variable node in V corresponds to an RA coded bit. The sum node in Y, associated with received symbol y_t in (4.1), denotes a superposition constraint between y_t and the two variable nodes from two users. Note that the sum node connects the dotted box parts of factor graph.

The iterative message-passing decoding is performed on the factor graph of the system and is accomplished by efficient local decoding at all nodes and interactions. A decoding iteration of the system starts from the local decoding at the sum nodes in Y. Based on the received superimposed

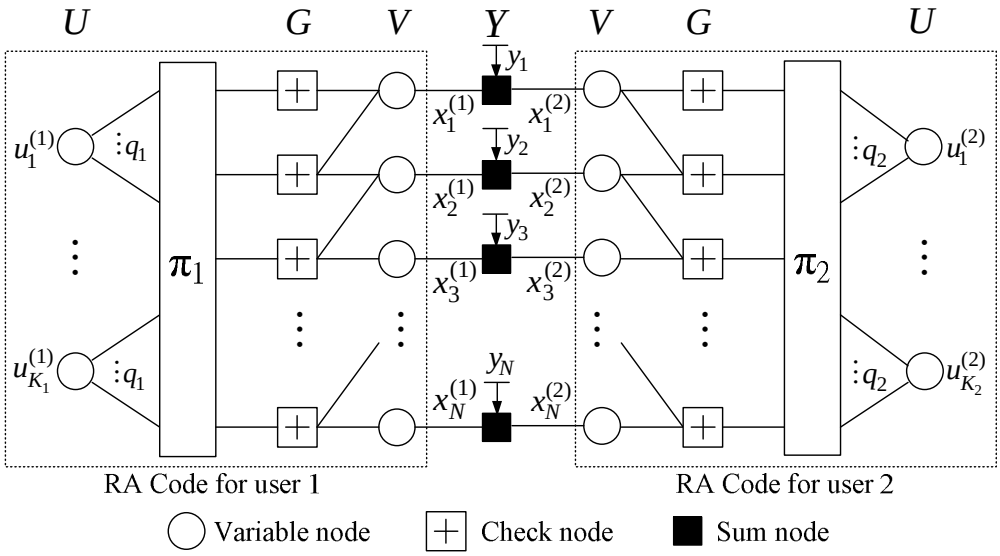

Figure 3.2: Factor graph representation of regular RA codes and superposition of two-user Gaussian MAC

signal and the input from the other user (obtained from the previous iteration), a sum node in Y performs a local decoding and outputs an estimation for the transmitted symbol of user j. This local decoding is maximum a posteriori probability (MAP) decoding, which minimize the probability of information-bit error. Based on this estimation, user j performs a single-user decoding on its own factor graph (see the dotted parts in Fig. 3.2). The decoding subsequently includes the local decodings at the nodes in $V \rightarrow G \rightarrow U \rightarrow G \rightarrow V$. The local decoding at the dashed box part is belief propagation (BP) decoding [11–13], in which the processing of variable node and check node is a standardized node processing [28] in the graph-based decoding.

Based on the one output from the sum nodes in Y and the two outputs (obtained from the previous iteration) from the check nodes in G, a variable node in V performs a local decoding, similar to the decoding for a repetition code [6, 10, 12, 14–17], and outputs an extrinsic message to each of its adjacent nodes in G. Based on the two outputs from the variable nodes in V, a check node in G performs a local decoding, similar to the decoding for a single-parity-check code [6, 10, 12, 14–17], and outputs an extrinsic message from the check nodes in G, a variable node in U performs a local decoding and outputs an extrinsic message to each of its adjacent nodes in

G. A similar process will be performed on nodes in G and V again to produce the final extrinsic message output to the sum nodes in Y as a prior message for the next iteration of the other user. After a large number of iterations, hard decisions can be made at the outputs of variable nodes in U to recover transmitted vectors $\boldsymbol{u}^{(1)}$ and $\boldsymbol{u}^{(2)}$.

3.3 Extrinsic Information Transfer (EXIT) Functions

Before proceeding, we formulate an extrinsic mutual information transfer (EXIT) function for the local decoding at each node in Fig. 3.2. We also give monotone properties of EXIT functions.

In our formulation, input and output messages of a decoding are represented by log-likelihood ratios (LLRs). We suppose an infinite code length and an infinite number of decoding iterations. Moreover, assume that the input and output LLRs are Gaussian variables (variance of each variable is twice of its mean). We give the EXIT function, which describes the relation between their mutual information forms (i.e., mutual information between the out LLR by the node and its associated message bit) [12, 14–17].

3.3.1 Variable Nodes

Before formulating the EXIT function, function J($*$) is defined as [10, 12, 14, 15, 17].

$$\mathrm{J}(\sigma_A) = 1 - \int_{-\infty}^{+\infty} \frac{e^{-((x-\sigma_A^2/2)^2/(2\sigma_A^2))}}{\sqrt{2\pi}\sigma_A} \log(1+e^{-x})dx. \tag{3.2}$$

The local decoding at a variable node with d (Fig. 3.2, $d = q_1$ in U for user 1 or $d = q_2$ in U for user 2 or $d = 3$ in V) connected edges is same as the decoding for a $[d, 1, d]$ repetition code with code length d, information length 1, and minimum distance d. The update rule for the LLR output at the jth edge is

$$L_{E,j} = \sum_{i=1, i\neq j}^{d} L_{A,i}, \tag{3.3}$$

where $L_{A,i}$ is the input LLR from check node i to variable node j. EXIT function T_v, which describes the mutual information (MI) output of the variable node, becomes [12, 14, 17]

$$\mathrm{T}_v(I_{A,1}, \cdots, I_{A,d-1}) = \mathrm{J}\left(\sqrt{\sum_{i=1}^{d-1}\left[\mathrm{J}^{-1}(I_{A,i})\right]^2}\right), \tag{3.4}$$

where $0 \le I_{A,i} \le 1$ is the input MI from check node i to variable node j and $\mathrm{J}^{-1}(*)$ is the inverse function of $\mathrm{J}(*)$. For simplicity, if e input MIs are the same, i.e., $I_{A,i} = I_A, i = 1, \ldots, e$, we represent this EXIT function as $\mathrm{T}_v(I_A \times e, I_{A,e+1}, \ldots, I_{A,d-1})$.

3.3.2 Check Nodes

The local decoding at the check node in G with d (Fig. 3.2, $d = 3$) connected edges is the same as the decoding for a $[d, d-1, 2]$ single-parity-check code. The updata rule at the jth edge is

$$L_{E,j} = 2\tanh^{-1}\left(\prod_{i=1, i\neq j}^{d}\tanh\left(\frac{L_{A,i}}{2}\right)\right), \tag{3.5}$$

where $L_{A,i}$ is the input LLR from variable node i to check node j. EXIT function T_c, i.e., the MI output of the check node, is [12, 14, 17]

$$\mathrm{T}_c(I_{A,1}, \cdots, I_{A,d-1}) = 1 - \mathrm{T}_v(1 - I_{A,1}, \cdots, 1 - I_{A,d-1}), \tag{3.6}$$

where $0 \le I_{A,i} \le 1$ is the input MI from variable node i to check node j. Similarly, for $I_{A,i} = I_A, i = 1, \ldots, e$, we represent this EXIT function as $\mathrm{T}_c(I_A \times e, I_{A,e+1}, \ldots, I_{A,d-1})$.

3.3.3 Sum Nodes

During message-passing decoding, MAP decoding at a sum node in Y estimates the transmitted symbol of each user by using a input LLR about the transmitted symbols of the other user.

Let $L_A^{(k)}, k = 1, 2$, denote a input LLR about $x_t^{(k)}$ in (4.1). By MAP decoding, the LLR output of $x_t^{(k)}$ is estimated as [26]

$$L_E^{(k)} = \log\frac{e^{(2y_t-2)/\sigma^2}e^{L_A^{(3-k)}} + 1}{e^{L_A^{(3-k)}} + e^{(-2y_t-2)/\sigma^2}}. \tag{3.7}$$

Transmitted symbols $x_t^{(k)}$, $k = 1, 2$, are independent of each other and uniformly distributed on set $\{+1, -1\}$. Moreover, input LLRs $L_A^{(k)}, k = 1, 2$, are independent of each other. Since there is a relationship between the mutual information and the LLR mean, we first obtain the expectation of the LLR output $\mathrm{E}[x_t^{(k)} L_E^{(k)}]$ with random variables $x_t^{(k)}$ and $L_A^{(k)}$, and get EXIT function T_s

$$\mathrm{T}_s(I_A, \sigma) = \mathrm{J}\left(\sqrt{2\mathrm{E}[x_t^{(k)} L_E^{(k)}]}\right) \tag{3.8}$$

of MAP decoding at a sum node, where we have used $I = \mathrm{J}(\sqrt{2m})$ to transform LLR mean m to mutual information form I.

3.4 Code Optimization

In this chapter, we give the maximum sum rate of two-user unequal rate RA code by fixed point analysis. In this theory, we obtain a system equation array of repeat numbers q_1 and q_2. This permits us to represent q_1 and q_2 as functions of fixed point, respectively. For a given channel noise level with unitary-power signal transmission, we get a reliable region of (q_1, q_2) over which the decoding error rate is less than a given arbitrary small value ϵ. Then in the reliable region, we find the optimal repeat numbers q_1^* and q_2^* that give the maximum sum rate of $1/q_1^* + 1/q_2^*$.

3.4.1 Fixed Point Theory

Now we consider the statistical output of each node during the iterative decoding. To see the flow of MI more explicitly, in Fig. 3.3 we give a protograph representation of the regular RA code and superposition for user 1. The protograph can be regarded as a simplification of the original factor graph in Fig. 3.2. Since the distribution of node degree in the original factor graph is preserved in the protograph, from the view point of MI flow, the protograph is equivalent to the original factor graph. Due to a regular RA code for each user, Fig. 3.3 is a case of regular protograph, and the MI outputs on the same side of the same node set are the same. Similar to the EXIT functions described in Chapter 3.3, the message output is measured by the MI.

At the l-th decoding iteration, $l = 0, 1, 2, \ldots$, each node in the protograph outputs an extrinsic

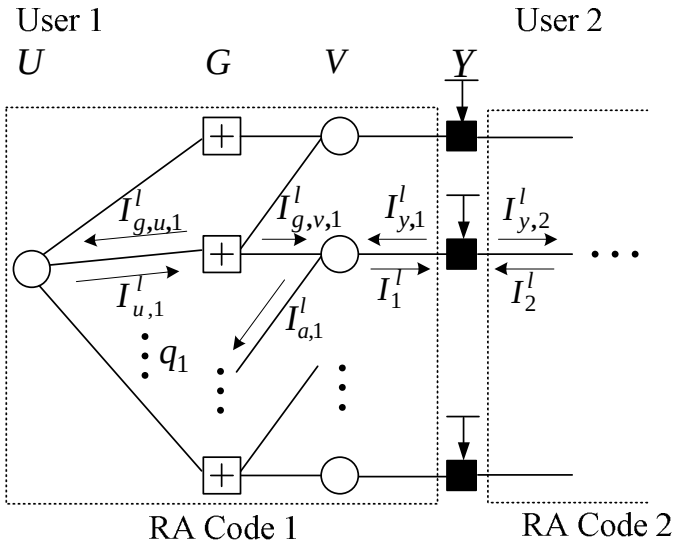

Figure 3.3: Protograph representation of regular RA code and superposition for user 1

message on each edge connected to it. Based on the message-passing decoding of the system, the MI output $I^l_{y,1}$ on the left side of a sum node in Y can be represented as a function of I^{l-1}_2

$$I^l_{y,1} = \mathrm{T}_s(I^{l-1}_2, \sigma). \tag{3.9}$$

When message-passing decoding from variable node V to check node G, the MI output $I^l_{a,1}$ on the left side of a variable node in V is

$$\begin{aligned} I^l_{a,1} &= \mathrm{T}_v(I^l_{y,1}, I^{l-1}_{g,v,1}) \\ &= \mathrm{T}_v\left(\mathrm{T}_s(I^{l-1}_2, \sigma), \mathrm{J}\left(\frac{1}{\sqrt{2}}\mathrm{J}^{-1}(I^{l-1}_1)\right)\right) \end{aligned} \tag{3.10}$$

where the last equality holds for $I^{l-1}_1 = \mathrm{T}_v(I^{l-1}_{g,v,1} \times 2)$ (see (4.2)). Subsequently, from check node G to variable node U, the MI output $I^l_{g,u,1}$ on the left side of a check node in G is written as following

$$I^l_{g,u,1} = \mathrm{T}_c(I^l_{a,1} \times 2). \tag{3.11}$$

Afterwards, accoding to the decoding order $U \rightarrow G$, we get the MI output $I^l_{u,1}$ on the right side of a variable node in U can be represented as function of $I^l_{a,1}$ and q_1

$$\begin{aligned} I^l_{u,1} &= \mathrm{T}_v(I^l_{g,u,1} \times (q_1 - 1)) \\ &= \mathrm{T}_v\left(\mathrm{T}_c(I^l_{a,1} \times 2) \times (q_1 - 1)\right). \end{aligned} \tag{3.12}$$

In a similar way, about $G \rightarrow V$, the MI output $I^l_{g,v,1}$ on the right side of a check node in G is obtained by

$$\begin{aligned} I^l_{g,v,1} &= \mathrm{T}_c(I^l_{u,1}, I^l_{a,1}) \\ &= \mathrm{T}_c\left(\mathrm{T}_v\left(\mathrm{T}_c(I^l_{a,1} \times 2) \times (q_1 - 1)\right), I^l_{a,1}\right) \end{aligned} \tag{3.13}$$

Finally, focusing on the MI output I^l_1 from variable node V to sum node Y, we have the following equation

$$I^l_1 = \mathrm{T}_v(I^l_{g,v,1} \times 2). \tag{3.14}$$

Substituting (3.13) into (3.14) and using (3.10), we have

$$I^l_1 = f(I^{l-1}_1, I^{l-1}_2, q_1, \sigma) \tag{3.15}$$

where

$$\begin{aligned} &f\left(I^{l-1}_1, I^{l-1}_2, q_1, \sigma\right) \\ &= \mathrm{T}_v\left(\mathrm{T}_c\left(\mathrm{T}_v\left(\mathrm{T}_c\left(\mathrm{T}_v\left(\mathrm{T}_s(I^{l-1}_2, \sigma), \mathrm{J}\left(\frac{1}{\sqrt{2}}\mathrm{J}^{-1}(I^{l-1}_1)\right)\right)\times 2\right)\times(q_1-1)\right), \mathrm{T}_v\left(\mathrm{T}_s(I^{l-1}_2, \sigma), \mathrm{J}\left(\frac{1}{\sqrt{2}}\mathrm{J}^{-1}(I^{l-1}_1)\right)\right)\right) \\ &\quad \times 2\Bigg). \end{aligned} \tag{3.16}$$

Similarly, for user 2, we get equation

$$\begin{aligned} I^l_2 &= \mathrm{T}_v(I^l_{g,v,2} \times 2) \\ &= f(I^{l-1}_2, I^{l-1}_1, q_2, \sigma). \end{aligned} \tag{3.17}$$

We know that with $l \rightarrow \infty$, the MI output of each edge converges to a constant [15]. For a given channel noise level and a pair $(1/q_1, 1/q_2)$ of rates, it holds that

$$\lim_{l\rightarrow\infty}(I^l_1, I^l_2) = (I_1, I_2) \tag{3.18}$$

where (I_1, I_2) is the minimum element [6] in solution set $\mathcal{I}$ of the equation array

$$\begin{cases} I_1 = f(I_1, I_2, q_1, \sigma) \\ I_2 = f(I_2, I_1, q_2, \sigma). \end{cases} \tag{3.19}$$

The equation array of (3.19) is referred to as a system equation array. Each solution $(I_1, I_2) \in \mathcal{I}$ of the system equation array is referred to as a fixed point. The minimum fixed point (I_1, I_2) is the convergence point of the decoding as the iteration approaches infinity.

Remark 3.1 The fixed point theory can be explained from the viewpoint of an EXIT chart [15]. The protograph in Fig. 3.3 corresponds to an RA code 1, and the omitted graph corresponds to an RA code 2. If we plot the EXIT charts of the RA decoder 1 and 2 in a two-dimensional plane, a fixed point, in fact, is an intersection of these two EXIT curves. There may be more than one intersection for these two EXIT curves, and the minimum intersection nearest the origin corresponds to the convergence point of the iterative decoding. □

It is well known that as the decoding iteration approaches infinity, each output I on an edge in a protograph, the corresponding error rate is [16]

$$\mathrm{P}_e(I) = \frac{1}{2}\mathrm{erfc}\left(\frac{\mathrm{J}^{-1}(I)}{2\sqrt{2}}\right) \tag{3.20}$$

where $\mathrm{erfc}(x) = \frac{2}{\sqrt{\pi}}\int_x^\infty e^{-t^2}dt$ is a complementary error function. In Fig. 3.3, for the MI outputs I_1 and I_2, the corresponding error rates are $\mathrm{P}_e(I_1)$ and $\mathrm{P}_e(I_2)$, respectively. By the property of complementary error function, if pair (I_1, I_2) of MI outputs satisfies that

$$(I_1, I_2) = (1, 1) \tag{3.21}$$

decoding error rates $\mathrm{P}_e(I_1)$ and $\mathrm{P}_e(I_2)$ of the RA coded bits are approach 0, respectively. Let the average decoding error rate of the RA coded bits be

$$\mathrm{P}_e = \frac{1}{2}\mathrm{P}_e(I_1) + \frac{1}{2}\mathrm{P}_e(I_2). \tag{3.22}$$

If the condition (3.21) is satisfied, P_e is less than a given arbitrary small value ϵ for sufficiently large N, i.e.,

$$\mathrm{P}_e < \epsilon \quad \text{as} \quad N \to \infty. \tag{3.23}$$

When P_e approaches 0, the average decoding error rate of the information bits approaches 0 (see Remark 3.2). This means that the decoding of two-user unequal rate RA code with pair $(1/q_1, 1/q_2)$ of rates is error-free.

Remark 3.2 In general, the average decoding error rate of a system is the average decoding error rate of information bits. In our system, it is given by

$$\mathrm{P}_e^u = \frac{K_1}{K_1+K_2}\mathrm{P}_e(I_{u,1}) + \frac{K_2}{K_1+K_2}\mathrm{P}_e(I_{u,2}) \tag{3.24}$$

where $I_{u,j} = \lim_{l\to\infty} I_{u,j}^l$ and $\mathrm{P}_e(I_{u,j})$ is decoding error rate of information bits of user j ($j = 1, 2$). In [6], it is shown that $\mathrm{P}_e(I_{u,j})$ approaches 0 if and only if $\mathrm{P}_e(I_j)$ approaches 0. Therefore, when P_e of (3.22) approaches 0, P_e^u of (3.24) approaches 0. □

3.4.2 Explicit Representations of q_1 and q_2

In this chapter, by solving the system equation array (3.19), we explicitly represent repeat numbers q_1 and q_2 of two-user RA code as functions of the fixed point, respectively.

As stated in Sect. 3.4.1, the decoding of two-user unequal rate unequal rate RA code is error-free if and only if $(I_1, I_2) = (1, 1)$. In general, repeat numbers q_1 and q_2 with which two-user unequal rate RA code is decodable can be obtained by substituting $I_1 = I_2 = 1$ into the functions of the fixed point, respectively. Unfortunately, for pair $(I_1, I_2) = (1, 1)$, we can't obtain the values of q_1 and q_2 directly with which two-user unequal rate RA code is decodable due to $\mathrm{J}^{-1}(I_1 = I_2 = 1) = \infty$ contained in function f of (3.19). A possible way is to obtain all values q_1 and q_2 with which two-user unequal rate RA code is undecodable firstly, namely an unreliable region (q_1, q_2). Then we obtain the reliable region (q_1, q_2) over which two-user unequal rate RA code is decodable via complementary set of unreliable region.

For two-user unequal rate RA code is undecodable, we consider three cases. Firstly, both RA code 1 and 2 are undecodable. Secondly, RA code 1 is undecodable even though RA code 2 is decodable. Thirdly, RA code 2 is undecodable even though RA code 1 is undecodable. This can be represented in Table 3.1.

Case 1: Now, we consider the case of the pair $(I_1, I_2) \in \mathcal{I}_{1,2}$. We consider system equation array (3.19) again. Using the definition of EXIT functions (4.2), (4.3) and (3.8), we solve q_1 and

Table 3.1: Undecodable and decodable

Case	Code $1/I_1$	Code $2/I_2$	$\mathcal{I} = \mathcal{I}_{1,2} \cup \mathcal{I}_1 \cup \mathcal{I}_2 \cup \mathcal{I}_0$
1	undecodable/$[0,1)$	undecodable/$[0,1)$	$\mathcal{I}_{1,2} = \{(I_1, I_2) \mid I_1, I_2 \in [0,1)\}$
2	undecodable/$[0,1)$	decodable/1	$\mathcal{I}_1 = \{(I_1, I_2) \mid I_1 \in [0,1), I_2 = 1\}$
3	decodable/1	undecodable/$[0,1)$	$\mathcal{I}_2 = \{(I_1, I_2) \mid I_1 = 1, I_2 \in [0,1)\}$
4	decodable/1	decodable/1	$\mathcal{I}_0 = \{(I_1, I_2) \mid I_1 = I_2 = 1\}$

q_2 in (3.19) explicitly

$$\begin{cases} q_1 = \dfrac{\left[\mathrm{J}^{-1}\left(1-\mathrm{J}\left(\sqrt{\left[\mathrm{J}^{-1}\left(1-\mathrm{J}\left(\frac{\mathrm{J}^{-1}(I_1)}{\sqrt{2}}\right)\right)\right]^2-\left[\mathrm{J}^{-1}(1-I_{a,1})\right]^2}\right)\right)\right]^2}{\left[\mathrm{J}^{-1}\left(1-\mathrm{J}\left(\sqrt{2\left[\mathrm{J}^{-1}(1-I_{a,1})\right]^2}\right)\right)\right]^2}+1 \\ q_2 = \dfrac{\left[\mathrm{J}^{-1}\left(1-\mathrm{J}\left(\sqrt{\left[\mathrm{J}^{-1}\left(1-\mathrm{J}\left(\frac{\mathrm{J}^{-1}(I_2)}{\sqrt{2}}\right)\right)\right]^2-\left[\mathrm{J}^{-1}(1-I_{a,2})\right]^2}\right)\right)\right]^2}{\left[\mathrm{J}^{-1}\left(1-\mathrm{J}\left(\sqrt{2\left[\mathrm{J}^{-1}(1-I_{a,2})\right]^2}\right)\right)\right]^2}+1 \\ \qquad\qquad (I_1, I_2) \in \mathcal{I}_{1,2} \end{cases} \tag{3.25}$$

where

$$\begin{cases} I_{a,1} = \mathrm{J}\left(\sqrt{\left[\mathrm{J}^{-1}\left(\mathrm{T}_s(I_2,\sigma)\right)\right]^2+\left[\mathrm{J}^{-1}(I_1)\right]^2/2}\right) \\ I_{a,2} = \mathrm{J}\left(\sqrt{\left[\mathrm{J}^{-1}\left(\mathrm{T}_s(I_1,\sigma)\right)\right]^2+\left[\mathrm{J}^{-1}(I_2)\right]^2/2}\right). \end{cases}$$

To facilitate discussion, we assume temporarily that repeat numbers q_1 and q_2 in (3.25) are real.

Given a pair of $(I_1, I_2) \in \mathcal{I}_{1,2}$, we can obtain an unique pair of $(q_1, q_2) = (q_1(I_1, I_2), q_2(I_1, I_2))$. Therefore, we can get all possible value of q_1 and q_2 for the range $\mathcal{I}_{1,2}$ of (I_1, I_2). The corresponding unreliable region is $\Lambda_{1,2} \triangleq \{(q_1(I_1, I_2), q_2(I_1, I_2)) \mid (I_1, I_2) \in \mathcal{I}_{1,2}\}$.

Case 2: Subsequently, we consider the case of the pair $(I_1, I_2) \in \mathcal{I}_1$. Fortunately, the first equation of equation array (3.25) is still hold on due to not contain $\mathrm{J}^{-1}(I_2 = 1) = \infty$. Therefore,

we can obtain all possible value of q_1 of RA code 1 for the range $\mathcal{I}_1$ of (I_1, I_2). Since RA code 2 is decodable ($I_2 = 1$), we don't have to get the value of q_2. The corresponding unreliable region is $\Lambda_1 \triangleq \{q_1(I_1, I_2) \mid (I_1, I_2) \in \mathcal{I}_1\}$.

In fact, it can be viewed as the single-user case. Obviously, we just need to get the value of q_1.

Case 3: For the pair $(I_1, I_2) \in \mathcal{I}_2$, in a similar way, we can also get all possible value of q_2 of RA code 2 for the range $\mathcal{I}_2$ of (I_1, I_2) and the corresponding unreliable region $\Lambda_2 \triangleq \{q_2(I_1, I_2) \mid (I_1, I_2) \in \mathcal{I}_2\}$.

3.4.3 Reliable Region and Maximum Sum Rate

In this chapter, we give the reliable region and the maximum sum rate of two-user unequal rate RA code where the average decoding error rate approaches zero.

Based on the expressions of $q_1(I_1, I_2)$ and $q_2(I_1, I_2)$ derived above, we get an union unreliable region

$$\Lambda = \Lambda_1 \cup \Lambda_2 \cup \Lambda_{1,2}. \tag{3.26}$$

Complementary region $\overline{\Lambda}$ of Λ

$$\overline{\Lambda} = \overline{\Lambda}_1 \cap \overline{\Lambda}_2 \cap \overline{\Lambda}_{1,2} \tag{3.27}$$

corresponds to the reliable region of (q_1, q_2) with decoding error rate $\mathrm{P}_e \to 0$.

Each integer pair of $(q_1, q_2) \in (\overline{\Lambda} \cap \mathbb{Z}^2)$ guarantees that a sum rate of $1/q_1 + 1/q_2$ is achievable in the sense of decoding error rate less than ϵ, where $\mathbb{Z}^2$ is the set of all integer pairs. Then we find the optimal q_1^* and q_2^* over the reliable region that give the maximum sum rate of two-user unequal rate RA system in the following theorem:

Theorem 3.1 Given a channel noise level σ, the optimal q_1^* and q_2^* are

$$(q_1^*, q_2^*) = \arg \max_{(q_1^*, q_2^*) \in (\overline{\Lambda} \cap \mathbb{Z}^2)} (1/q_1 + 1/q_2)$$

which give maximum sum rate $R_{sum}^{max} = 1/q_1^* + 1/q_2^*$. □

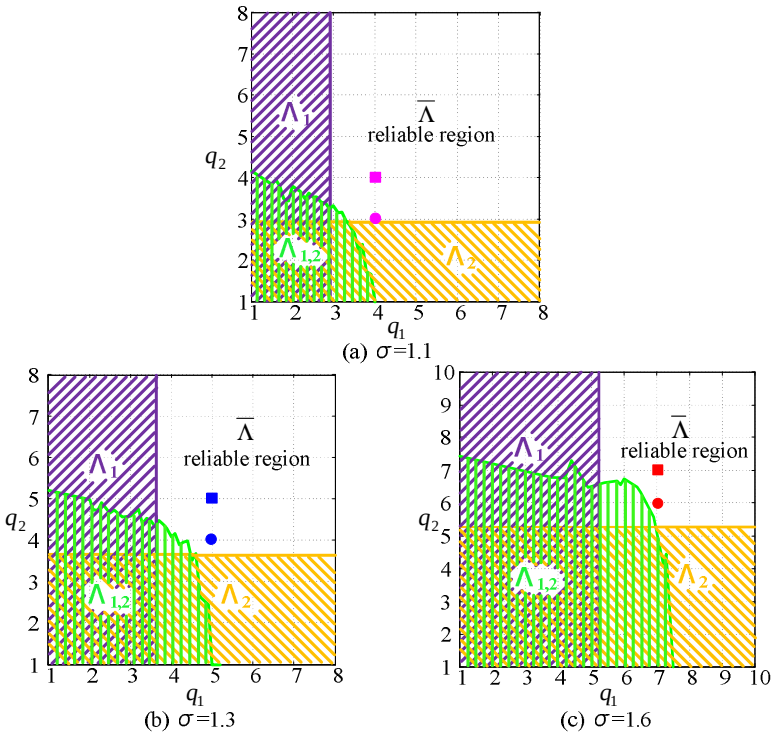

Figure 3.4: Reliable and unreliable regions for the two-user case

From the above analysis, it is clear that for a given channel noise level σ, we obtain the pair $(1/q_1^*, 1/q_2^*)$ of rates in the sense that the average decoding error rate approaches 0. The threshold of message-passing decoding is then

$$\text{EbN0}_{\text{th}} = 10 \cdot \log_{10} \frac{1}{(\sigma)^2 \cdot (1/q_1^* + 1/q_2^*)} \text{ [dB]}. \tag{3.28}$$

3.5 Numerical Results

In this chapter, we present some numerical results of fixed point analysis.

For an arbitrary channel noise level, e.g., $\sigma = 1.1$, we first consider the case of the pair $(I_1, I_2) \in \mathcal{I}_1$ and $\mathcal{I}_2$, then get two unreliable regions $\Lambda_1 = \{1 \le q_1 \le 2.9\}$ and $\Lambda_2 = \{1 \le q_2 \le 2.9\}$. Then consider the case of the pair $(I_1, I_2) \in \mathcal{I}_{1,2}$, we also obtain an unreliable region $\Lambda_{1,2}$ by (3.25). Subsequently, we get the unreliable region Λ by (3.26). The reliable region is also obtained in Fig. 3.4 (a). Obviously, the optimal point in the reliable region is $(q_1^*, q_2^*) = (4, 3)$, which gives the

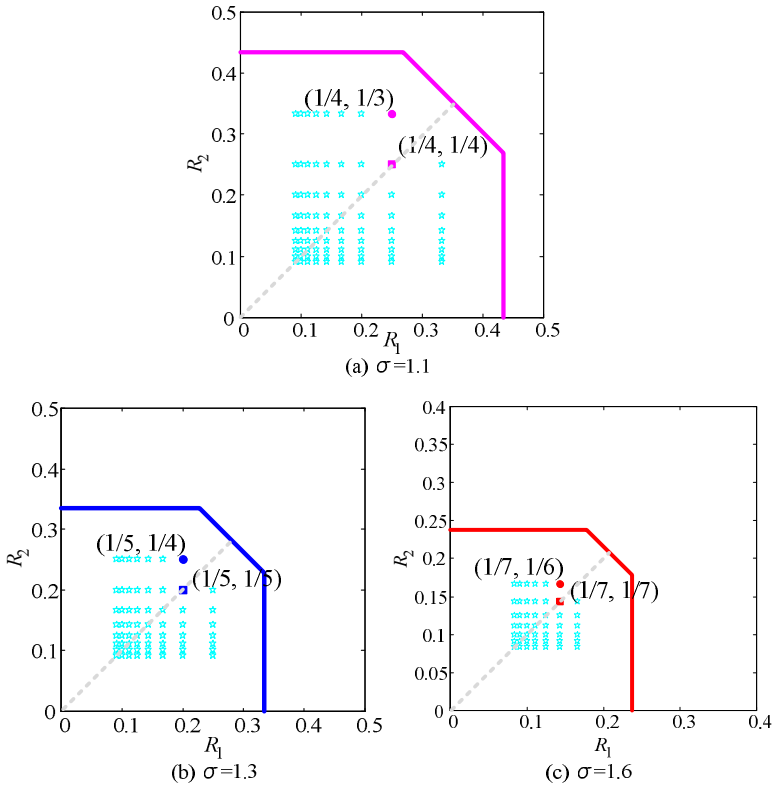

Figure 3.5: Maximum achievable pair of (equal or unequal) rates in the capacity region of two-user Gaussian multiple access channel

sum rate of $R_{sum}^{max} = 7/12$ bit/symbol. Also, we see that point (4,4) is in the reliable region, but gives a slightly smaller sum rate of 1/2. It means that the two-user unequal rate RA code can achieve larger sum rates than two-user equal rate RA code.

Similarly, for $\sigma = 1.3$ (Fig. 3.4 (b)), we get the reliable region $\overline{\Lambda}$ of (q_1, q_2) over which the average decoding error rate approaches 0. The optimal point $(q_1^*, q_2^*) = (5, 4)$ gives the maximum sum rate of 9/20 bit/symbol. For $\sigma = 1.6$, the reliable region $\overline{\Lambda}$ is shown in Fig. 3.4 (c). The optimal point $(q_1^*, q_2^*) = (7, 6)$ gives the maximum sum rate of 13/42 bit/symbol.

We also give the maximum achievable pair of rates obtained by EXIT charts in the capacity region [1, 29] of two-user GMAC. For $\sigma = 1.1$, among pairs of rates over the capacity region (see Fig. 3.5 (a)), we find the optimal pair of unequal rates which has the maximum sum rate is $(1/q_1^*, 1/q_2^*) = (1/4, 1/3)$. Similarly, for $\sigma = 1.3$ and 1.6, $(1/q_1^*, 1/q_2^*) = (1/5, 1/4)$ and (1/7, 1/6),

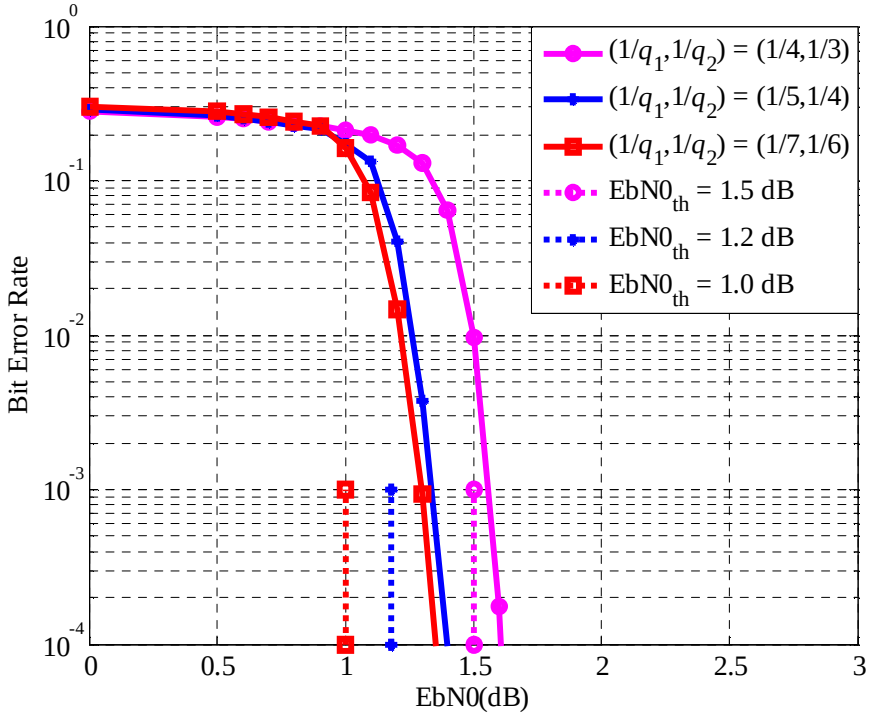

Figure 3.6: BER performance of two-user unequal rate RA code

respectively. All these optimal pairs of unequal rates obtained by EXIT charts in Fig. 3.5 coincide with our fixed point analysis.

The optimal point (q_1^*, q_2^*) of reliable region by fixed point analysis is based on assumptions of infinite code length and infinite iterations. For finite code length $N = 42000$ and finite iterations $l = 100$, the bit error rate (BER) curves of $(1/q_1^*, 1/q_2^*) = (1/4, 1/3), (1/5, 1/4)$ and $(1/7, 1/6)$ are given by Monte Carlo simulations, respectively (see Fig. 3.6). The corresponding thresholds of (3.28) are also plotted in Fig. 3.6. It is shown that the receiver can decode successfully and two-user unequal rate RA codes converge to their thresholds very well within a gap less than 0.4 dB at error rate 10^{-4}. This verifies that fixed point analysis is accurate in the joint design of two-user unequal rate RA code.

3.6 Conclusions

For a multiple access channel, we proposed a two-user unequal rate RA code with binary inputs, equal-power and symbol synchronization. In this scheme, a regular RA code whose rate can be changed freely is employed for each user. Two-user message-passing decoding is performed on a single factor graph. Based on message-passing decoding, we developed a fixed point analysis to explicitly obtain a system equation array of q_1 and q_2. This permits us to represent q_1 and q_2 explicitly as functions of fixed point, respectively. For a given channel noise level with unitary-power signal transmission, we obtained a reliable region of (q_1, q_2) in which the error rate of detected information bits approaches zero. Then in the reliable region, we found the optimal repeat numbers q_1^* and q_2^* which achieves the maximum sum rate $R_{sum}^{max} = 1/q_1^* + 1/q_2^*$. Monte Carlo simulations verified that fixed point analysis is accurate in the jointly design of the two-user unequal rate RA code.

Works [30] and [31] addressed spatial coupled LDPC code over MAC. Numerical results show that spatial coupled LDPC code has a noticeable performance over two-user MAC. Our two-user unequal rate RA code can be considered as a base code before spatial coupling, and the decoding threshold of our code can also be improved by spatial coupling method.

Chapter 4

Rate Optimization in Multi-User Communications

In this chapter, we introduce a multi-rate transmission in multi-user multiple access communication systems. We equally divide K users into M groups, and users in identical group has a same transmission rate. For each user, we employ a RA code serially concatenated with a spreading to implement various rates by adjusting both repeat number in RA encoder and length of spreading in spreader. Here the spreading is to lower the rate and thus to combat the user interference, since an increase in the number of users results in very serious multi-user interference. At the receiver, we perform a joint iterative BP decoding (Iterative Joint Decoding, IJD) on a single factor graph, where at sum (multi-user superimposed signals) node, the elementary signal estimation (ESE) is carried out. We develop a bivariate fixed point analysis to explicitly represent repeat numbers q_m of RA code and spreading lengths L_m as a function of mutual information outputs, $m = 1, \cdots, M$. Based on these basic explicit representations, a united unreliable region is given, where users in at least one group are undecodable. The complementary set of the united unreliable region gives the optimal parameters (repeat numbers) of RA code and spreading lengths, corresponding to the optimal rate profile, that achieves the maximum sum rate. With the increment of groups, the maximum sum rates of our optimized multi-rate code increase, and approach the Shannon limit, and exceeds those of conventional equal-rate transmission.

Instead of global IJD above, in the receiver we perform hybrid interference cancellation (HIC) decoding, where successive interference cancellation (SIC) is employed between the groups, and IJD is employed within the group. The HIC scheme provides much lower decoding complexity than the global IJD scheme with little degradation in the maximum sum rate, and outperforms the pure SIC scheme.

4.1 Introduction

For a K-user multiple access channel (MAC) [3, 4, 6, 32–34], a serial concatenation of error correction code (ECC) C_k and length-L_k spreading $\mathcal{S}_k$ for each user k, $1 \leq k \leq K$, is shown to be an effective coding scheme. In this scheme, ECC mainly overcomes the channel noise, and the spreading mainly overcomes the multi-user interference. K-user coding-spreading schemes based on this idea are coded code-division multiple-access (CDMA) [32–34] and coded interleave-division multiple-access (IDMA) [3,4,6], where the challenge is optimizing the ECC and spreading profile $\{(C_1, \mathcal{S}_1), \cdots, (C_K, \mathcal{S}_K)\}$ that approaches the Shannon limit of MAC.

The IDMA scheme can provide an even larger load-carrying capability than the CDMA scheme [35, 36], since the conventional CDMA scheme is regarded as a special case of the IDMA scheme [37]. For a K-user IDMA system, in general, the same ECC and spreading, i.e., $C_1 = \cdots = C_K \triangleq C$, $\mathcal{S}_1 = \cdots = \mathcal{S}_K \triangleq \mathcal{S}$, are employed by each user, and user-specific interleavers, π_k, $1 \leq k \leq K$, are followed for user separation. This is equal rate transmission. In principle, to approach the Shannon limit, ECC and spreading should be jointly designed, for instance, by extrinsic information transfer (EXIT) analysis. By employing identical C and $\mathcal{S}$ for K users, the K mutual information (MI) outputs of the decoder-despreader are the same. The decoding error is judged by observing the EXIT charts of the multi-user detector and the decoder-despreader. However, a tremendous amount of observation on the EXIT charts for various parameters of C and $\mathcal{S}$ prevents us from doing the joint design. In practice, the previous works [3,4] optimized the spreading length for a given ECC. Zhang *et al*. considered a convolutional coded IDMA [3], where the optimal spreading length is obtained by observing the EXIT chart for a given convolutional code. They gave some examples

of EXIT charts when repetition code and repeat-accumulate (RA) code were employed [4]. Also, an optimal non-binary spreading length for a given non-binary low-density parity-check code was given [5]. Joint design of ECC and spreading can be found in our previous work [6], where we focused on jointly optimizing regular RA code and the spreading length by bivariate fixed-point analysis, which is based on the MI transfer function. Related to the serial concatenating scheme of ECC and spreading stated above, recently the parallel concatenating scheme of ECC and spreading can be found in [7, 8]. However, these works [3–8] only addressed equal rate transmission.

In practice, multi-rate transmission [38,39] is required in wireless communications, which support various multimedia services such as voice, data, and video. For example, in the IDMA system, K users are separated into M groups of transmission rates $R_1, \cdots, R_M$, where the data users transmit at lower rates, and the video users transmit at higher rates. From the viewpoint of information theory, for such systems with equal-power distribution, the Shannon limit can be achieved as long as M is sufficiently large [2]. It is required to give a practical multi-rate coding-spreading scheme and optimize it to approach the Shannon limit. Similar to EXIT analysis, we can track M different MI outputs, each of which represents the same MI outputs of K/M users within the mth group. However, this optimization's complexity is prohibitive. To the best of our knowledge, relatively few works have focused on the joint optimization of practical coding-spreading for multi-rate transmission. Previous work [9] optimized the spreading length profile $(L_1, \cdots, L_M)$ in uncoded IDMA systems by a linear programming method. This approach is restricted to no ECC and the all-ones spreading sequence and may be not extended to coded systems. The bit error rate (BER) performance is about 5 dB away from the Shannon limit.

In this chapter, we propose a multi-rate coding-spreading scheme for the Gaussian MAC with binary inputs, equal-power, and symbol synchronization. In this multi-rate transmission, we equally divide K users into M groups. For each user in the mth group, we employ code rate-$1/q_m$ regular RA code $\mathcal{C}_m$ serially concatenated with length-L_m spreading $\mathcal{S}_m$, where repeat number q_m and spreading length L_m can be changed ($1 \le m \le M$). The transmission rate of each user in the mth group is $R_m^{(1)} = R_m^{(2)} = \cdots = R_m^{(K/M)} \triangleq R_m = 1/(q_m L_m)$. For convenience, $\{(\mathcal{C}_1, \mathcal{S}_1), \cdots, (\mathcal{C}_M, \mathcal{S}_M)\}$ is called a K-user multi-rate code, which includes spreading. One key advantage of employing RA

codes is that the encoder structure is simple and the encoding complexity is linear with the code length [17]. Moreover, the RA codes are a class of the simplest forms of turbo codes that provide capacity-approaching performance [40]. For M independent information bit sequences with different lengths, the corresponding adjustable q_m and L_m guarantee the same length of transmitted vectors and realize multi-rate transmission. At the receiver, iterative joint decoding (IJD) and hybrid interference cancellation (HIC) schemes are performed on a single factor graph with a belief propagation (BP) decoder.

For the design of our K-user multi-rate code, we applied bivariate fixed-point analysis [6] to our multi-rate transmission and obtained a system equation array of M different MI outputs $I_1, \cdots, I_M$, which has M pairs-of-equations. By solving the mth pair-of-equations, we represent (q_m, L_m) explicitly as a function of $I_1, \cdots, I_M$, only when $0 \leq I_m < 1$ and $0 \leq I_{m'} \leq 1$ $(m' \neq m)$. This implies that we only obtain all the possible values of (q_m, L_m) over which users in the mth group are undecodable due to $I_m \neq 1$. Based on these basic explicit representations, from T corresponding simultaneous pairs-of-equations, we obtain a combined region of $((q_1, L_1), \cdots, (q_M, L_M))$ over which the users in any T groups are undecodable $(1 \leq T \leq M)$. Then, we have a united (unreliable) region over which users in at least one group are undecodable. The reliable region, i.e., the complementary set of the united unreliable region, gives the optimal repeat number and the spreading length profile $((q_1^*, L_1^*), \cdots, (q_M^*, L_M^*))$ that corresponds to optimal rate profile $(R_1^*, \cdots, R_M^*)$, which achieves the maximum sum rate.

The remainder of this chapter is organized as follows. Section 4.2 briefly describes the system model. The design of the K-user multi-rate code is given in Section 4.3. Numerical results are shown in Section 4.4, and Section 4.5 draws our conclusion.

4.2 System Model

In this chapter, we describe our K-user multi-rate code and two decoding schemes for the Gaussian MAC.

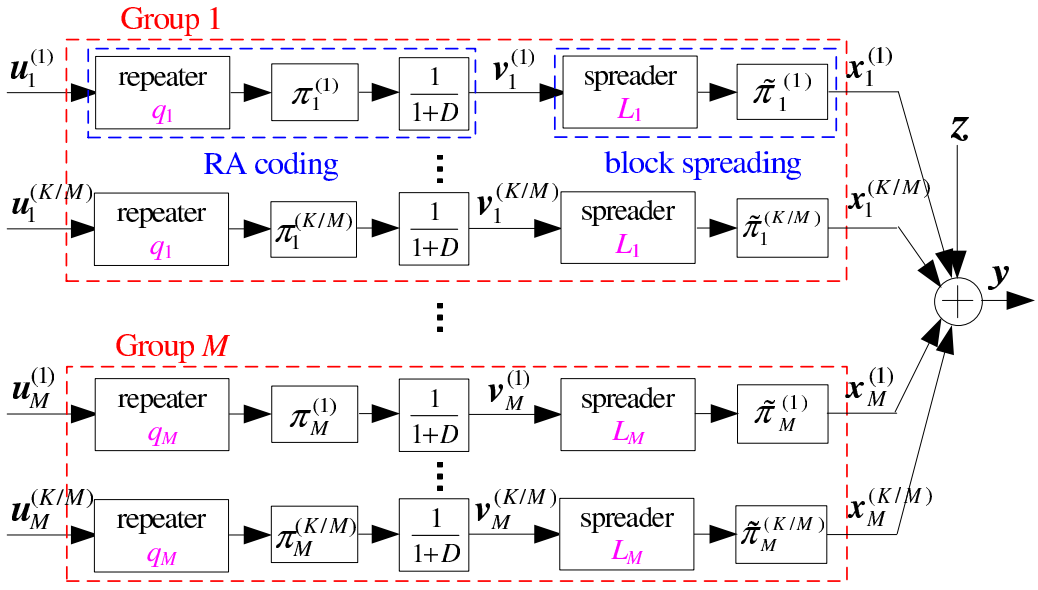

Figure 4.1: System model

4.2.1 Coding Scheme

In this chapter, we give our K-user multi-rate code for the Gaussian MAC. A block diagram of a multi-user multi-rate transmission system is depicted in Fig. 4.1.

In our scheme, we equally divide K users into M groups. The mth group contains K/M users with identical transmission rates $R_m^{(1)} = R_m^{(2)} = \cdots = R_m^{(K/M)} \triangleq R_m$ $(1 \le m \le M)$. Length-K_m information bit vector $\boldsymbol{u}_m^{(k)} = (u_{m,1}^{(k)}, u_{m,2}^{(k)}, \cdots, u_{m,K_m}^{(k)}), u_{m,i}^{(k)} \in \{0,1\}, 1 \le i \le K_m$, of the kth $(1 \le k \le K/M)$ user in the mth group, is first encoded by a regular RA code $\mathcal{C}_m$, which is a serial concatenation of a code rate-$1/q_m$ repeater with a $1/(1+D)$ accumulator linked by interleaver $\pi_m^{(k)}$ [41]. The output coded vector is denoted as $\boldsymbol{v}_m^{(k)} = (v_{m,1}^{(k)}, v_{m,2}^{(k)}, \cdots, v_{m,K_m q_m}^{(k)}), v_{m,j}^{(k)} \in \{0,1\}, 1 \le j \le K_m q_m$. A block spreading $\mathcal{S}_m$, which consists of bit spreading and chip-level interleaving, is then performed on $\boldsymbol{v}_m^{(k)}$. Each bit of $\boldsymbol{v}_m^{(k)}$ is spread by length-L_m sequence $\boldsymbol{s}_m^{(k)}$ into vector $(1 - 2v_{m,j}^{(k)})\boldsymbol{s}_m^{(k)}$. Here, $\boldsymbol{s}_m^{(k)} = (s_1^{(k)}, s_2^{(k)}, \cdots, s_{L_m}^{(k)})$ with $s_{2l-1}^{(k)} = +1, s_{2l}^{(k)} = -1, 1 \le l \le \lfloor \frac{L_m+1}{2} \rfloor$, where $\lfloor p \rfloor$ is the greatest integer less than or equal to p [37]. The spreader output is a length-$K_m q_m L_m$ sequence, which is referred to as a chip sequence. After spreading, user-specific chip-level interleaver $\tilde{\pi}_m^{(k)}$ with

length-$K_m q_m L_m$ is employed to produce transmitted signal vector $\boldsymbol{x}_m^{(k)} = (x_{m,1}^{(k)}, x_{m,2}^{(k)}, \cdots, x_{m,K_m q_m L_m}^{(k)})$, which is transmitted to the Gaussian MAC. Here, transmitted signal vector $\boldsymbol{x}_m^{(k)}$ is referred to as a codeword of the kth user in the mth group. The transmission rate of each user in the mth group is $R_m = 1/(q_m L_m)$. Denote by $\{(\mathcal{C}_1, \mathcal{S}_1), \cdots, (\mathcal{C}_M, \mathcal{S}_M)\}$ a K-user multi-rate code, which includes spreading. Note that although the transmission rates of different groups vary, it is not difficult to have identical length N by an adjustment of information bit lengths K_m, i.e., $K_m q_m L_m \triangleq N$, to realize multi-rate transmission with rate profile $(R_1, R_2, \cdots, R_M)$. The overall transmission rate, i.e., the sum rate, is given as

$$R_{sum} = \frac{K}{M} \sum_{m=1}^{M} R_m = \frac{K}{M} \sum_{m=1}^{M} \frac{1}{q_m L_m}.$$

The symbols and codeword synchronization are assumed.

Our K-user multi-rate coding scheme can also be described by a factor graph. Since the factor graph can be obtained by a "copy-and-permute" operation from a protograph [18], it is equivalent for us to describe the coding scheme using it. Moreover, since each user's protograph in the mth group is the same, $1 \leq m \leq M$, we only give the protograph of the kth user in the mth group associated with the Gaussian MAC in Fig. 4.2. The graph has three kinds of nodes: variable nodes in U and V, which correspond to the information bits and the RA coded bits, check nodes in G, which correspond to a constrain where the mod-2 addition of the variable nodes connected to it is 0, and sum nodes in Y, which correspond to the received signals. The dashed box part is a protograph of the rate-$1/q_m$ regular RA code, which represents information bits that are repeated q_m times in $U \to G$ and passed through an accumulator in $G \to V$. The remaining part in $V \to Y$ corresponds to block spreading by length-L_m. At the sum node in Y, the K users' signals are superimposed, among which the K/M users' signals are from the mth group (left side of the sum node) and the $\frac{K}{M}(M-1)$ users' signals are from the remaining $M-1$ groups (right side of the sum node). Each of the K edges in the sum node is connected to its corresponding user's protograph. In Fig. 4.2, only the protograph of the kth user in the mth group is shown.

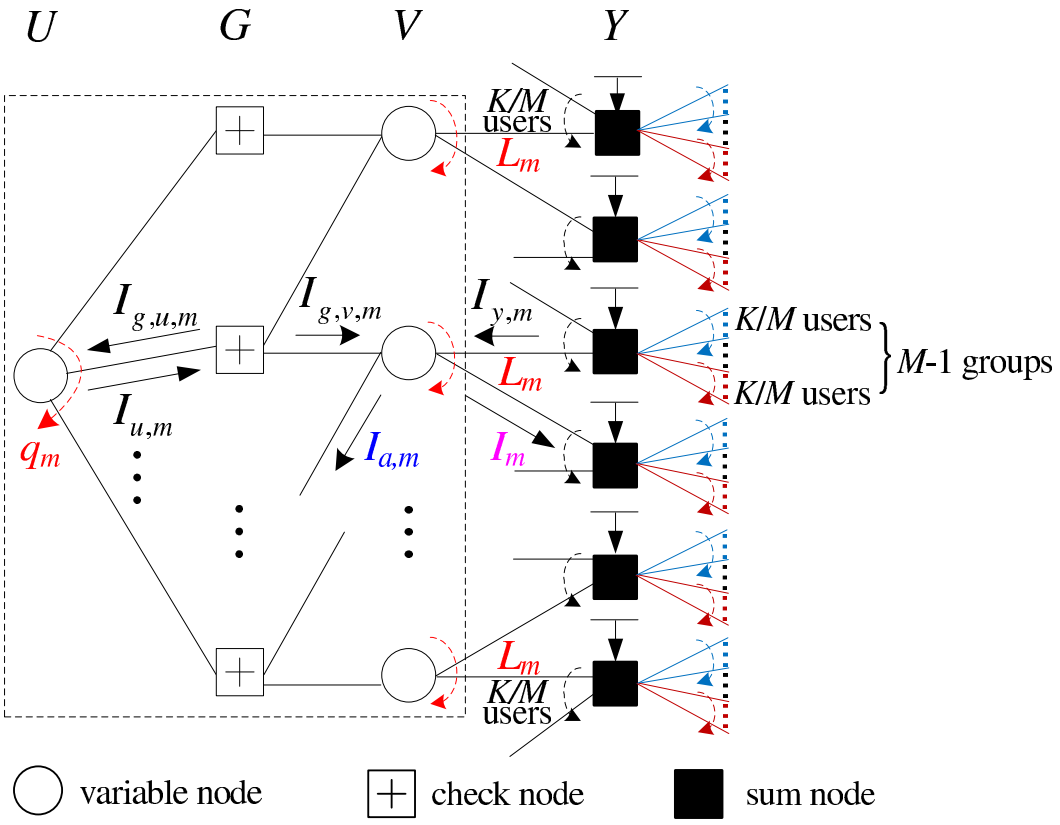

Figure 4.2: Protograph representation of regular RA code and block spreading associated with Gaussian MAC for kth user in mth group ($1 \le k \le K/M, 1 \le m \le M$)

4.2.2 Decoding Scheme

In this section, we briefly give IJD and HIC schemes for our multi-rate transmission. Our decoding schemes are performed on a factor graph. For convenience, we describe them on the protograph (Fig. 4.2).

The receiver gets a superimposed signal vector $\boldsymbol{y} = (y_1, y_2, \cdots, y_N)$ with

$$y_t = \sum_{m=1}^{M} \sum_{k=1}^{K/M} x_{m,t}^{(k)} + z_t, \ t = 1, 2, \cdots, N, \tag{4.1}$$

where z_t is a zero-mean Gaussian variable with a variance of σ^2, i.e., $\mathrm{E}[z_t] = 0, \mathrm{Var}[z_t] = \sigma^2$. The IJD and HIC schemes are performed to recover information bit vectors $\boldsymbol{u}_m^{(k)}, 1 \le m \le M, 1 \le k \le$

K/M.

4.2.2.1 Iterative Joint Decoding

The IJD scheme is accomplished by efficient local decoding at all the nodes and interactions. During a decoding iteration, each node acts once to perform local decoding and updates the message on the edges to each of its adjacent nodes.

A decoding iteration starts from the local decoding at the sum nodes in Y. The local decoding at a sum node is elementary signal estimation (ESE) [35, 36, 42], in which the sum signal of the other users is regarded as Gaussian. Then the local decodings are subsequently done at the nodes in $V \to G \to U \to G \to V \to Y$. The local decoding at the dashed box part is BP decoding [11–13], in which the processing of variable node and check node is a standardized node processing [28] in the graph-based decoding. After a large number of iterations, hard decisions are made at the outputs of the variable nodes in U to recover the transmitted vectors. The message update rules at sum node, variable node and check node will be given later in Section 4.3.1.

4.2.2.2 Hybrid Interference Cancellation

The HIC scheme is accomplished by a local IJD within the groups and successive interference cancellation (SIC) [1, 43, 44] among the groups. It provides much lower decoding complexity than the global IJD described in Section 4.2.2.1, since it does not require global iteration among all the users.

Without loss of generality, assume that $R_1 \leq R_2 \leq \cdots \leq R_M$. At the receiver in the mth step of the HIC scheme, $1 \leq m \leq M$, K/M users' information in the mth group is decoded by a local IJD, regarding the signals transmitted from the $M - m$ groups as "noise". Then the replicas of the transmitted vectors in the mth groups are generated and cancelled from the received signal. This process is performed successively until the users' information in all the groups has been recovered.

4.3 Code Optimization

The design of the K-user multi-rate code is to find the optimal repeat number and spreading length profile $((q_1^*, L_1^*), \cdots, (q_m^*, L_m^*))$, which gives the maximum sum rate. In this section, after introducing the EXIT function at each node for the local decoding in the protograph, we give a bivariate fixed-point analysis to explicitly represent (q_m, L_m) as a function of MI outputs. Based on these basic explicit representations, we have a united unreliable region over which users in at least one group are undecodable. The reliable region, i.e., the complementary set of the united unreliable region, gives optimal profile $((q_1^*, L_1^*), \cdots, (q_m^*, L_m^*))$.

4.3.1 Node Processing and EXIT Functions

Generally during decoding, the input or output message of a local decoding is a log-likelihood ratio (LLR) for its associated bit. The EXIT function describes a statistical property of the decoding, where both the input and output are measured by the MI between the LLR and its associated message bit [12, 14–17]. Moreover, the EXIT function theory is based on assumptions of infinite code length, infinite iterations, and the Gaussian approximation, where both the input and output LLRs are assumed to be Gaussian variables (variance of each variable is twice its mean). In the following, we introduce the EXIT function for the local decoding at each node.

4.3.1.1 Preliminaries

The update rules of all the LLRs at the variable and check nodes follow from usual BP decoding [14, 17]. For the local decoding at a variable node with degree d (Fig. 4.2, $d = q_m$ in U or $L_m + 2$ in V for kth user in mth group), the EXIT function T_v, which describes the MI output of the variable node, becomes

$$\mathrm{T}_v(I_{A,1}, \cdots, I_{A,d-1}) = \mathrm{J}\left(\sqrt{\sum_{i=1}^{d-1}\left[\mathrm{J}^{-1}(I_{A,i})\right]^2}\right), \tag{4.2}$$

where $0 \leq I_{A,i} \leq 1$ is the input MI from check node i to variable node j. For simplicity, if e inputs are the same, i.e., $I_{A,i} = I_A, i = 1, \ldots, e$, we represent this EXIT function as $\mathrm{T}_v(I_A \times$

$e, I_{A,e+1}, \ldots, I_{A,d-1}$). For the local decoding at a check node in G with degree d (Fig. 4.2, $d = 3$), the EXIT function T_c, i.e., the MI output of the check node, is

$$\mathrm{T}_c(I_{A,1}, \cdots, I_{A,d-1}) = 1 - \mathrm{T}_v(1 - I_{A,1}, \cdots, 1 - I_{A,d-1}), \tag{4.3}$$

where $0 \le I_{A,i} \le 1$ is the input MI from variable node i to check node j. Similarly, for $I_{A,i} = I_A, i = 1, \ldots, e$, we represent the EXIT function as $\mathrm{T}_c(I_A \times e, I_{A,e+1}, \ldots, I_{A,d-1})$.

4.3.1.2 Sum Node for IJD

For the IJD and HIC decoding schemes, the EXIT functions, i.e., the MI outputs, at a sum node are different. For the IJD scheme, since the sum node has K edges, its MI output is a function of $K - 1$ input MIs.

We rewrite (4.1) as

$$y_t = x_{m,t}^{(k)} + \zeta_{m,t}^{(k)} + z_t, \tag{4.4}$$

where

$$\zeta_{m,t}^{(k)} \triangleq \sum_{m'=1}^{M} \sum_{k'=1}^{K/M} x_{m',t}^{(k')} - x_{m,t}^{(k)} = \sum_{m'=1}^{M} \sum_{\substack{k'=1 \\ (m' \neq m)\&(k' \neq k)}}^{K/M} x_{m',t}^{(k')} \tag{4.5}$$

is regarded as a Gaussian variable.

The local decoding at the sum node in Y estimates LLR output $L_{E,m}^{(k)}$ of $x_{m,t}^{(k)}$ from received signal y_t and input LLRs $L_{A,m}^{(k)}$. Since $\zeta_{m,t}^{(k)}$ is a Gaussian variable, we have [35, 36]

$$L_{E,m}^{(k)} = \log\left(\frac{\Pr\left(y_t | x_{m,t}^{(k)} = +1\right)}{\Pr\left(y_t | x_{m,t}^{(k)} = -1\right)}\right) = \frac{2\left(y_t - \mathrm{E}\left[\zeta_{m,t}^{(k)}\right] - \mathrm{E}\left[z_t\right]\right)}{\mathrm{Var}\left[\zeta_{m,t}^{(k)}\right] + \mathrm{Var}\left[z_t\right]}, \tag{4.6}$$

where

$$\begin{aligned}
\mathrm{E}\left[\zeta_{m,t}^{(k)}\right] &= \sum_{m'=1}^{M} \sum_{\substack{k'=1 \\ (m' \neq m)\&(k' \neq k)}}^{K/M} \tanh\left(\frac{L_{A,m'}^{(k')}}{2}\right), \\
\mathrm{Var}\left[\zeta_{m,t}^{(k)}\right] &= \sum_{m'=1}^{M} \sum_{\substack{k'=1 \\ (m' \neq m)\&(k' \neq k)}}^{K/M} \left(1 - \left(\tanh\left(\frac{L_{A,m'}^{(k')}}{2}\right)\right)^2\right)
\end{aligned}$$

due to $\mathrm{E}\left[x_{m,t}^{(k)}\right] = \tanh\left(\frac{L_{A,m}^{(k)}}{2}\right)$, $\mathrm{Var}\left[x_{m,t}^{(k)}\right] = 1 - \left(\mathrm{E}\left[x_{m,t}^{(k)}\right]\right)^2$ [35, 36].

Since transmitted signals $x_{m,t}^{(k)}$ are independent of each other and uniformly distributed on $\{+1, -1\}$, we derive the expectation of the LLR output with random variable $x_{m,t}^{(k)}$

$$\mathrm{E}_{\mathrm{IJD}}\left[x_{m,t}^{(k)} L_{E,m}^{(k)}\right] = \mathrm{E}\left[\frac{2}{\sum_{m'=1}^{M} \sum_{\substack{k'=1 \\ (m' \neq m)\&(k' \neq k)}}^{K/M} \left(1 - \left(\tanh\left(\frac{L_{A,m'}^{(k')}}{2}\right)\right)^2\right) + \sigma^2}\right]. \tag{4.7}$$

The expectation above can be obtained by the Monte Carlo method [18]. Note that the assumption that the all-ones signals, i.e., $x_{m,t}^{(k)} = 1$, were transmitted in the single-user case is not suitable for the multi-user case.

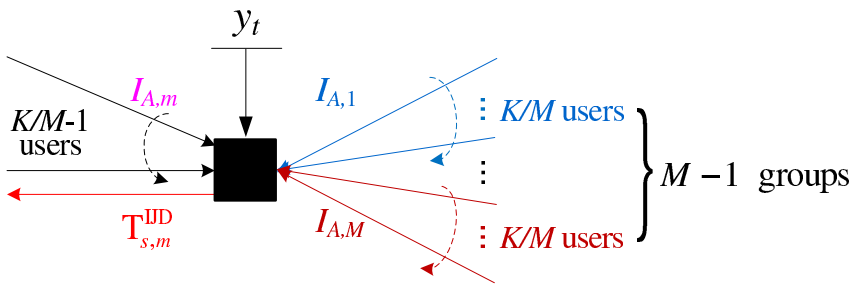

Figure 4.3: Sum node for IJD scheme

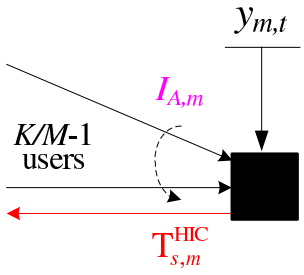

Figure 4.4: Sum node for HIC scheme

Now we are ready to give an EXIT function at the sum node for the IJD scheme. Similar to the

variable and check nodes, the input and output LLRs are modeled by Gaussian variables with mean μ and variance 2μ. The MI is $I = \mathrm{J}(\sqrt{2\mu})$ [18]. We redraw the sum node in Fig. 4.2 as in Fig. 4.3, where the K edges are connected to the node, one labeled by MI output $\mathrm{T}_{s,m}^{\mathrm{IJD}}$ and the others labeled by input MIs $I_{A,m}$, $1 \le m \le M$. The input MIs come from the MI outputs of the decoder-despreader (Fig. 4.2). Within the mth group, users have the same input MI, i.e., $I_{A,m}^{(1)} = \cdots = I_{A,m}^{(K/M)} \triangleq I_{A,m}$, since they employ the same RA code and spreading. As a result, we have M kinds of input MIs $(I_{A,1}, \cdots, I_{A,M})$, which are associated with rate profile $(R_1, \cdots, R_M)$. In our Monte Carlo simulation, we set $I_{A,m}$ and randomly generate input LLRs $L_{A,m}^{(k)}$ to compute the expectation of the LLR output in (4.7). Therefore, EXIT function $\mathrm{T}_{s,m}^{\mathrm{IJD}}$, i.e., the MI output of the sum node, can be formulated as

$$\mathrm{T}_{s,m}^{\mathrm{IJD}}\left(I_{A,1} \times \frac{K}{M}, \cdots, I_{A,m} \times \left(\frac{K}{M} - 1\right), \cdots, I_{A,M} \times \frac{K}{M}, \sigma^2\right) = \mathrm{J}\left(\sqrt{2\mathrm{E}_{\mathrm{IJD}}\left[x_{m,t}^{(k)} L_{E,m}^{(k)}\right]}\right), 1 \le m \le M. \quad (4.8)$$

Note that if the equal rate transmission is considered, i.e., $M = 1$, the EXIT function in (4.8) is reduced to [6, Eq. (8)].

4.3.1.3 Sum Node for HIC

For the HIC scheme, we employ the local IJD within the groups and the SIC among them. Assume that $R_1 \le \cdots \le R_M$. In the mth step, the replicas of $\hat{x}_{m-1,t}^{(k)}$, $1 \le k \le K/M$ are generated and cancelled from $y_{m-1,t}$, and the remaining received signal is given by

$$y_{m,t} = x_{m,t}^{(k)} + \zeta'^{(k)}_{m,t} + z'_{m,t}, \quad (4.9)$$

where $y_{1,t} = y_t$ in (4.1). Here, $\zeta'^{(k)}_{m,t} \triangleq \sum_{k'=1,k' \ne k}^{K/M} x_{m,t}^{(k')}$ is a Gaussian variable, and

$$z'_{m,t} = \begin{cases} \sum_{j=m+1}^{M} \sum_{k=1}^{K/M} x_{j,t}^{(k)} + z_t & \text{if } 1 \le m < M, \\ z_t & \text{if } m = M \end{cases}$$

is regarded as "noise" for SIC.

For the local IJD within the mth group, similar to the global IJD in (4.7), we obtain the expec-

tation of the LLR output with $x_{m,t}^{(k)}$

$$\mathrm{E}_{\mathrm{HIC}}\left[x_{m,t}^{(k)}L_{E,m}^{(k)}\right]=\mathrm{E}\left[\frac{2}{\sum\limits_{k'=1,k'\neq k}^{K/M}\left(1-\left(\tanh\left(\frac{L_{A,m}^{(k')}}{2}\right)\right)^2\right)+\frac{K}{M}(M-m)+\sigma^2}\right]. \tag{4.10}$$

Note that the second term in the denominator denotes the interfering signal power of the users in the remaining $M-m$ groups, which is regarded as "noise".

Obviously, users within the mth group have identical input MI $I_{A,m}$. We set $I_{A,m}$ and randomly generate input LLRs $L_{A,m}^{(k)}$ to compute the expectation of the LLR output in (4.10), where $\frac{K}{M}(M-m)$ is the total interfering signal power of the remaining $M-m$ groups. Since the replicas of the transmitted vectors in the preceding $m-1$ groups are cancelled from received signal y_t of (4.4), the remaining received signal is $y_{m,t}$ of (4.9) in Fig. 4.4. EXIT function $\mathrm{T}_{s,m}^{\mathrm{HIC}}$, i.e., the MI output of the sum node, is

$$\mathrm{T}_{s,m}^{\mathrm{HIC}}\left(I_{A,m}\times\left(\frac{K}{M}-1\right),\frac{K}{M}(M-m)+\sigma^2\right)=\mathrm{J}\left(\sqrt{2\mathrm{E}_{\mathrm{HIC}}\left[x_{m,t}^{(k)}L_{E,m}^{(k)}\right]}\right),1\leq m\leq M. \tag{4.11}$$

4.3.2 Bivariate Fixed-Point Analysis

In this section, we apply bivariate fixed-point analysis to our multi-rate transmission and represent each (q_m, L_m) as a function of M different MI outputs by solving the mth pair-of-equations in the system equation array.

Due to the monotone increasing property of the EXIT functions at each node, the MI output on each edge on the protograph in Fig. 4.2 is increasing and converges to a fixed value as the decoding iteration approaches infinity [6]. In the following, we directly give the convergence value on the protograph.

As stated in Section 4.3.1, there are M kinds of input MIs to the sum nodes in Fig. 4.3 for the IJD scheme, but there is only one in Fig. 4.4 for the HIC scheme. Thus, the MI output of $I_{y,m}$ at a sum node in Y on the protograph is

$$I_{y,m}=\begin{cases}\mathrm{T}_{s,m}^{\mathrm{IJD}}\left(I_1\times\frac{K}{M},\cdots,I_m\times\left(\frac{K}{M}-1\right),\cdots,I_M\times\frac{K}{M},\sigma^2\right) & \text{for the IJD scheme,} \quad (4.12a)\\ \mathrm{T}_{s,m}^{\mathrm{HIC}}\left(I_m\times\left(\frac{K}{M}-1\right),\frac{K}{M}(M-m)+\sigma^2\right) & \text{for the HIC scheme.} \quad (4.12b)\end{cases}$$

Moreover, for a given pair of (q_m, L_m) at a variable node, MI outputs of $I_{u,m}$ in U and $I_{a,m}, I_m$ in V are obtained by (4.2). At a check node, MI outputs of $I_{g,u,m}$ and $I_{g,v,m}$ in G are obtained by (4.3). According to the MI evolution $Y \to V \to G \to U \to G \to V \to Y$ in Fig. 4.2, we obtain the mth pair-of-equations

$$\begin{cases} I_m &= \mathrm{T}_v\left(\mathrm{T}_c\left(\mathrm{T}_v\left(\mathrm{T}_c\left((I_{a,m}\times 2)\times(q_m-1)\right)\right), I_{a,m}\right)\times 2, I_{y,m}\times(L_m-1)\right) \quad (4.13a)\\ I_{a,m} &= \mathrm{T}_v\left(\mathrm{T}_c\left(\mathrm{T}_v\left(\mathrm{T}_c\left((I_{a,m}\times 2)\times(q_m-1)\right)\right), I_{a,m}\right), I_{y,m}\times L_m\right) \quad (4.13b)\end{cases}$$

$$m = 1, 2, \cdots, M.$$

In the mth pair-of-equations, each value $(I_m, I_{a,m})$ is referred to as a bivariate fixed-point. Minimum fixed-point $(I^*_m, I^*_{a,m})$ is the convergence point of the decoding as the iteration approaches infinity [6].

The convergence behavior of the decoding can be predicted by the average bit error rate of the RA coded bits (variable nodes in V in Fig. 4.2), i.e.,

$$\overline{\mathrm{P}}_e = \sum_{m=1}^{M} \frac{K_m q_m}{\sum_{m'=1}^{M} K_{m'} q_{m'}} \mathrm{P}_e(I^*_m), \quad (4.14)$$

where $\mathrm{P}_e(I^*_m) = \mathrm{erfc}(\mathrm{J}^{-1}(I^*_m)/(2\sqrt{2}))/2$. By the property of complementary error function erfc$(*)$, if $I^*_m = 1$, $\mathrm{P}_e(I^*_m) \to 0$, thus $\overline{\mathrm{P}}_e \to 0$. Instead of the average bit error rate $\overline{\mathrm{P}}^u_e = \sum_{m=1}^{M} \frac{K_m}{\sum_{m'=1}^{M} K_{m'}} \mathrm{P}_e(I_{u,m})$ of the information bits (variable nodes in U in Fig. 4.2), we employ $\overline{\mathrm{P}}_e$ to judge whether the decoding is successful, since $\mathrm{P}_e(I_{u,m}) \to 0$ if and only if $\mathrm{P}_e(I^*_m) \to 0$ [6]. Note that if $I^*_m \neq 1, \mathrm{P}_e(I^*_m) \neq 0$. This means that K/M users in the mth group are undecodable if $I^*_m \neq 1$. If the users in any one group are undecodable, the decoding of our K-user multi-rate code is regarded as fail, i.e., $\forall m$, if $\mathrm{P}_e(I^*_m) \neq 0$, $\overline{\mathrm{P}}_e \neq 0$.

Next, we consider the mth pair-of-equations (4.13) again. For given $I^*_1, \cdots, I^*_M$ and auxiliary variable $I^*_{a,m}$, by (4.13b) $\times 2 -$ (4.13a) using (4.2), (4.3) and (4.12), we can solve L_m in (4.15b).

Then, substituting L_m into (4.13a) (or (4.13b)), we also explicitly solve q_m in (4.15a):

$$\begin{cases} \dot{q}_m(I_1^*,\cdots,I_m^*,\cdots,I_M^*,I_{a,m}^*) \\ \quad = \dfrac{\left[\mathrm{J}^{-1}\left(1-\mathrm{J}\left(\sqrt{\left[\mathrm{J}^{-1}\left(1-\mathrm{J}\left(\sqrt{\left[\mathrm{J}^{-1}(I_{y,m})\right]^2+\left[\mathrm{J}^{-1}(I_m^*)\right]^2-\left[\mathrm{J}^{-1}(I_{a,m}^*)\right]^2}\right)\right)\right]^2-\left[\mathrm{J}^{-1}(1-I_{a,m}^*)\right]^2}\right)\right)\right]^2}{\left[\mathrm{J}^{-1}\left(1-\mathrm{J}\left(\sqrt{2[\mathrm{J}^{-1}(1-I_{a,m}^*)]^2}\right)\right)\right]^2}+1 \quad (4.15a) \\ \dot{L}_m(I_1^*,\cdots,I_m^*,\cdots,I_M^*,I_{a,m}^*) \\ \quad = \dfrac{2\left[\mathrm{J}^{-1}(I_{a,m}^*)\right]^2-\left[\mathrm{J}^{-1}(I_m^*)\right]^2}{\left[\mathrm{J}^{-1}(I_{y,m})\right]^2}-1 \quad (4.15b) \end{cases}$$

$$0 \le I_m^*, I_{a,m}^* < 1,\ 0 \le I_{m'}^* \le 1,\ m' \ne m$$

where

$$I_{y,m} = \begin{cases} \mathrm{J}\left(\sqrt{2\mathrm{E}_{\mathrm{IJD}}\left[x_{m,t}^{(k)}L_{E,m}^{(k)}\right]}\right) & \text{for the IJD scheme,} \\ \mathrm{J}\left(\sqrt{2\mathrm{E}_{\mathrm{HIC}}\left[x_{m,t}^{(k)}L_{E,m}^{(k)}\right]}\right) & \text{for the HIC scheme.} \end{cases}$$

For a given m, $(\dot{q}_m, \dot{L}_m)$ in (4.15), is calculated over the range $0 \le I_m^*, I_{a,m}^* < 1$. It should be emphasized that 1 is excluded from the range of I_m^* and $I_{a,m}^*$, since function $\mathrm{J}^{-1}(I = 1) = \infty$. As we stated above, $\mathrm{P}_e(I_m^*) \ne 0$, when $I_m^* \ne 1$. This means that the values of $(\dot{q}_m, \dot{L}_m)$ in (4.15) are unreliable in the sense that K/M users in the mth group are undecodable, i.e., $I_m^* \ne 1$.

4.3.3 Reliable and United Unreliable Regions

As stated in Section 4.3.2, we can not directly obtain the (reliable) values of (q_m, L_m) that guarantee the error-free decoding, since 1 is excluded from the range of MI output I_m^*. Our objective is to obtain a reliable region, over which our K-user multi-rate code is decodable, by taking the complement of a union of M combined unreliable regions. Note that the unreliable values of $(\dot{q}_m, \dot{L}_m)$ in the unreliable region are calculated from (4.15). Specifically, based on the above basic explicit representations of (4.15a) and (4.15b), from T corresponding simultaneous pairs-of-equations ($1 \le T \le M$), we first give a combined unreliable region over which users in any T groups are undecodable. Then we have a united unreliable region over which the users in at least

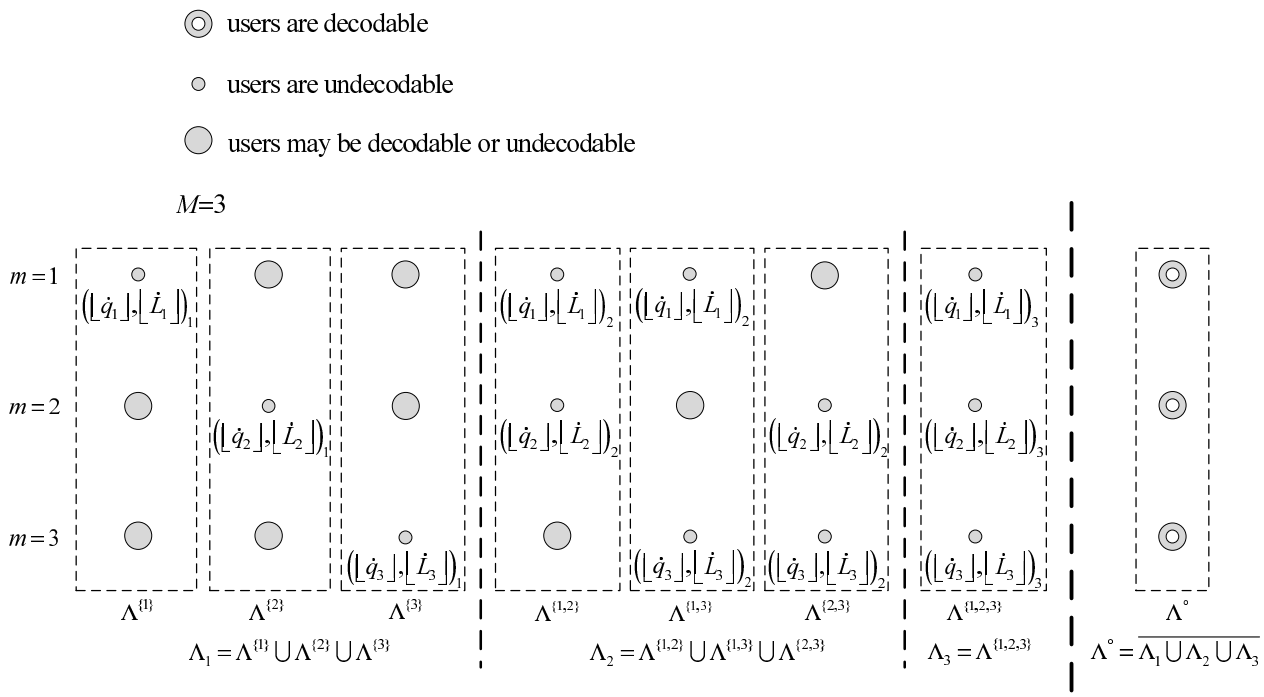

Figure 4.5: Reliable and unreliable regions for our K-user multi-rate code ($M = 3$)

one group are undecodable. Finally, the reliable region gives the optimal repeat number and the spreading length profile, which achieves the maximum sum rate.

For a given T, denote by $\mathcal{S}_T = \{s_1, \cdots, s_T\}$ a subset of T-distinct elements of $\mathcal{M} = \{1, \cdots, M\}$, which is referred to as a T-combination of $\mathcal{M}$. Region

$$\Lambda^{\mathcal{S}_T} = \{((q_1, L_1), \cdots, (q_M, L_M)) \mid ((q_{s_1}, L_{s_1}), \cdots, (q_{s_T}, L_{s_T})) = ((\lfloor \dot{q}_{s_1} \rfloor, \lfloor \dot{L}_{s_1} \rfloor)_T, \cdots, (\lfloor \dot{q}_{s_T} \rfloor, \lfloor \dot{L}_{s_T} \rfloor)_T), \\ \text{and } \forall (q_{m'}, L_{m'}) \in \mathbb{Z}^2, m' \in \mathcal{M} \setminus \mathcal{S}_T\} \tag{4.16}$$

is unreliable, in the sense that all the users in $\mathcal{S}_T$ are undecodable, regardless whether the users in the remaining groups $\mathcal{M} \setminus \mathcal{S}_T$ are decodable or undecodable, where $\mathbb{Z}^2$ is the set of 2-dimensional integers. Here, $((\dot{q}_{s_1}, \dot{L}_{s_1})_T, \cdots, (\dot{q}_{s_T}, \dot{L}_{s_T})_T)$ are obtained simultaneously from T corresponding pairs-of-equations in (4.15). Note that the values of $(\dot{q}_m, \dot{L}_m)_T$ depend on I^*_m and $I^*_{m'}$ (see (4.15)). Here, I^*_m, $m \in \mathcal{S}_T$, excludes 1, and $I^*_{m'}$, $m' \in \mathcal{M} \setminus \mathcal{S}_T$, includes 1. Thus a different T may give different

Table 4.1: IJD scheme: optimal repeat number and spreading length profiles

K	M	SNR (dB)	$((q_1^*, L_1^*), \cdots, (q_M^*, L_M^*))$	R_{sum}^{max}	Shannon limit	SNR_{th}	Gap
12	1	2	$(4, 6)$	0.5000	0.01	1.88	1.87
		4	$(3, 6)$	0.6667	1.82	3.45	1.63
		6	$(2, 7)$	0.8571	3.59	5.41	1.82
	2	2	$((3, 8), (4, 5))$	0.5500	0.59	1.90	1.31
			$((4, 6), (4, 5))$			1.92	1.33
			$((3, 8), (5, 4))$			1.95	1.36
		4	$((3, 6), (3, 5))$	0.7333	2.47	3.87	1.40
		6	$((2, 7), (2, 6))$	0.9286	4.20	5.67	1.47
			$((2, 7), (3, 4))$			5.86	1.66
	3	2	$((3, 8), (4, 5), (4, 5))$	0.5667	0.77	1.98	1.21
			$((4, 6), (4, 5), (4, 5))$				
			$((3, 8), (4, 5), (5, 4))$				
		4	$((3, 6), (3, 6), (4, 3))$	0.7778	2.88	3.92	1.04
		6	$((2, 7), (2, 7), (3, 3))$	1.0159	4.91	5.97	1.06

values of $(\dot{q}_m, \dot{L}_m)_T$. Moreover, for another distinct T-combination $\tilde{\mathcal{S}}_T$ of $\mathcal{M}$, since all the values of the vectors in regions $\Lambda^{\mathcal{S}_T}$ and $\Lambda^{\tilde{\mathcal{S}}_T}$ are from T pairs-of-equations in (4.15) with the only difference in $m \in \tilde{\mathcal{S}}_T$ or $\mathcal{S}_T$, the vector in region $\Lambda^{\tilde{\mathcal{S}}_T}$ is a permutation of a corresponding vector in $\Lambda^{\mathcal{S}_T}$. Thus, region $\Lambda^{\tilde{\mathcal{S}}_T}$ is obtained by setting $(\dot{q}_m, \dot{L}_m)_T$ in region $\Lambda^{\mathcal{S}_T}$, $m \in \mathcal{S}_T$ into the corresponding locations in $\Lambda^{\tilde{\mathcal{S}}_T}$ in a particular order of $\tilde{\mathcal{S}}_T$.

Let $\mathcal{S}_T^c$, $1 \le c \le \binom{M}{T}$, be a T-combination of $\mathcal{M}$, e.g., $\mathcal{S}_T^1 = \{1, \cdots, T\}$. Combined region $\Lambda_T = \bigcup_{c=1}^{\binom{M}{T}} \Lambda^{\mathcal{S}_T^c}$ is unreliable over which all the users in any T groups are undecodable. Then, we have a united unreliable region

$$\Lambda_1 \cup \cdots \cup \Lambda_M \tag{4.17}$$

Table 4.2: HIC and SIC schemes: optimal repeat number and spreading length profiles

	K	M	SNR (dB)	$((q_1^*, L_1^*), \cdots, (q_M^*, L_M^*))$	R_{sum}^{max}	Shannon limit	SNR_{th}	Gap
HIC	12	2	2	((4, 8), (4, 5))	0.4875	-0.15	1.61	1.76
				((4, 8), (5, 4))			1.89	2.04
			4	((3, 9), (3, 5))	0.6222	1.37	3.69	2.32
				((3, 9), (5, 4))				
			6	((4, 6), (3, 4))	0.7500	2.63	4.41	1.78
				((4, 6), (4, 3))			4.75	2.12
				((3, 8), (3, 4))			4.99	2.36
				((3, 8), (4, 3))				
		3	2	((5, 7), (4, 7), (4, 5))	0.4571	-0.53	1.65	2.18
				((5, 7), (4, 7), (5, 4))				
			4	((4, 7), (4, 5), (4, 3))	0.6762	1.92	3.87	1.95
			6	((4, 6), (3, 6), (3, 3))	0.8333	3.38	5.96	2.58
		12	2	((5, 8), (5, 7), (5, 7), (5, 7), (5, 6), (4, 7), (5, 5), (6, 4), (6, 4), (5, 4), (6, 3), (4, 4))	0.4713	-0.35	1.69	2.04
			4	((5, 7), (5, 6), (5, 6), (4, 7), (5, 5), (6, 4), (5, 4), (5, 4), (6, 3), (5, 3), (6, 2), (5, 2))	0.6182	1.33	3.96	2.63
			6	((5, 6), (4, 7), (5, 5), (6, 4), (5, 4), (5, 4), (6, 3), (5, 3), (7, 2), (5, 2), (9, 1), (7, 1))	0.7984	3.07	5.70	2.63
SIC	12	12	2	((6, 7), (5, 8), (6, 6), (5, 7), (4, 8), (5, 6), (4, 7), (5, 5), (6, 4), (5, 4), (6, 3), (4, 4))	0.4553	-0.55	1.90	2.45
			4	((5, 7), (4, 8), (5, 6), (4, 7), (5, 5), (6, 4), (7, 3), (5, 4), (6, 3), (5, 3), (6, 2), (5, 2))	0.6138	1.28	3.96	2.68
			6	((5, 6), (4, 7), (9, 3), (5, 5), (6, 4), (5, 4), (6, 3), (5, 3), (7, 2), (4, 3), (5, 2), (7, 1))	0.7576	2.70	5.89	3.19

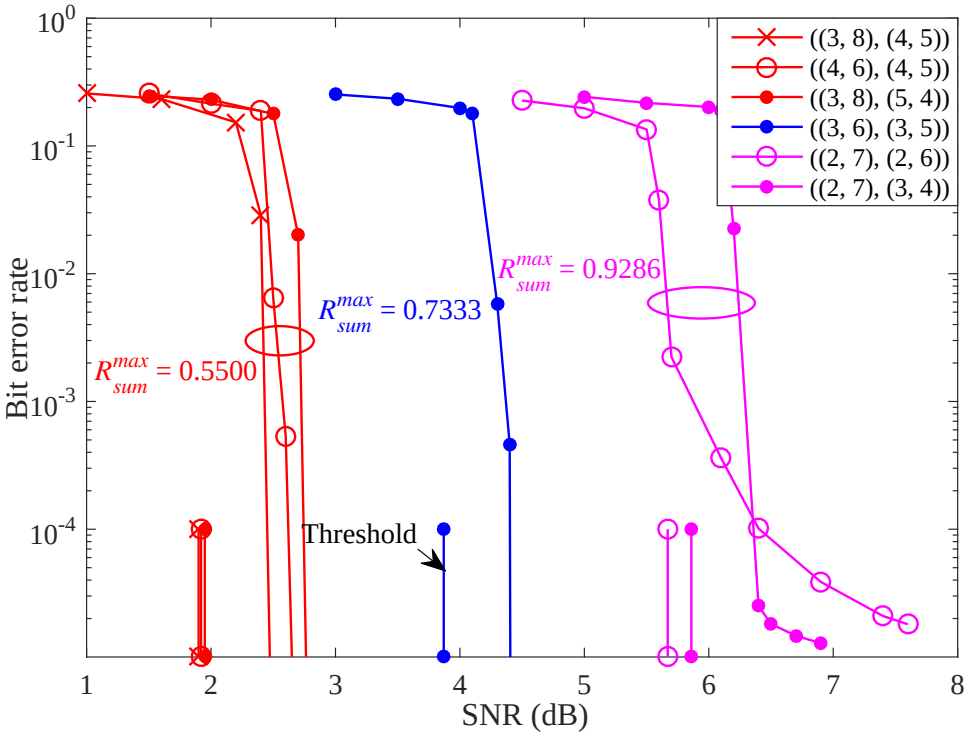

Figure 4.6: BERs of K-user multi-rate code under IJD scheme for $K = 12$ and $M = 2$

over which users in at least one group are undecodable.

Finally, we have a complementary region of (4.17), called a reliable region,

$$\Lambda^{\circ} = \overline{\Lambda_1 \cup \cdots \cup \Lambda_M}, \tag{4.18}$$

over which the decoding for our K-user multi-rate code is error-free.

For simplicity, we give an example of reliable and unreliable regions for our K-user multi-rate code in Fig. 4.5. Let $M = 3$. Consider $T = 2$ and $\mathcal{S}_2^1 = \{1, 2\}$ for an instance. We have unreliable region $\Lambda^{\mathcal{S}_2^1=\{1,2\}} = \{((\lfloor \dot{q}_1 \rfloor, \lfloor \dot{L}_1 \rfloor)_2, (\lfloor \dot{q}_2 \rfloor, \lfloor \dot{L}_2 \rfloor)_2, (q_3, L_3)) \mid \forall (q_3, L_3) \in \mathbb{Z}^2\}$, where the values of $((\dot{q}_1, \dot{L}_1)_2, (\dot{q}_2, \dot{L}_2)_2)$ are obtained simultaneously from two corresponding pairs-of-equations in (4.15) by setting $I_1^*, I_2^*, I_3^*, I_{a,1}^*, I_{a,2}^*$ over range $0 \leq I_1^*, I_2^*, I_{a,1}^*, I_{a,2}^* < 1$ and $0 \leq I_3^* \leq 1$. In Fig. 4.5, over unreliable region $\Lambda^{\mathcal{S}_2^1=\{1,2\}}$, the users in the 1st and 2nd groups are undecodable, regardless whether the users in the 3rd group are decodable or undecodable. Unreliable regions $\Lambda^{\mathcal{S}_2^2=\{1,3\}}$ and $\Lambda^{\mathcal{S}_2^3=\{2,3\}}$ are given by permuting $\Lambda^{\mathcal{S}_2^1=\{1,2\}}$. Combined region $\Lambda_2 = \Lambda^{\mathcal{S}_2^1=\{1,2\}} \cup \Lambda^{\mathcal{S}_2^2=\{1,3\}} \cup \Lambda^{\mathcal{S}_2^3=\{2,3\}}$ is

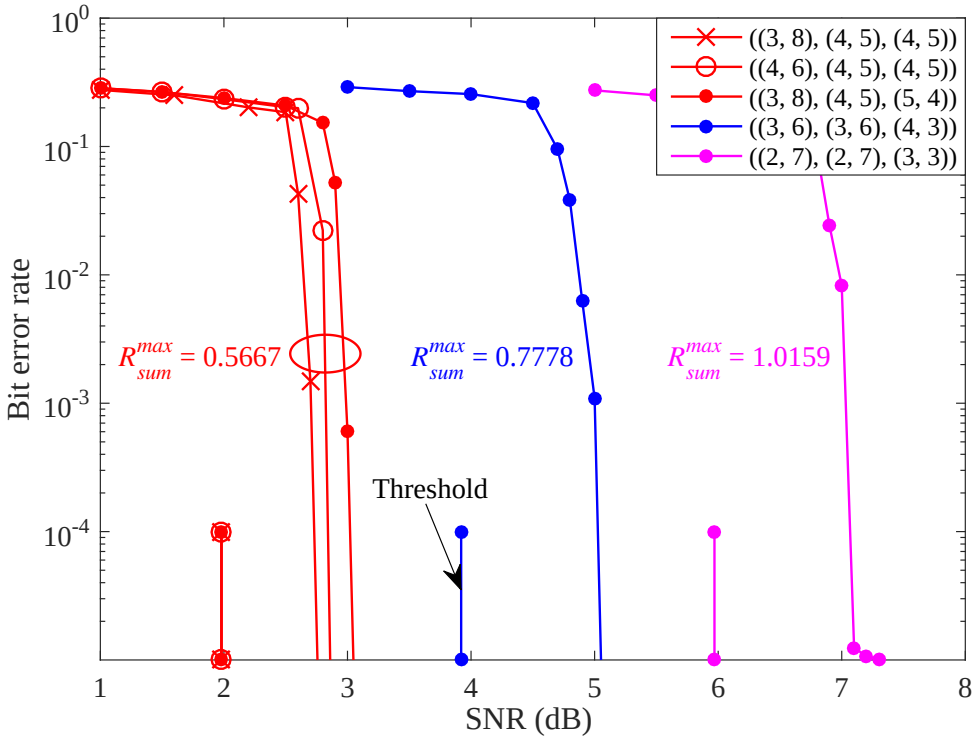

Figure 4.7: BERs of K-user multi-rate code under IJD scheme for $K = 12$ and $M = 3$

also unreliable, where all the users in any two groups are undecodable. Finally, we obtain a reliable region of $\Lambda^\circ = \overline{\Lambda_1 \cup \Lambda_2 \cup \Lambda_3}$. Note that we cannot directly obtain Λ° in Fig. 4.5, since $(\dot{q}_m, \dot{L}_m)$ cannot be obtained when I_m^* or $I_{a,m}^* = 1$.

Next, we find the optimal repeat number and the spreading length profile is

$$((q_1^*, L_1^*), \cdots, (q_M^*, L_M^*)) = \arg \max_{((q_1,L_1),\cdots,(q_M,L_M))\in\Lambda^\circ} \frac{K}{M} \sum_{m=1}^{M} \frac{1}{q_m L_m}, \tag{4.19}$$

which gives maximum sum rate $R_{sum}^{max} = (K/M) \sum_{m=1}^{M} 1/q_m^* L_m^*$.

For our multi-rate transmission, the threshold of the decoding is the minimum channel signal-to-noise ratio (SNR) that makes $((q_1, L_1), \cdots, (q_M, L_M))$ in the reliable region Λ°, i.e.,

$$\text{SNR}_{\text{th}} = 10 \cdot \log_{10} \frac{K}{\sup\{\sigma^2 \mid ((q_1, L_1), \cdots, (q_M, L_M)) \in \Lambda^\circ\}} \text{ [dB]}. \tag{4.20}$$

We summarize the above optimization of our K-user multi-rate code as follows.

Search algorithm for $((q_1^*, L_1^*), \cdots, (q_M^*, L_M^*))$:

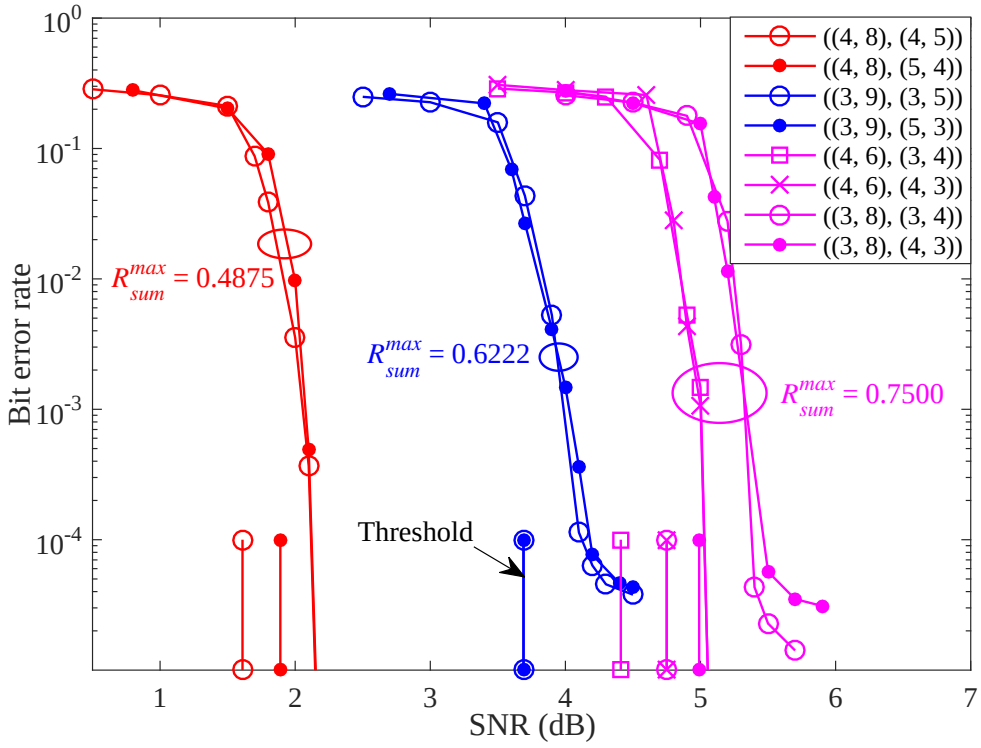

Figure 4.8: BERs of K-user multi-rate code under HIC scheme for $K = 12$ and $M = 2$

// given number of users K, groups M, and σ

for $(T = 1; T <= M; T = T + 1)$

obtain $\Lambda^{\mathcal{S}_T^1}$ from T simultaneous pairs-of-equations of (4.15);

for $(c = 2; c <= \binom{M}{T}; c = c + 1)$

obtain $\Lambda^{\mathcal{S}_T^c}$ by permuting $\Lambda^{\mathcal{S}_T^1}$;

end

$\Lambda_T = \bigcup_{c=1}^{\binom{M}{T}} \Lambda^{\mathcal{S}_T^c}$;

end

$\Lambda^\circ = \overline{\Lambda_1 \cup \cdots \cup \Lambda_M}$;

give $((q_1^*, L_1^*), \cdots, (q_M^*, L_M^*))$ in (4.19). □

Remark 4.1 The work in this paper is an extension of code optimization of equal rate transmission [6] to multi-rate transmission. For HIC scheme, the optimized code C_m and spreading $\mathcal{S}_m$ is

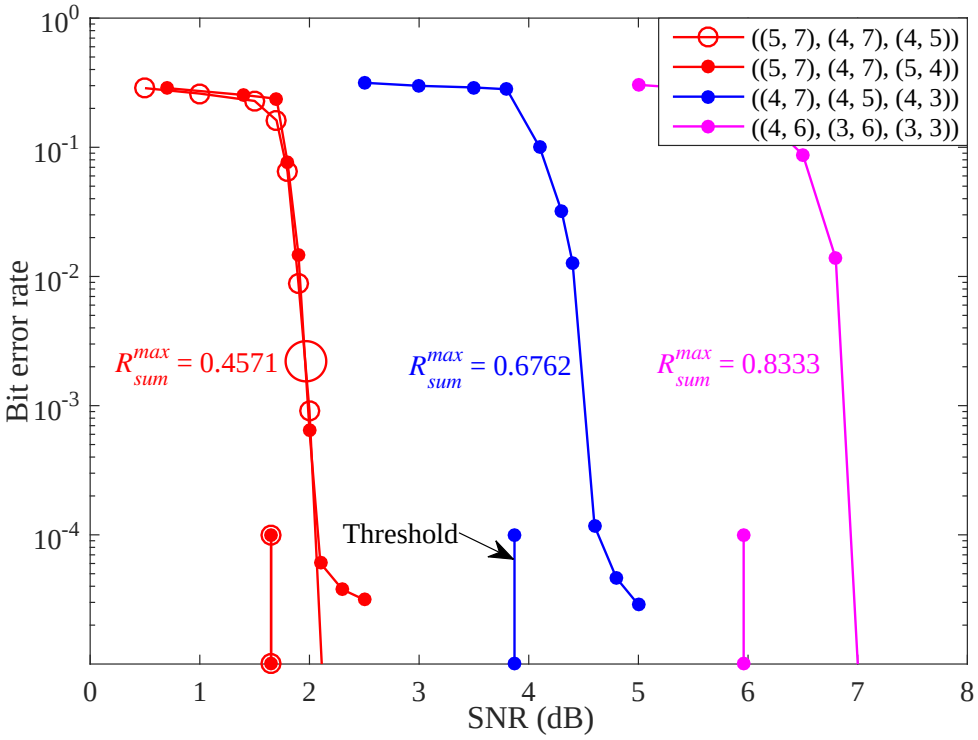

Figure 4.9: BERs of K-user multi-rate code under HIC scheme for $K = 12$ and $M = 3$

the same as that obtained in [6], since at the mth step, the replicas of the signals from the users in the previous $m-1$ groups are cancelled (see (4.9)), and the signals from the users in the remaining $M-m$ groups are regarded as noise (see (4.9) and (4.12b)). In fact, the code optimization of HIC is proceeded by independently repeating the code optimization of [6] for M different groups of users, and thus provide us a multi-rate transmission.

For IJD scheme, in the special case of $M = 1$, i.e., a single-rate transmission, the code optimization is reduced to that of [6]. Setting $M > 1$ provides us the M-rate transmission. We observe that in the sum node of Fig. 4.3, there are K edges, each of which is labeled by one of M input MIs, corresponding to M rates. Thus (q_m, L_m) in (4.15a) and (4.15b) is a function of M variables of $I_1, I_2, \cdots I_M$. As a result, the complement of a union of M combined unreliable regions guarantees reliable multi-rate transmission. On the other hand, in [6], although the number of edges in the sum node is still K, the same input MI I labels each of edges due to same rate transmission. Thus

repeat number q and spreading length L is a function of the single MI, and the complement of an unreliable region of (q, L) guarantees reliable equal rate transmission.

Note that although our code optimization is slightly more complex than that in [6], we provide a multi-rate transmission service and improve the maximum sum rate (see Figs. 4.10, 4.11, 4.12 below), compared with [6]. □

4.4 Numerical Results

In this chapter, we present some numerical results of our K-user multi-rate code under both the IJD and HIC schemes by the above code optimization in Sections 4.3.2 and 4.3.3. In our numerical computation, the intervals are set to $\Delta_m^* = \Delta_{a,m}^* = 0.001$. We set the maximum of $I_m^* = 0.999$, and thus the target BER for each group is 1.3×10^{-4}.

4.4.1 Iterative Joint Decoding Scheme

For the IJD scheme, let $K = 12$, $M = 2$, and SNR $= K/\sigma^2 = 2$ dB. In Table 4.1, we give three optimal profiles, $((q_1^*, L_1^*), (q_2^*, L_2^*)) = ((3, 8), (4, 5)), ((4, 6), (4, 5))$, and $((3, 8), (5, 4))$, which were obtained in Sections 4.3.2 and 4.3.3. All have the same rate profile, $(R_1^*, R_2^*) = (1/24, 1/20)$, which gives a maximum sum rate of $R_{sum}^{max} = 0.55$. The corresponding thresholds of (4.20) are $\text{SNR}_{\text{th}}^{\text{IJD}} =$ 1.90, 1.92, and 1.95 dB. We know that the profile $((3, 8), (4, 5))$ is optimal since the 1.31-dB gap between the threshold and the Shannon limit is minimum.

When $M = 1$, our multi-rate transmission is reduced to a conventional equal rate transmission [6]. In Table 4.1, when SNR = 2 dB, optimal profile $(q_1^*, L_1^*) = (4, 6)$ gives a maximum sum rate of $R_{sum}^{max} = 0.5$. Compared with this conventional equal rate code, our K-user multi-rate code with $M = 2$ improves the maximum sum rate by 0.05.

Similarly, for $M = 3$, we obtain the corresponding results, as shown in Table 4.1. The maximum sum rate improved from $M = 2$ to 3. For SNR = 2 dB, $(q_2^*, L_2^*) = (q_3^*, L_3^*) = (4, 5)$. As a result, eight users are assigned to rate 1/20 and four to rate 1/24. This results in unequal group-division, although in our analysis the number of users in each group is assumed to be equal.

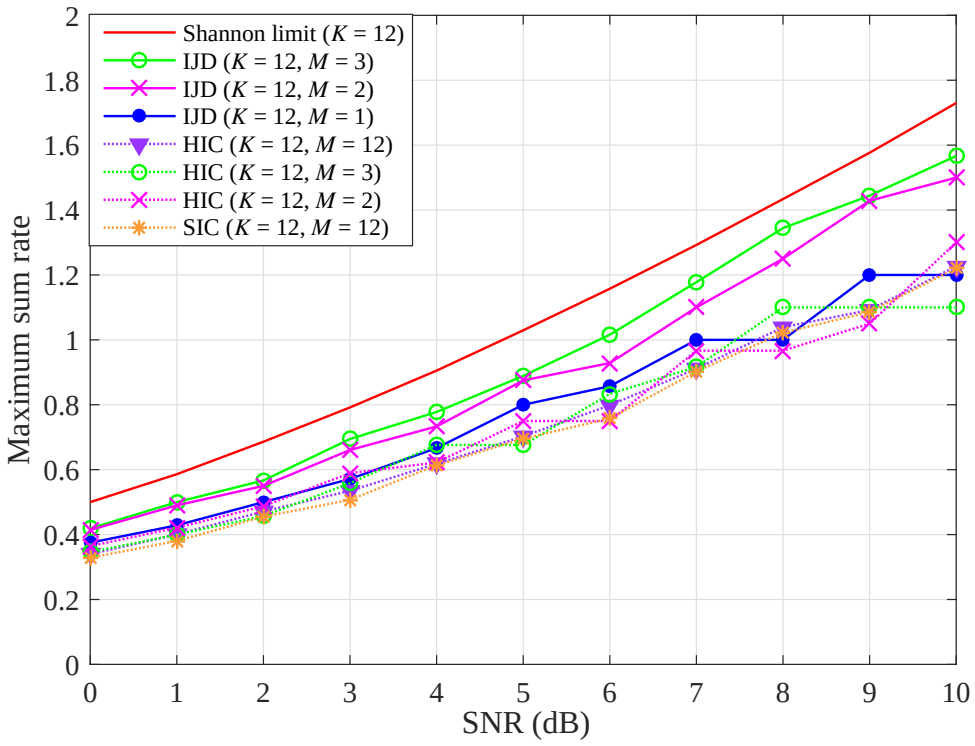

Figure 4.10: Maximum sum rate of K-user multi-rate code under IJD, HIC, and SIC schemes for $K = 12$ and $M = 1, 2, 3, 12$

To verify our analysis, we did Monte Carlo simulations to evaluate the BERs of our K-user multi-rate code obtained in Table 4.1. In the simulation, our K-user multi-rate code with chip lengths of $N = 60480$ was used for each user. All the interleavers are random. The number of iterations was $L_{\text{IJD}} = 500$ for $M = 2$ and $L_{\text{IJD}} = 750$ for $M = 3$. In Figs. 4.6 and 4.7, the BERs of our K-user multi-rate codes converged well to their thresholds. This verifies that the design of our K-user multi-rate code for the IJD scheme is accurate. For a given SNR, our designed codes have slightly different BER performances, although these codes have the same sum rate.

4.4.2 Hybrid Interference Cancellation Scheme

For the HIC scheme, we also obtained the optimal repeat number and the spreading length profile, which gave the maximum sum rate (Table 4.2). The gaps between the thresholds of our

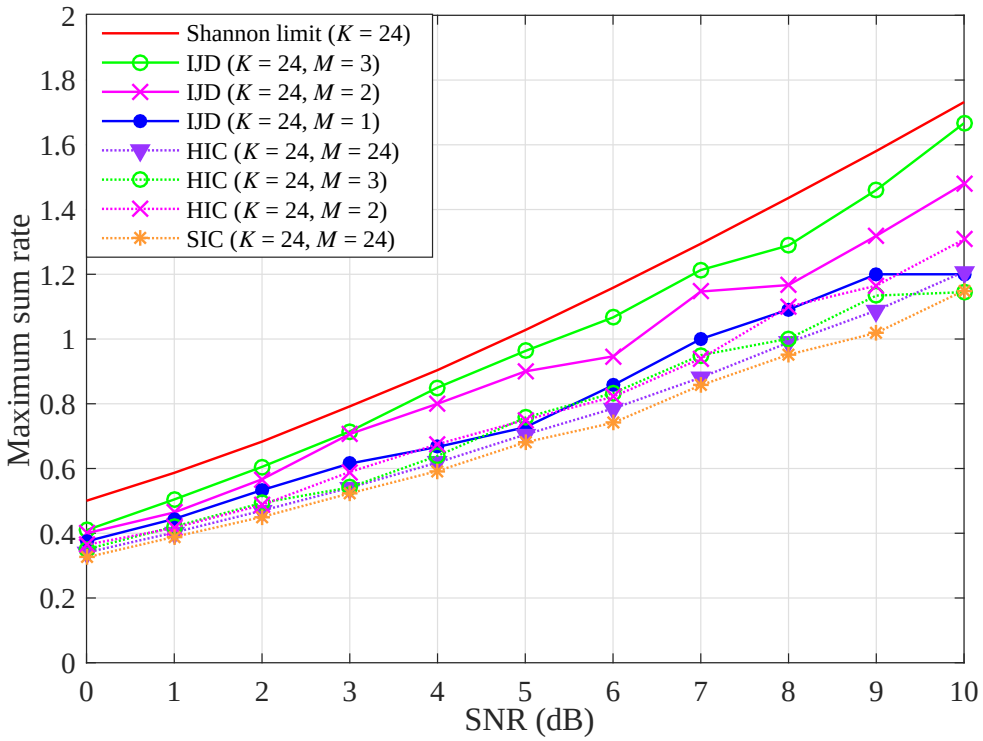

Figure 4.11: Maximum sum rate of K-user multi-rate code under IJD, HIC, and SIC schemes for $K = 24$ and $M = 1, 2, 3, 24$

optimized K-user multi-rate codes and the Shannon limit are less than 3 dB. In contrast to the IJD scheme, the maximum sum rate did not improve with M increments.

When $M = 12$ and SNR = 2 dB, we obtained $(q_2^*, L_2^*) = (q_3^*, L_3^*) = (q_4^*, L_4^*) = (5, 7)$, and $(q_8^*, L_8^*) = (q_9^*, L_9^*) = (6, 4)$. In fact, this is a 9-group rate profile, i.e., $M_{\text{true}} = 9$, since our HIC scheme allows $R_1 \leq \cdots \leq R_M$. Our HIC scheme is superior to a pure SIC scheme [1, 44] in the maximum sum rate and the gap between the threshold and Shannon limit (Table 4.2), since the SIC scheme is limited to $R_1 < \cdots < R_M$ when the power allocation is equal.

We also give the Monto Carlo simulation of our optimized K-user multi-rate codes in Figs. 4.8 and 4.9. The same parameters were set with the IJD scheme. The total number of iterations was $L_{\text{HIC}} = ML_{\text{HIC}}^{\text{G}}$, where $L_{\text{HIC}}^{\text{G}}$ is the number of decoding iterations within the groups in the mth step, $1 \leq m \leq M$. When $L_{\text{HIC}} = L_{\text{IJD}}$, the decoding complexity of the HIC scheme was reduced to $1/M$

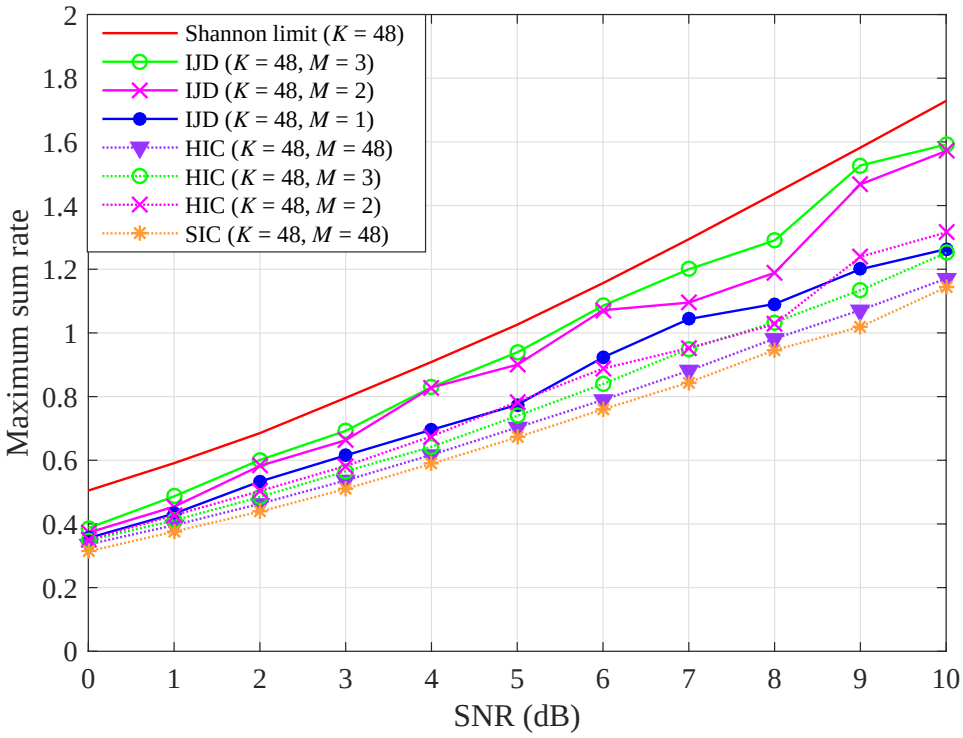

Figure 4.12: Maximum sum rate of K-user multi-rate code under IJD, HIC, and SIC schemes for $K = 48$ and $M = 1, 2, 3, 48$

of the IJD scheme's (see Appendix B). In Figs. 4.8 and 4.9, the BER curves of our optimized codes still converged well to their thresholds. This means that the design of our K-user multi-rate code for the HIC scheme is accurate.

4.4.3 Comparison

The maximum sum rates illustrated in Tables 4.1 and 4.2 are only at SNR = 2, 4, 6 dB. We also give a graphical representation at SNR from 0 to 10 dB with 1-dB intervals for $K = 12$, 24, and 48 in Figs. 4.10, 4.11, and 4.12.

For the IJD scheme, we observed that with the increment of groups M, the maximum sum rates increase and approach the Shannon limit. The gap between the curve of the maximum sum rate and the Shannon limit is within 1 dB in a large SNR range for $M = 3$. Moreover, the maximum

sum rates are higher than those of conventional equal rate transmission, i.e., $M = 1$. For the HIC scheme, the maximum sum rates are higher than those of the pure SIC scheme and lower than those of the IJD scheme. However, it provides much lower decoding complexity than the IJD scheme.

4.5 Conclusion

For a Gaussian MAC, we proposed a K-user multi-rate code with binary inputs, equal-power, and symbol synchronization. In this multi-rate transmission, we equally divided K users into M groups. For each user in the mth group, a code rate-$1/q_m$ regular RA code serially concatenated with a length-L_m spreading was employed. The transmission rate of each user was $R_m^{(1)} = \cdots = R_m^{(K/M)} \triangleq 1/(q_m L_m)$. At the receiver, the IJD and HIC schemes were performed on a single factor graph with a BP decoder. For each decoding scheme, we applied bivariate fixed-point analysis to explicitly represent (q_m, L_m) as a function of MI outputs by solving the mth pair-of-equations. Based on these basic explicit representations, from T corresponding simultaneous pairs-of-equations, we obtained a region of $((q_1, L_1), \cdots, (q_M, L_M))$ over which users in any T groups are undecodable. Then, a united (unreliable) region is given over which users in at least one group are undecodable. The reliable region, i.e., the complementary set of the united unreliable region, gives an optimal profile, $((q_1^*, L_1^*), \cdots, (q_M^*, L_M^*))$, that corresponds to optimal rate profile $(R_1^*, \cdots, R_M^*)$, which achieves the maximum sum rate.

Numerical results verified that the design of our K-user multi-rate code is accurate for both the IJD and HIC schemes. For the IJD scheme, with increments of groups M, the maximum sum rates of our K-user multi-rate codes increased and approached the Shannon limit, exceeding those of conventional equal rate transmissions. The HIC scheme provided much lower decoding complexity than the IJD scheme and outperformed the pure SIC scheme in maximum sum rate.

Chapter 5

Joint Rate and Power Optimization in Multi-User Communications

In this chapter, we also consider the multi-rate transmission in the multi-user systems but with the SIC decoding in the receiver. The SIC decoding has lower decoding complexity, compared with IJD and HIC schemes. We propose a joint rate and power optimization (RPO) to obtain the optimal rate and power profile, that achieves the optimal sum rate by the assumption of equal-ratio power allocation. Our RPO employs multiple equal-ratio power, and choose the optimal ratio, which gives the power profile well matched with the rate profile. It shows that our optimized multi-rate code with joint RPO, supporting the multi-rate transmission with the same structure of encoder, is close to the Shannon limit, and outperforms conventional rate-only optimization and power-only optimization.

5.1 Introduction

For non-orthogonal multiple access (NOMA) systems with successive interference cancellation (SIC), the Shannon limit can be achieved by power-only optimization (PO) as long as each user has an ideal channel code. Previous works [45–47] are mainly based on this assumption of ideal code. It is intuitively to think that code design for NOMA systems is not necessary, since each user

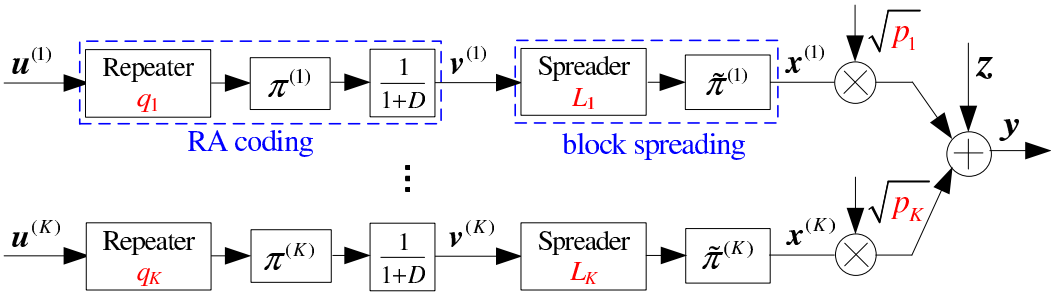

Figure 5.1: K-user multi-rate multi-power transmitters with multiple access channel

can employ the conventional well-designed channel codes directly.

However, NOMA systems need to support massive of users and multiple rates to meet the requirements for diverse services. An increase in the number of users will result in very serious multi-user interference, so that some users need low-rate codes to guarantee the decoding performance. Moreover, such systems should support various rates for the various multimedia services. Employing conventional well-designed low-rate LDPC or Turbo code, is impractical since users have to employ difference encoders to realize multi-rate transmission. It is required to design a bank of variable, low-rate channel codes with the same structure of encoder.

In this chapter, for K-user multi-rate multi-power NOMA systems with SIC, we use a repeat accumulator (RA) code serially concatenated with a spreading for each user to implement a variable, low-rate coding, where the transmission rate can be changed flexibly by varying the repeat number and spreading length. Here, users employ the identical RA encoder, although their transmission rates are different. Moreover, both RA and repetition (spreading) codes are simple and computationally efficient. To enhance the system performance, we propose a joint rate and power optimization (RPO) to maximize the sum rate. Numerical results show that our proposed coding-spreading scheme with joint RPO, supporting the multi-rate transmission with the same structure of encoder, approaches the Shannon limit.

5.2 System Model

In this chapter, we simply introduce K-user multi-rate multi-power NOMA systems in Fig. 5.1.

5.2.1 Coding Scheme

Suppose there are K active users simultaneously transmitted information to a base station. The length-n_k information bit vector $\boldsymbol{u}^{(k)} = (u_1^{(k)}, \cdots, u_{n_k}^{(k)})$, $u_i^{(k)} \in \{0, 1\}$, $1 \leq i \leq K_k$, of the kth ($1 \leq k \leq K$) user, is first encoded by a regular RA code, which is a serial concatenation of a code rate-$1/q_k$ repeater with a $1/(1 + D)$ accumulator linked by interleaver $\pi^{(k)}$. The output coded vector is denoted as $\boldsymbol{v}^{(k)} = (v_1^{(k)}, \cdots, v_{K_k q_k}^{(k)})$, $v_t^{(k)} \in \{0, 1\}$, $1 \leq t \leq K_k q_k$. A block spreading, which consists of bit spreading and chip-level interleaving, is then performed on $\boldsymbol{v}^{(k)}$. Each bit of $\boldsymbol{v}^{(k)}$ is spread by length-l_k sequence $\boldsymbol{s}^{(k)}$ into vector $(1 - 2v_t^{(k)})\boldsymbol{s}^{(k)}$. Here, $\boldsymbol{s}^{(k)} = (s_1^{(k)}, \cdots, s_{l_k}^{(k)})$ with $s_{2m-1}^{(k)} = +1, s_{2m}^{(k)} = -1, 1 \leq m \leq \lfloor \frac{l_k+1}{2} \rfloor$, where $\lfloor p \rfloor$ is the greatest integer less than or equal to p. The spreader output is a length-$K_k q_k l_k$ sequence, which is referred to as a chip sequence. After spreading, user-specific chip-level interleaver $\tilde{\pi}^{(k)}$ with length-$K_k q_k l_k$ is employed to produce transmitted signal vector $\boldsymbol{x}^{(k)} = (x_1^{(k)}, \cdots, x_{K_k q_k l_k}^{(k)})$. The kth user's transmission rate is $r_k = 1/(q_k l_k)$. Note that although the transmission rates of different users vary, it is not difficult to have identical length N by an adjustment of information bit lengths K_k, i.e., $K_k q_k l_k \triangleq N$, to realize multi-rate transmission. The sum rate is $R_{sum} = \sum_{k=1}^{K} r_k$. The symbols and codeword synchronisation are assumed. Let p_k be the transmission power of the kth user. The total power is $P_{sum} = \sum_{k=1}^{K} p_k$. The receiver gets a superimposed signal vector $\boldsymbol{y} = (y_1, \cdots, y_N)$ at time j is

$$y_j = \sum_{k=1}^{K} \sqrt{p_k} x_j^{(k)} + z_j, \ \ j = 1, \cdots, N. \tag{5.1}$$

where z_j is a zero-mean Gaussian variable with a variance of σ^2, i.e., $\mathrm{E}(z_j) = 0, \mathrm{Var}(z_j) = \sigma^2$.

5.2.2 Successive Interference Cancellation Scheme

An SIC receiver decodes the K users' information successively [1]. Suppose the decoding is in order of increasing user index. For the kth user, after recovering the information of the first $k - 1$

users, the corresponding replicas of signals are generated and subtracted from the received signal. The remaining received signal is given by

$$y_j^{(k)} = \sqrt{p_k} x_j^{(k)} + \omega_j^{(k)} + z_j \tag{5.2}$$

where $y_j^{(1)} = y_j$ in (5.1), and $\omega_j^{(k)} = \sum_{k'=k+1}^{K} \sqrt{p_{k'}} x_j^{(k')}$. From this remaining received signal, the kth user's information is decoded by treating the signals of remaining $K-k$ users as interferences with power $\varsigma_k = \sum_{k'=k+1}^{K} p_{k'}$. Subsequently, BP decoding is performed at the part of block spreading and RA coding. Then, hard decisions are made to recover the kth user's information. This process is performed successively until all the users' information has been recovered.

5.3 Joint Rate and Power Optimization

In this chapter, for given number of users K, total power P_{sum}, and noise power σ^2, we gives the optimal rate and power profile, which achieves the maximum sum rate of multi-rate multi-power NOMA system with error free decoding.

5.3.1 EXIT Function for a single-user system

Before proceeding, let us consider a single-user system with a rate-$1/q$ regular RA code serially concatenated with a length-l spreading under the interference power ς and noise power σ^2. For a given transmission power p, we find an optimal pair of (q^*, l^*) that gives the maximum transmission rate of $1/(q^* l^*)$ with error free decoding. Specifically, for the single-user system with a pair of (q, l) and signal-to-interference-plus-noise ratio (SINR) $p/(\varsigma + \sigma^2)$, we draw an EXIT chart. The decoding is successful if there is a clear swath between the curves in the chart [34]. Since the transmission rate must be less the AWGN channel capacity, the successful pair of (q, l) must fall in $1/(ql) \leq C(p/(\varsigma + \sigma^2))$, where $C(x) = 0.5 \log_2(1 + x)$ is the channel capacity with SINR x. The maximum transmission rate of $1/(q^* l^*)$ gives the optimal pair of (q^*, l^*). Hereafter, for simplicity's sake, we still use (q, l) to represent the optimal pair of (q^*, l^*).

5.3.2 Equal-Ratio Power Allocation

Now, let us turn back to our multi-rate multi-power NOMA system. As stated in Section 5.2, the SIC receiver decodes the K users' information in the order of increasing user index by assumption. For the kth user, we assume that the information bits of the first $k-1$ users are error-freely recovered, and their corresponding signals are completely removed from the received signal. From the remaining received signal, the receiver decodes the kth user's information bits, by regarding signals from the remaining $K-k$ users as interference with power $\varsigma_k = \sum_{k'=k+1}^{K} p_{k'}$.

For the joint optimization of rate and power profile, let us first consider the K real powers. Multi-user information theory tells us that an arbitrary power allocation can provide the sum rate to approach the capacity of K-user Gaussian multiple access channel [1]

$$\sum_{k=1}^{K} C\left(\frac{p_k}{\sum_{k'=k+1}^{K} p_{k'} + \sigma^2}\right) = C\left(\frac{\sum_{k=1}^{K} p_k}{\sigma^2}\right). \tag{5.3}$$

if K optimal random codes are used. This implies a reasonable assumption of a equal-ratio power allocation, i.e.,

$$p_k / p_{k+1} = \mu. \tag{5.4}$$

Since $P_{sum} = \sum_{k=1}^{K} p_k$, we have

$$p_k = \begin{cases} \mu^{K-k} \cdot \dfrac{1-\mu}{1-\mu^K} P_{sum}, & \mu \neq 1 \quad (5.5a) \\ \dfrac{P_{sum}}{K}, & \mu = 1 \quad (5.5b) \end{cases}$$

with $k = 1, \cdots, K$.

For the kth user with interference power ς_k, given power p_k in (5.5), the EXIT chart analysis (see above) give the optimal (q_k, l_k) that provides the maximum rate $1/(q_k l_k)$ in SINR_k $p_k/(\varsigma_k + \sigma^2)$. Since this optimization is given at the power ratio of μ, hereafter we denote this optimal rate and power profile by $\Omega^\mu \triangleq ((q_1^\mu, l_1^\mu, p_1^\mu), \cdots, (q_K^\mu, l_K^\mu, p_K^\mu))$, that provides the corresponding maximum sum rate $R_{max}^\mu = \sum_{k=1}^{K} 1/(q_k^\mu l_k^\mu)$.

5.3.3 Optimal Rate and Power Profile and Optimal Sum Rate

The assumption of the equal-ratio power allocation above is based on the optimal random codes which are theoretically used to approach the channel capacity. The random codes have arbitrary rates and thus are flexible to their corresponding real powers. In our work, each user employs RA code concatenated with spreading. The kth user's transmission rate $1/(q_k l_k)$ is discrete with the restriction of integers q_k and l_k. Therefore, the simple equal-ratio power allocation above may results in a sum-rate loss. For this reason, we set $\mu \in [\mu_{min}, \mu_{max}]$. Over this range, we obtain the optimal rate and power profile Ω^{μ^*} as

$$\Omega^{\mu^*} = ((q_1^{\mu^*}, l_1^{\mu^*}, p_1^{\mu^*}), \cdots, (q_K^{\mu^*}, l_K^{\mu^*}, p_K^{\mu^*})) = \arg \max_{\mu \in [\mu_{min}, \mu_{max}]} \sum_{k=1}^{K} \frac{1}{q_k^{\mu} l_k^{\mu}} \tag{5.6}$$

which gives the optimal sum rate $R_{sum}^{\mu^*} = \sum_{k=1}^{K} 1/(q_k^{\mu^*} l_k^{\mu^*})$ with error free decoding.

We determine the values of μ_{max} and μ_{min}. Assume that our multi-rate multi-power NOMA system has a minimum transmission rate requirement of r_{min} for each user. Let $\mu_{er} = \sqrt[K]{P_{sum}/\sigma^2 + 1}$, where users have the identical SINR, corresponding to the identical transmission rate [1]. For $\mu > \mu_{er}$, it holds that $\mathrm{SINR}_1 > \cdots > \mathrm{SINR}_K$, i.e., the Kth user has the minimum achievable rate of $C(\mathrm{SINR}_K)$. Let $r_{min} + \Delta r = C(\mathrm{SINR}_K) = C\left(\frac{1-\mu}{1-\mu^K} \cdot \frac{P_{sum}}{\sigma^2}\right)$. The solution μ_{max} is obtained for given r_{min} and Δr, where Δr is a given small positive offset between the achievable rate of the RA concatenated with spreading scheme and an ideal channel coding scheme. Similarly, for $\mu < \mu_{er}$, it holds that $\mathrm{SINR}_1 < \cdots < \mathrm{SINR}_K$. Let $r_{min} + \Delta r = C(\mathrm{SINR}_1)$, the solution μ_{min} is obtained for given r_{min} and Δr.

For our multi-rate multi-power NOMA system, the threshold of the decoding is the minimum SNR that makes our multi-rate multi-power code with Ω^{μ^*} is error-free, i.e.,

$$\mathrm{SNR}_{\mathrm{th}} = 10 \cdot \log_{10} \frac{P_{sum}}{\sup\{\sigma^2 \mid \Omega^{\mu^*}\}} \text{ [dB]}. \tag{5.7}$$

In our RPO, there are two special cases. When $\mu = 1$, users have the same power, and only rate profile is optimised [48]. In the case of each user's rate being the same, information theory shows that its optimized power profile satisfies (5.4) with $\mu = \mu_{er}$ [49].

Table 5.1: Optimal rate and power profiles

SNR	Sch.	$\Omega^{\mu} = \left((q_1^{\mu}, l_1^{\mu}, p_1^{\mu}), \cdots, (q_K^{\mu}, l_K^{\mu}, p_K^{\mu})\right)$	R_{sum}^{μ}	SNR_{th}	S. L.	Gap
2	RPO	(5, 42, 0.20), (5, 32, 0.25), (5, 25, 0.32), (5, 19, 0.41), (5, 15, 0.51), (5, 11, 0.65), (5, 8, 0.82), (5, 6, 1.04), (4, 6, 1.32), (5, 3, 1.67), (5, 2, 2.12), (6, 1, 2.68)	0.4944	2.03	-0.07	2.10
	RO	(4, 10, 1.00), (4, 10, 1.00), (5, 7, 1.00), (5, 7, 1.00) (5, 6, 1.00), (5, 6, 1.00), (4, 7, 1.00), (6, 4, 1.00) (4, 6, 1.00), (5, 4, 1.00), (6, 3, 1.00), (6, 3, 1.00)	0.4540	1.94	-0.57	2.51
	PO	(5, 5, 1.47), (5, 5, 1.37), (5, 5, 1.26), (5, 5, 1.17), (5, 5, 1.08), (5, 5, 1.00), (5, 5, 0.93), (5, 5, 0.86), (5, 5, 0.80), (5, 5, 0.74), (5, 5, 0.68), (5, 5, 0.63)	0.4800	1.86	-0.24	2.30
4	RPO	(5, 32, 0.22), (5, 25, 0.28), (5, 19, 0.35), (5, 15, 0.43), (4, 15, 0.54), (5, 9, 0.68), (5, 7, 0.84), (5, 5, 1.06), (6, 3, 1.32), (6, 2, 1.65), (4, 2, 2.06), (4, 1, 2.58)	0.6595	3.99	1.75	2.24
	RO	(5, 7, 1.00), (5, 6, 1.00), (5, 6, 1.00), (4, 7, 1.00), (5, 5, 1.00), (4, 6, 1.00), (5, 4, 1.00), (6, 3, 1.00), (6, 3, 1.00), (5, 3, 1.00), (6, 2, 1.00), (5, 2, 1.00)	0.6237	4.03	1.38	2.65
	PO	(4, 5, 1.68), (4, 5, 1.50), (4, 5, 1.35), (4, 5, 1.22), (4, 5, 1.10), (4, 5, 0.99), (4, 5, 0.89), (4, 5, 0.80), (4, 5, 0.72), (4, 5, 0.65), (4, 5, 0.59), (4, 5, 0.53)	0.6000	1.13	3.64	2.51

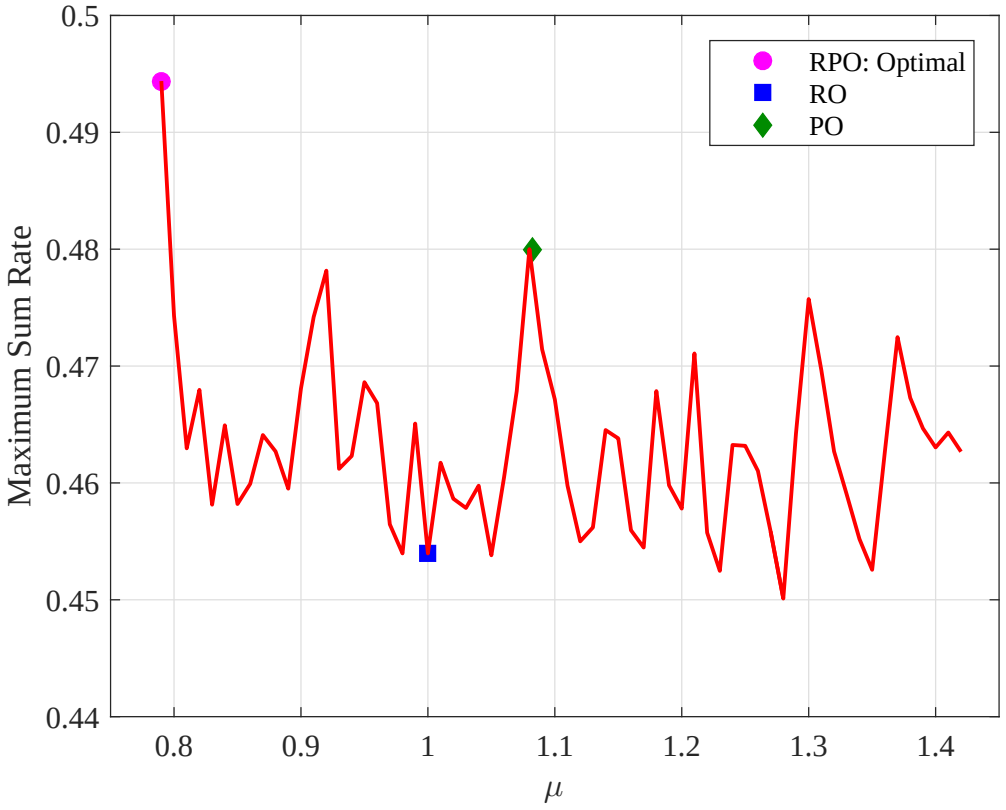

Figure 5.2: Maximum sum rate R^{μ}_{sum} and gap for $K = 12$, SNR = 2 dB

5.4 Numerical Results

In this section, we present some numerical results by the above joint RPO. In our numerical computation, we set $K = 12$, $P_{sum} = 12$, $r_{min} = 0.01$, and $\Delta r = 0.005$.

Let's set SNR $= P_{sum}/\sigma^2 = 2$ dB. Our RPO provides sum rate R^{μ}_{sum} for $\mu \in [\mu_{min} = 0.79, \mu_{max} = 1.42]$ with intervals $\Delta\mu = 0.01$ (see Fig. 5.2). Among R^{μ}_{sum}, $R^{\mu^*}_{sum} = 0.4944$ is the maximum at $\mu^* = 0.79$ and thus is the optimal sum rate with the minimum gap of 2.10 dB. The corresponding optimal rate and power profile Ω^{μ^*} and it's threshold are illustrated in Table 5.1. In Ω^{μ^*}, the first user's transmission rate of 0.0048 is very low, which is implemented by the rate-1/5 RA code and the length-42 spreading.

Also in Fig. 5.2 and Table 5.1, the rate-only optimization (RO) [48] ($\mu = 1.00$, equal power) gives sum rate $R^{\mu}_{sum} = 0.4540$, the gap of 2.51 dB, and the corresponding optimal profile. On the

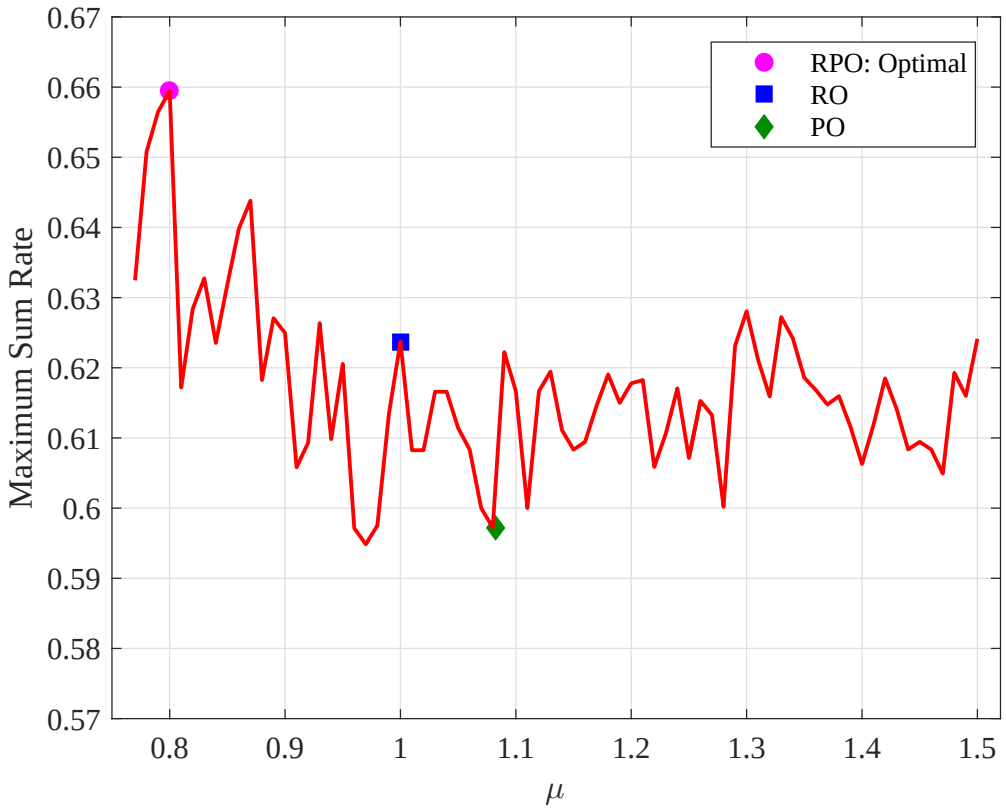

Figure 5.3: Maximum sum rate R^{μ}_{sum} and gap for $K = 12$, SNR = 4 dB

other hand, the power-only optimization (PO) [49] ($\mu = 1.08$, equal rate) also gives these optimal values. Compared with RO and PO, our RPO improves the maximum sum rate by 0.0404 and 0.0144, and decreases the gap by 0.41 and 0.20 dB, respectively. The reason is that RPO employs multiple equal-ratio power μ, and choose the optimal ratio μ^*, which gives the power profile well matched with the rate profile, and compensates the sum-rate loss due to the restriction of discrete rates of RA code and spreading.

In addition, at SNR = 4 dB, we obtain the optimal profile in Table 5.1. Our optimal sum rate and gap are superior to those of RO and PO (see Fig. 5.3).

The maximum sum rate illustrated in Table 5.1 are only at SNR = 2 and 4 dB. We also give a graphical representation of maximum sum rate R^{μ}_{sum} at SNR from 0 to 20 dB with 1-dB intervals in Fig. 5.4. We observed that our RPO outperforms RO and PO.

It is interesting to give a comparison of sum rates between the coding-spreading and coding-

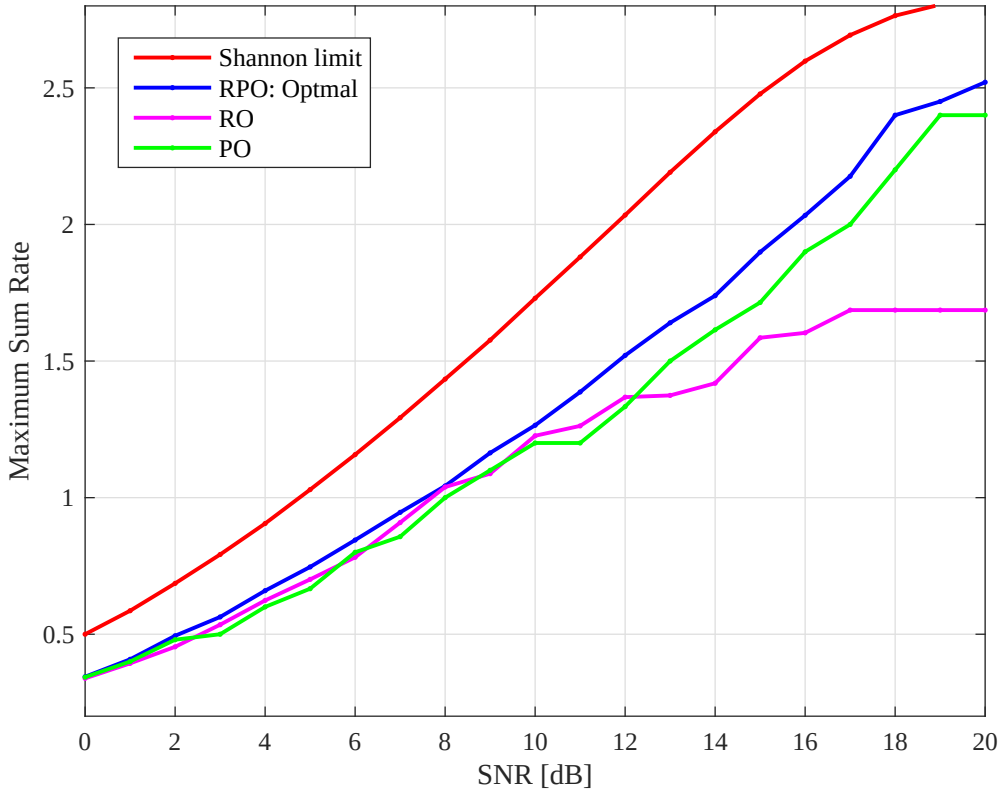

Figure 5.4: Maximum sum rate R_{sum}^{μ} for $K = 12$

only in Fig. 5.5. In the coding-only system, user only employ a RA code ($l = 1$), where the repetition number q is optimized. Obviously, our coding-spreading scheme outperforms the coding-only scheme, especially in the lower SINR of $p/(\varsigma + \sigma^2)$. This is the reason why we employ coding-spreading instead of coding-only in our K-user system. Note that, in the coding-only scheme, employing some conventional well-designed low-rate LDPC or Turbo codes, may also approach the Shannon limit, but is impractical since users have to employ difference encoders.

We also give a comparison of maximum sum rates between the IJD, HIC schemes, as stated in Chapter 4, and our RPO scheme, i.e., SIC/power scheme, for $K = 12$ in Fig. 5.6. We observed that the maximum sum rate of our SIC/power scheme superior to that of HIC scheme, and approach that of IJD scheme.

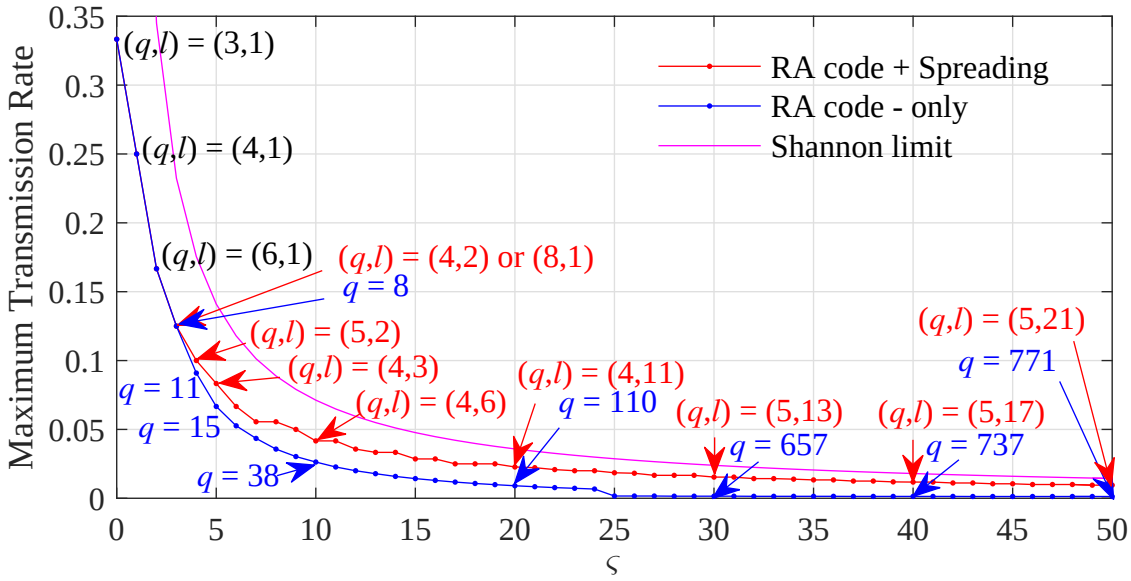

Figure 5.5: Maximum transmission rate for $K = 1$, $p = 1$, SNR = 2 dB

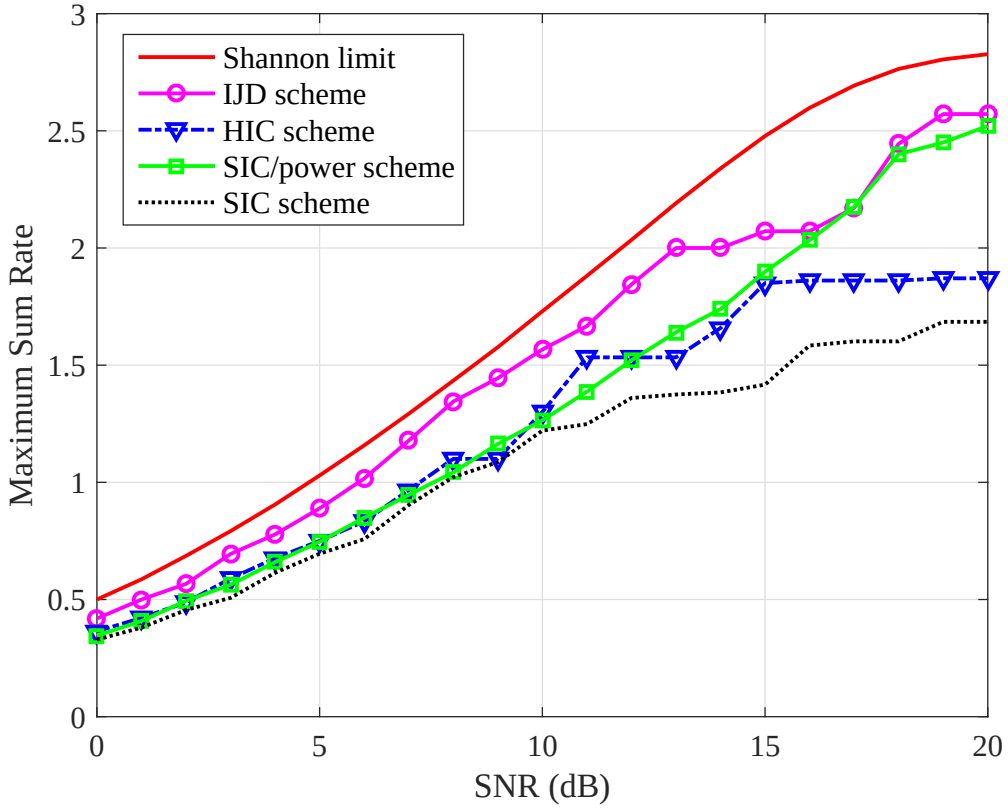

Figure 5.6: The comparison of maximum sum rate for $K = 12$

5.5 Conclusions

In multi-rate multi-power NOMA system with SIC, we employed an RA code serially concatenated with a spreading for each user to implement a variable, low-rate coding. We proposed a joint RPO to maximize the sum rate with error free decoding. Numerical results show that our proposed coding-spreading scheme with joint RPO, supporting the multi-rate transmission with the same structure of encoder, approaches the Shannon limit.

For multi-rate coding scheme with IJD, HIC, and SIC/power schemes, if power control is considered, the SIC/power is optimal, since it has the lowest decoding complexity. If power control is not considered, the IJD scheme is optimal in maximum sum rate, while the HIC scheme provides much lower decoding complexity with little degradation in maximum sum rate.

Chapter 6

Concluding Remarks

In multi-rate communication systems, a central problem is to assign K constituent code to K transmitters so that they can communicate simultaneously, at various transmission rates, with a common receiver through the Gaussian MAC. However, it is impractical for users to employ different encoders.

In this dissertation, we proposed multi-rate coding schemes for Gaussian MAC. In our schemes, each user employs a same structure of encoder serially concatenated with a spreader and a user-specific interleaver. Here, the different interleavers are used for user separation, and the spreader is employed to lower the transmission rate and thus to combat the multi-user interference. The different rate transmission is realized by adjusting the parameter of the encoder and the length of spreading. We analyzed the decoding performances of our coding schemes, and obtained the optimal coding parameters and spreading lengths, which gives the maximum sum rates and approach the theoretical limits of the channel. The proposed coding schemes support multimedia services, and avoid employing multiple channel encoders to implement the multi-rate transmission.

Our three multi-rate coding schemes, roughly speaking, have almost the same structure with the same encoder, spreader, and interleaver. We discuss the optimization of the multi-rate coding based on three decoding algorithms employed in the multiple access communication systems. The three decoding algorithms are the belief propagation (BP) with the maximum a priori (MAP) detection, elementary signal estimation (ESE), and successive interference cancellation (SIC).

First, for the multi-rate transmission in two-user multiple access communication systems with the MAP detection, the same RA encoder but with different parameters, i.e., the repeat numbers, in the encoder, is employed for each user. Here, the coding-only (without spreading) scheme is performed, since multi-user interference is small for two users. At the receiver, the BP decoding on a single factor graph is performed, where at sum (two-user superimposed signals) node, the MAP detection is carried out. A univariate fixed point analysis is developed to obtain a system equation array of parameters of RA codes. This makes it possible to represent the parameters of RA codes explicitly as functions of the fixed point. The optimal parameters of RA codes is found to give the maximum sum rate. Our optimized two-user multi-rate RA code is superior to the conventional equal rate code in maximum sum rate, and approach the Shannon limit.

Second, for the multi-rate transmission in multi-user multiple access communication systems with the ESE detection, K users are equally divided into multiple groups, and users in identical group has a same transmission rate. For each user, a RA code serially concatenated with a spreading sequence and a user-specific interleaver pattern is employed to implement various rates by adjusting both repeat number in RA encoder and length of spreading in spreader. Here, the interleaver patterns are different for user sepatation, and the spreading sequence is to lower the rate and thus to combat the user interference, since an increase in the number of users results in very serious multi-user interference. At the receiver, a joint iterative BP decoding (Iterative Joint Decoding, IJD) on a single factor graph is performed, where at sum (multi-user superimposed signals) node, the ESE detection is carried out. A bivariate fixed point analysis is developed to obtain the optimal parameters (repeat numbers) of RA code and spreading lengths, which give the maximum sum rate. With the increment of groups, the maximum sum rates of our optimized multi-rate code increase, and approach the Shannon limit, and exceeds those of conventional equal-rate transmission.

Instead of global IJD above, in the receiver hybrid interference cancellation (HIC) decoding is also performed, where SIC is employed between the groups, and IJD is employed within the group. The HIC scheme provides much lower decoding complexity than the global IJD scheme with little degradation in the maximum sum rate, and outperforms the pure SIC scheme.

Finally, we also consider the multi-rate transmission in the multi-user systems but with the

SIC decoding. The SIC decoding has lower decoding complexity, compared with IJD and HIC schemes. The optimal rate and power profile is given and provides the sum rate which approach the Shannon limits.

We now briefly summarize our contributions. We have proposed the multi-rate coding schemes for the Gaussian MAC, and analytically gave the maximum sum rate which approach the theoretical limits of the channel. The proposed multi-rate coding schemes support multimedia services in practical communication systems.

Acknowledgments

The author would like to thank her advisor, Prof. Jun Cheng, for his continual guidance and suggestions during this work. Without his insightful instructions and constant support, it would be impossible to complete this work.

The author also wishes to express her heartfelt thanks and appreciation to Prof. Y. Watanabe, Prof. Ying Li, and Prof. Li Ping for their guidance and suggestion.

The author is also very grateful to Dr. G. Song in her laboratory, who collaborated to this research work. The author is delighted to thank the members of her laboratory, Dr. S. Lu, Dr. W. Hou, Mr. Y. Ren, Mr. S. Liu, and Mr. H. Han. A number of valuable discussions with them are acknowledged.

The scholarships supplied by Ministry of Education, Culture, Sports, Science and Technology (MEXT) and Doshisha University are the financial support to the author during this work.

Finally, the author would like to thank her parents, her husband, and her son for their loving considerations, great confidence, and continuing support throughout this work.

Bibliography

[1] T. M. Cover and J. A. Thomas, *Elements of Information Theory*, John Wiley and Sons, Inc., 2006.

[2] C. Schlege, Z. Shi, and M. Burnashev, "Optimal power/rate allocation and code selection for iterative joint detection of coded random CDMA," *IEEE Trans. Inf. Theory*, vol. 52, no. 9, pp. 2657-2673, Sep. 2006.

[3] R. Zhang and L. Hanzo, "EXIT chart based joint code-rate and spreading-factor optimisation of single-carrier interleave division multiple access," in *Proc. IEEE WCNC*, 2007, pp. 735-739.

[4] R. Zhang and L. Hanzo, "Three design aspects of multicarrier interleave division multiple access," *IEEE Trans. Veh. Technol.*, vol. 57, no. 6, pp. 3607-3617, Nov. 2008.

[5] G. Song, Y. Tsujii, J. Cheng, and W. Yoichiro, "Finite field spreading for multiple-access channel," *IEEE Trans. Commun.*, vol. 62, no. 3, pp. 1001-1010, 2014.

[6] G. Song, J. Cheng, and Y. Watanabe, "Maximum sum rate of repeat-accumulate interleave-division system by fixed-point analysis," *IEEE Trans. Commun.*, vol. 60, no. 10, pp. 3011-3022, Oct. 2012.

[7] G. Song and J. Cheng, "K-user parallel concatenated code for multiple-access channel," *IEICE Trans. Fundamentals*, vol. E98-A, no. 9, pp. 1953-1963, 2015.

[8] G. Song and J. Cheng, "Low-complexity coding scheme to approach multiple-access channel capacity," *Proc. IEEE Int. Symp. on Information Theory*, pp. 2106-2110, HongKong, China, June 2015.

[9] T. Yang, J. H. Yuan, and Z. N. Shi, "Rate optimization for IDMA systems with iterative joint multi-user decoding," *IEEE Trans. Wireless Commun.*, vol. 8, no. 3, pp. 1148-1153, Mar. 2009.

[10] T. J. Richardson, A. Shokrollahi, and R. L. Urbanke, "Design of capacity-approaching low-density parity-check codes," *IEEE Trans. Inf. Theory*, vol. 47, no. 2, pp. 619-637, Feb. 2001.

[11] F. R. Kschischang, B. J. Frey, and H. A. Loeliger, "Factor graphs and the sum-product algorithm," *IEEE Trans. Inf. Theory*, vol. 47, no. 2, pp. 498-519, 2001.

[12] T. J. Richardson and R. Urbanke, *Modern Coding Theory.*, Cambridge, Cambridge University Press, 2008.

[13] T. J. Richardson and R. L. Urbanke, "The capacity of low-density parity-check codes under message-passing decoding," *IEEE Trans. Inf. Theory*, vol. 47, no. 2, pp. 599-618, Feb. 2001.

[14] A. Ashikhmin, G. Kramer, and S. ten Brink, "Extrinsic information transfer functions: model and erasure channel properties," *IEEE Trans. Inf. Theory*, vol. 50, no. 11, pp. 2657-2673, Nov. 2004.

[15] S. ten Brink, "Convergence behavior of iteratively decoded parallel concatenated codes," *IEEE Trans. Commun.*, vol. 49, no. 10, pp. 1727-1737, Oct. 2001.

[16] S. Y. Chung, T. J. Richardson, and R. L. Urbanke, "Analysis of sum-product decoding of low-density parity-check codes using a Gaussian approximation," *IEEE Trans. Commun.*, vol. 47, no. 2, pp. 657-670, Feb. 2001.

[17] S. ten Brink and G. Kramer, "Design of repeat-accumulate codes for iterative detection and decoding," *IEEE Trans. Signal Process.*, vol. 51, no. 11, pp. 2764-2772, Nov. 2003.

[18] W. E. Ryan and S. Lin, *Channel Codes: Classical and Modern*, Cambridge University Press, 2009.

[19] S. ten Brink, G. Kramer, and A. Ashikhmin, "Design of low-density parity-check codes for modulation and detection," *IEEE Trans. Commun.*, vol. 52, no. 4, pp. 670-678, Apr. 2004.

[20] E. Sharon, A. Ashikhmin, and S. Litsyn, "EXIT functions for the Gaussian channel," in *Proc. 40th Annu. Allerton Conf. on Communication, Control, Computer*, Allerton, IL, Oct. 2003, pp. 972-981.

[21] E. Sharon, A. Ashikhmin, and S. Litsyn, "EXIT functions for binary input memoryless symmetric channels," *IEEE Trans. Commun.*, vol. 54, no. 7, pp. 1207-1214, Jul. 2006.

[22] B. Rimoldi and R. Urbanke, "A rate-splitting approach to the Gaussian multiple-access channel," *IEEE Trans. Inf. Theory*, vol. 42, no. 2, pp. 364-375, Mar. 1996.

[23] R. Ahlswede, "Multi-way communication channels," in *Proceedings of the 2nd IEEE International Symposium on Information Theory (ISIT'71)*, pp. 23-52, Aremenian Prague, Czech Republic, 1971.

[24] H. Liao, *Multiple access channels*, Ph.D. dissertation, Dept. Elec. Eng., University of Hawaii, Honolulu, Hawaii, USA, 1972.

[25] A. Roumy, D. Declercq and E. Fabre, "Low complexity code design for the 2-user Gaussian multiple access channel," in *Proc. IEEE ISIT*, 2004, p. 481.

[26] A. Roumy and D. Declercq, "Characterization and optimization of LDPC codes for the 2-user Gaussian multiple-access channel," *EURASIP Journal on Wireless Communications and Networking*, vol. 2007, ID: 74890, 2007.

[27] D. Divsalar, H. Jin, and R. J. McEliece, "Coding theorem for turbo-like codes," in *Proc. Annu. Allerton Conf. Commun. Control, Comput.*, 1998, pp. 201-210.

[28] S. J. Johnson, *Iterative error correction.*, Cambridge, Cambridge University Press, 2010.

[29] S. Verdu, "The capacity region of the symbol-asynchronous Gaussian multiple-access channel," *IEEE Trans. Inf. Theory*, vol. 35, no. 4, pp. 733-751, Jul. 1989.

[30] S. Kudekar and K. Kasai, "Spatially coupled codes over the multiple access channel," in *Proc. IEEE ISIT*, 2011, pp. 2816-2820.

[31] A. Yedla, P. S. Nguyen, H. D. Pfister, and K. R. Narayanan, "Universal codes for the Gaussian MAC via spatial coupling," in *Proc. Forty-Ninth Annual Allerton Conference Allerton House, UIUC, Illinois, USA*, 2011, pp. 1801-1808.

[32] V. V. Veeravalli and A. Mantravadi, "The coding-spreading tradeoff in CDMA systems," *IEEE J. Sel. Areas Commun.*, vol. 20, no. 2, pp. 396-408, Feb. 2002.

[33] S. Verd*ú* and S. Shamai, "Spectral efficiency of CDMA with random spreading," *IEEE Trans. Inf. Theory*, vol. 45, no. 2, pp. 622-640, Mar. 1999.

[34] G. S. Yue and X. D. Wang, "Coding-spreading tradeoff in LDPC-coded CDMA with Turbo multiuser detection," *IEEE Trans. Wireless Commun.*, vol. 3, no. 5, pp. 1734-1745, Sep. 2004.

[35] W. K. Leung, L. H. Liu, and P. Li, "Interleaving-based multiple access and iterative chip-by-chip multi-user detection," *IEICE Trans. Commun.*, vol. E86-B, no. 12, pp. 3634-3637, Dec. 2003.

[36] P. Li, L. H. Liu, K. Y. Wu, and W. K. Leung, "Interleaving-division multiple access," *IEEE Trans. Wireless Commun.*, vol. 5, no. 4, pp. 938-947, Apr. 2006.

[37] G. Song, J. Cheng, and W. Yoichiro, "Spreading and interleaving design for synchronous interleave-division multiple-access," *IEICE Trans. Fundamentals.*, vol. E95-A, no. 3, pp. 646-656, 2012.

[38] T. Ojanpera and R. Prasad, "An overview of air interface multiple access for IMT-2000/UMTS," *IEEE Commun. Mag.*, vol. 38, no. 10, pp. 82-95, Sep. 1998.

[39] J. F. Huber, D. Weiler, and H. Brand, "UMTS, the mobile multimedia vision for IMT-2000: A focus on standardization," *IEEE Commun. Mag.*, vol. 38, no. 9, pp. 129-136, Sep. 2000.

[40] C. Berrou and A. Glavieux, "Near optimum error correcting coding and decoding: turbo-codes," *IEEE Trans. Commun.*, vol. 44, no. 10, pp. 1261-1271, Oct. 1996.

[41] H. Jin and R. J. McEliece, "General coding theorems for turbo-like codes," in *Proc. IEEE ISIT*, 2000, pp. 201-210.

[42] K. Li, X. Wang, and P. Li, "Analysis and optimization of interleave-division multiple-access communication systems," *IEEE Trans. Wireless Commun.*, vol. 6, no. 5, pp. 1973-1983, May 2007.

[43] P. Patel and J. Holtzman, "Analysis of a simple successive interference cancellation scheme in a DS/CDMA system," *IEEE J. Select. Areas Commun.*, vol. 12, no. 5, pp. 796-807, Jun. 1994.

[44] David Tse and P. Viswanath, *Fundamentals of Wireless Communication*, Cambridge, Cambridge University Press, 2005.

[45] Y. Saito, Y. Kishiyama, A. Benjebbour, T. Nakamura, A. Li, and K. Higuchi, "Non-orthogonal multiple access (NOMA) for cellular future radio access," in *Proc. IEEE VTC spring 2013*, June 2013, pp. 1-5.

[46] Z. Ding, Z. Yang, P. Fan, and H. V. Poor, "On the performance of non-orthogonal multiple access in 5G systems with randomly deployed users," *IEEE Signal Process. Lett.*, vol. 21, no. 12, pp. 1501-1505, Dec. 2014.

[47] L. Dai, B. Wang, Y. Yuan, S. Han, C.-I. I, and Z. Wang, "Non-orthogonal multiple access for 5G: Solutions, challenges, opportunities, and future research trends," *IEEE Commun. Mag.*, vol. 53, no. 9, pp. 74-81, Sep. 2015.

[48] M. He, G. Song, and J. Cheng, "Optimal rate profile for multi-user multi-rate transmission systems by bivariate fixed-point analysis," *IET Commun.*, vol. 11, no. 5, pp. 628-638, Mar. 2017.

[49] F. A. Rabee, K. Davaslioglu, and R. Gitlin, "The Optimum Received Power Levels of Uplink NOMA Signals," in *Proc. IEEE WAMICOM*, Apr. 2017, pp. 1-4.

My Publications

[1] M. He, G. Song, and J. Cheng, "Joint rate and power optimization for successive interference cancellation in uplink NOMA systems," *IEICE Commun. Express.*, vol. 7, no. 2, pp. 48-53, Feb. 2018.

[2] J. Liu, M. He, and J. Cheng, "Improved sphere bound on the MLD performance of binary linear block codes via voronoi region," *IEICE Tranc. Fundamentals of Electronics.*, vol. E100-A, no. 12, pp. 2572-2577, Dec. 2017.

[3] M. He, G. Song, and J. Cheng, "Optimal rate profile for multi-user multi-rate transmission systems by bivariate fixed-point analysis," *IET Commun.*, vol. 11, no. 5, pp. 628-638, Mar. 2017.

[4] M. He, G. Song, and J. Cheng, "Unequal rate transmission for sum rate maximization over two-user Gaussian multiple access channel," *The Harris Science Review of Doshisha University*, vol. 57, no. 2, pp. 81-89, Jul. 2016.

[5] M. He, G. Song, and J. Cheng, "Optimal rate profile for multi-user multi-rate code with hybrid interference cancellation scheme," in *Proc. IEICE Int. Symposium on Information Theory and Its Applications (ISITA)*, California, USA, Oct. 2016, p. 552.

[6] M. He, G. Song, and J. Cheng, "Sum-rate maximization with hybrid interference cancellation scheme for multiple access channel," in *Proc. Croucher Summer Course in Information Theory (CSCIT)*, Hong Kong, China, Jun. 2015, p. 28.

[7] M. He, G. Song, and J. Cheng, "Rate optimization for RA-IDMA system by bivariate fixed point analysis," in *Proc. IEEE East Asian School of Information Theory (EASIT)*, Hong Kong, China, Jul. 2014, p. 16.

[8] M. He, G. Song, and J. Cheng, "Rate optimization for repeat-accumulate interleave-division system by fixed point analysis," in *Proc. IEEE Int. Conf. on Communications (ICC)*, Sydney, Australia, Jun. 2014, pp. 2015-2111.

[9] M. He, G. Song, and J. Cheng, "Rate allocation for repeat accumulate interleave division system by fixed point analysis," in *Proc. IEICE the 36th Symposium on Information Theory and its Applications (SITA)*, Shizuoka, Japan, Dec. 2013, pp. 249-254.

[10] M. He, G. Song, and J. Cheng, "Maximum sum rate of two-user unequal rate repeat accumulate code by fixed point analysis," in *Proc. 8th Joint Symposium between Chonnam National University and Doshisha University*, Kyoto, Japan, Oct. 2013, pp. 3-8.

[11] M. He, G. Song, and J. Cheng, "Unequal rate repeat accumulate codes for two-user Gaussian multiple access channel," in *Proc. IEICE the 35th Symposium on Information Theory and its Applications (SITA)*, Beppu, Japan, Dec. 2012, pp. 96-100.

[12] M. He, S. Lu, G. Song, J. Cheng, and Y. Watanabe, "Channel capacity with superposed *M*-PAM modulation," in *Proc. IEEE 4th Int. Conf. on Intelligent Computation Technology and Automation (ICICTA)*, Shenzhen, China, Mar. 2011, pp. 475-478.

Appendix A

Shannon Limit of Binary-Input K-User Gaussian Multiple Access Channel

The K-user Gaussian multiple access channel with binary input is modeled as

$$Y = \sum_{k=1}^{K} X^{(k)} + Z. \tag{A.1}$$

Here, binary inputs $X^{(k)}, k = 1, \cdots, K$, are i.i.d variables and uniformly distributed on $\mathcal{X} = \{+1, -1\}$. Noise Z is a Gaussian variable with root-mean-square value σ. It is not difficult to get the Shannon limit of the channel as [1]

$$\begin{aligned} C(K, \sigma) &= \max_{p(x^{(1)}), \cdots, p(x^{(K)})} I(X^{(1)}, \cdots, X^{(K)}; Y) && \text{(A.2)} \\ &= \max_{p(x^{(1)}), \cdots, p(x^{(K)})} H(Y) - H(Y|X^{(1)}, \cdots, X^{(K)}) && \text{(A.3)} \\ &= \max_{p(x^{(1)}), \cdots, p(x^{(K)})} \left\{ - \int_{-\infty}^{+\infty} p(y) \log_2 p(y) \mathrm{d}y \right\} - \frac{1}{2} \log_2(2\pi e \sigma^2) && \text{(A.4)} \\ &= - \int_{-\infty}^{+\infty} p'(y) \log_2 p'(y) \mathrm{d}y - \frac{1}{2} \log_2(2\pi e \sigma^2). && \text{(A.5)} \end{aligned}$$

The last equation is followed when transmitted symbols $x^{(k)}, k = 1, \cdots, K$, are statistically independent and equally likely to be +1 and -1, where $p'(y)$ is [6]

$$p'(y) = \sum_{i=0}^{K} \frac{C_K^i}{2^K} \frac{1}{\sqrt{2\pi\sigma^2}} \exp\left(- \frac{(y - (K - 2i))^2}{2\sigma^2} \right). \tag{A.6}$$

Appendix B

Computation Complexity for Chapter 4

The decoding complexity of IJD, HIC, and SIC schemes, described in Section 4.2.2, depends on the node operations at node sets U, G, V, and Y (see Fig. 4.2).

Let ψ_m be the arithmetic operation complexity performed on variable nodes in U and V and on check nodes in G per user in the mth group per iteration. The complexity ψ_m is specified by numbers of addition/subtraction, multiplication/division, and exponent/logarithm operations in (3.3) and (3.5). For IJD scheme, let L_{IJD} be the number of iterations in joint decoding. The decoding complexity at nodes U, V, and G for all the users is

$$\varphi_{\mathrm{IJD}} = \sum_{m=1}^{M} \psi_m L_{\mathrm{IJD}} \frac{K}{M}. \tag{B.1}$$

For HIC scheme, denoted by $L_{\mathrm{HIC}}^{\mathrm{G}}$ the number of iterations in decoding within each group. We have the decoding complexity

$$\varphi_{\mathrm{HIC}} = \sum_{m=1}^{M} \psi_m L_{\mathrm{HIC}}^{\mathrm{G}} \frac{K}{M}. \tag{B.2}$$

Let us turn to describe the computation complexity at sum nodes in Y. The operation at sum nodes depends on the number of edges connected to the nodes (see Fig. 4.3 and Fig. 4.4). For IJD, the K users are always connected to sum nodes. We denote by ϕ_K the arithmetic operation complexity performed on sum nodes with K users per iteration. The complexity ϕ_K can be obtained by observing (4.6). With number of iterations L_{IJD}, the computation complexity at sum nodes in Y

is

$$\chi_{\mathrm{IJD}} = \phi_K L_{\mathrm{IJD}}. \tag{B.3}$$

For the mth step of HIC, only K/M users in the mth group are connected to sum nodes and the signals from other users are cancelled or considered to be noise. The arithmetic operation complexity performed on sum nodes, in the mth step of HIC (see Section 4.2.2.2), is thus $\phi_{K/M} = \phi_K/M$. With the number of iterations $L^{\mathrm{G}}_{\mathrm{HIC}}$ within group and M-step cancelling, the computation complexity at sum nodes in Y is

$$\chi_{\mathrm{HIC}} = \phi_{(K/M)} L^{\mathrm{G}}_{\mathrm{HIC}} M. \tag{B.4}$$

When $L_{\mathrm{IJD}} = M L^{\mathrm{G}}_{\mathrm{HIC}}$, i.e., the total numbers of iterations at sum nodes are same, the overall complexity of HIC, i.e., the summation of (B.2) and (B.4), is $1/M$ of that of IJD. In addition, the overall complexity of SIC is $1/K$ of that of IJD.